(12) INTERNATIONAL APPLICATION PUBLISHED UNDER THE PATENT COOPERATION TREATY (PCT)

(19) World Intellectual Property Organization
International Bureau

(43) International Publication Date
5 November 2009 (05.11.2009)

PCT

(10) International Publication Number
WO 2009/135184 A2

(51) International Patent Classification:
A61K 31/352 (2006.01)

(21) International Application Number:
PCT/US2009/042614

(22) International Filing Date:
1 May 2009 (01.05.2009)

(25) Filing Language: English

(26) Publication Language: English

(30) Priority Data:

61/049,462	1 May 2008 (01.05.2008)	US
61/055,780	23 May 2008 (23.05.2008)	US

(71) Applicant *(for all designated States except US)*: **THE TRUSTEES OF COLUMBIA UNIVERSITY IN THE CITY OF NEW YORK** [US/US]; 412 Low Memorial Library, 535 West 116th Street, New York, NY 10027 (US).

(72) Inventors; and

(75) Inventors/Applicants *(for US only)*: **WORMAN, Howard, J.** [US/US]; 240 West 102nd Street, Apt. 41, New York, NY 10025 (US). **MUCHIR, Antoine** [FR/US]; 47 West 86th Street, Apt. 2R, New York, NY 10029 (US).

(74) Agents: **LOVE, Jane, M.** et al.; Wilmer Cutler Pickering Hale And Dorr LLP, 399 Park Avenue, New York, NY 10022 (US).

(81) Designated States *(unless otherwise indicated, for every kind of national protection available)*: AE, AG, AL, AM, AO, AT, AU, AZ, BA, BB, BG, BH, BR, BW, BY, BZ, CA, CH, CN, CO, CR, CU, CZ, DE, DK, DM, DO, DZ, EC, EE, EG, ES, FI, GB, GD, GE, GH, GM, GT, HN, HR, HU, ID, IL, IN, IS, JP, KE, KG, KM, KN, KP, KR, KZ, LA, LC, LK, LR, LS, LT, LU, LY, MA, MD, ME, MG, MK, MN, MW, MX, MY, MZ, NA, NG, NI, NO, NZ, OM, PG, PH, PL, PT, RO, RS, RU, SC, SD, SE, SG, SK, SL, SM, ST, SV, SY, TJ, TM, TN, TR, TT, TZ, UA, UG, US, UZ, VC, VN, ZA, ZM, ZW.

(84) Designated States *(unless otherwise indicated, for every kind of regional protection available)*: ARIPO (BW, GH, GM, KE, LS, MW, MZ, NA, SD, SL, SZ, TZ, UG, ZM, ZW), Eurasian (AM, AZ, BY, KG, KZ, MD, RU, TJ, TM), European (AT, BE, BG, CH, CY, CZ, DE, DK, EE, ES, FI, FR, GB, GR, HR, HU, IE, IS, IT, LT, LU, LV, MC, MK, MT, NL, NO, PL, PT, RO, SE, SI, SK, TR), OAPI (BF, BJ, CF, CG, CI, CM, GA, GN, GQ, GW, ML, MR, NE, SN, TD, TG).

Published:

— *without international search report and to be republished upon receipt of that report (Rule 48.2(g))*

WO 2009/135184 A2

(54) Title: METHODS FOR TREATING AND/OR PREVENTING CARDIOMYOPATHIES BY ERK OR JNK INHIBITION

(57) Abstract: Provided is a method of treating or preventing a cardiomyopathy associated with activation of at least one kinase in the MAP kinase signaling pathway in heart tissue by providing to a subject an inhibitor of at least one kinase in the ERK signaling pathway or in the JNK signaling pathway, or both. In some embodiments, the cardiomyopathy is associated with one or more mutations in the *LMNA* gene, which encodes A-type nuclear lamins, or in the *EMD* gene, which encodes an inner nuclear membrane protein.

METHODS FOR TREATING AND/OR PREVENTING CARDIOMYOPATHIES BY ERK OR JNK INHIBITION

[0001] This application claims the benefit of priority of U.S. provisional applications Serial No. 61/049,462, filed May 1, 2008, and Serial No. 61/055,780, filed May 23, 2008. The disclosure of the aforementioned provisional applications, and of all patents, patent applications, and publications cited herein, are hereby incorporated by reference in their entirety.

[0002] This invention was made in part with government support under grant No. R01AR048997 awarded by the National Institutes of Health. The United States government has certain rights in this invention.

BACKGROUND OF THE INVENTION

[0003] Cardiomyopathies may be caused a variety of factors, including environmental factors, genetic mutations, disruption of cell signaling pathways, and various other etiologies. The present invention is directed in part to methods of treating cardiomyopathies that are associated with activation of MAP kinase signaling pathways. Emery-Driefuss muscular dystrophy (EDMD) is characterized by genetic (inherited) cardiomyopathies. Acquired cardiomyopathies, such as hypertrophic cardiomyopathy, are also associated with MAP kinase activation (150).

[0004] Emery-Dreifuss muscular dystrophy (EDMD) results in cardiac disease, the initial presentation being atrioventricular conduction block followed by dilated cardiomyopathy (1). EDMD is also characterized by joint contractures in the spine, neck, elbows, and Achilles tendons, and progressive skeletal muscle weakness and wasting in a humero-peroneal distribution. EDMD was initially described as an X-linked inherited disorder, but it is now known that there are autosomal dominant and recessive forms of EDMD (100). X-linked EDMD is associated with mutations in the *EMD* gene (2, 4), while autosomal dominant and recessive EDMD is associated with mutations in the *LMNA* gene (5, 6).

[0005] The *EMD* gene encodes the ubiquitously expressed inner nuclear membrane protein emerin (3, 4). The *LMNA* gene encodes the widely expressed A-type nuclear lamins, of which lamin A and lamin C are the predominant somatic cell isoforms (8). Nuclear lamins are intermediate filament proteins that polymerize to form 10 nm diameter filaments on the inner aspect of the inner nuclear membrane (9-12). The lamina interacts with integral proteins

in the inner nuclear membrane and provides anchorage sites for chromatin and structural support to the nuclear envelope (7). Many of the disease-causing A-type lamin mutants lead to disruption of the nuclear lamina and abnormal nuclear envelope architecture when expressed in cells (7).

[0006] In addition to playing a role in EDMD, mutations in the *EMD* and *LMNA* genes are associated with other cardiomyopathies, and indeed other non-cardiac diseases. For example, mutations in *LMNA* encoding A-type nuclear lamins cause several diverse diseases often referred to as laminopathies (7, 128), which, in addition to autosomal dominant and recessive EDMD, include dilated cardiomyopathy type 1A with conduction defect (68) and limb-girdle muscular dystrophy type 1B (69). These are a subset of the laminopathies that affect striated muscle (5, 6, 63, 39). A common feature of these disorders is cardiomyopathy. Indeed it is believed that 8% of familial and sporadic cardiomyopathies may be caused by mutations in the *LMNA* gene (129). While implantable pacemakers and defibrillators can prevent complications of cardiac dysrhythmias that occur early in these disorders, affected individuals eventually develop heart failure for which there is no curative treatment and cardiac transplantation is ultimately necessary (129-131). *LMNA* mutations are also associated with Charcot-Marie-Tooth disease type 2B1 (70) (a peripheral neuropathy with secondary muscle wasting and weakness), Dunnigan-type familial partial lipodystrophy (71-73) which affects adipose tissue (74), mandibuloacral dysplasia (75), Hutchison-Gilford progeria syndrome (76, 77), atypical Werner syndrome (78), neonatal lethal restrictive dermopathy (79), and disorders characterized by accelerated aging.

[0007] Despite that widespread expression of the *EMD* and *LMNA* genes, EDMD selectively affects striated muscle and tendons. Two main hypotheses have been proposed attempting to connect the pathophysiology of EDMD to functions of A-type lamins and emerin (7). The "mechanical stress" hypothesis proposes that the ability of A-type lamins and emerin to maintain the mechanical integrity of cells subject to stress is altered when *LMNA* or *EMD* genes are mutated. The "gene expression" hypothesis proposes a specific role of A-type lamins and emerin in proper tissue-selective gene expression. These hypotheses are not necessarily mutually exclusive, as altered nuclear mechanics and abnormal expression of stress-response genes have both been observed in cells lacking A-type lamins (13). However, despite data obtained mostly from cultured cells and *in vitro* binding assays that have lead to the "mechanical stress" and "gene expression" hypotheses,

there are scant experimental results linking *LMNA* and *EMD* mutations to pathogenic pathways in affected tissues.

SUMMARY OF THE INVENTION

[0008] We have determined the effects of an *Lmna* H222P mutation on signaling pathways involved in the development of cardiomyopathy in a knock-in mouse model of autosomal dominant Emery-Dreifuss muscular dystrophy. This is a model of inherited or genetic cardiomyopathy. Analysis of genome-wide expression profiles in hearts using Affymetrix GeneChips showed statistically significant differences in expression of genes in the MAPK pathways at the incipience of the development of clinical disease. Using real-time PCR, we showed that activation of MAPK pathways preceded clinical signs or detectable molecular markers of cardiomyopathy. In heart tissue and isolated cardiomyocytes, there was activation of MAPK cascades and downstream targets, implicated previously in the pathogenesis of cardiomyopathy. Expression of H222P lamin A in cultured cells activated MAPKs and downstream target genes. Activation of MAPK signaling by mutant A-type lamins could be a cornerstone in the development of heart disease in autosomal dominant Emery-Dreifuss muscular dystrophy.

[0009] We used the JNK inhibitor SP600125 (Calbiochem), which is a cell-permeable and selective inhibitor of all JNK isoforms (80-82), and PD98059 (Calbiochem), U0126 (EMD Biosciences), and MEK1/2 (EMD Biosciences), which are cell-permeable and selective for ERK isoforms (83-88). These compounds specifically block the MAP kinase kinases responsible for phosphorylating (activating) JNKs and ERKs. $Lmna^{H222P/H222P}$ mice treated with MAPK inhibitors showed significantly improved ejection fraction and left ventricular end diastolic diameter as assessed by echocardiography, showing improvement in cardiac function. Kinase activation and activation of downstream genes were also inhibited in hearts of treated mice. Activation of ERK, JNK, or ERK plus JNK can lead to heart disease in Emery-Dreifuss muscular dystrophy and other cardiomyopathies. ERK, JNK, or ERK plus JNK inhibitors can block kinase activity and prevent onset of, improve or slow progression of, and/or improve cardiac function in cardiomyopathy in the $Lmna^{H222P/H222P}$ mouse model of Emery-Dreifuss muscular dystrophy. Inhibitors to decrease activation can be used as treatment.

[0010] Therefore, this invention is based, in part, on the discovery that the JNK and ERK branches of the MAP kinase cascade are activated in mouse models of autosomal and X-linked EDMD, and the discovery that this activation occurs prior to the appearance of cardiac disease, suggesting that it is a primary pathogenic mechanism. The invention is also based, in part, on the discovery that, along with activation of JNK and ERK, EDMD is also associated with increased expression of "downstream" transcription factors, such as c-Jun, and genes they activate encoding sarcomeric proteins such as myosins and sacrolipin.

[0011] In one aspect, the invention provides a method of treating or preventing a cardiomyopathy associated with activation of at least one kinase in the mitogen-activated protein kinase (MAPK) signaling pathway in heart tissue, the method comprising providing to a subject an inhibitor of at least one kinase in the extracellular signal-regulated kinase (ERK) signaling pathway, or an inhibitor of at least one kinase in the c-Jun N-terminal kinase (JNK) signaling pathway, or both.

[0012] In one embodiment, the cardiomyopathy is a genetic, or inherited, cardiomyopathy. For example, the cardiomyopathy can be associated with one or more mutations in *LMNA* or *EMD*. In another embodiment, the cardiomyopathy is an acquired cardimyopathy. In some embodiments, the cardiomyopathy can be a dilated cardiomyopathy or a hypertrophic cardiomyopathy.

[0013] The kinase in the ERK signaling pathway can be, for example, a MAPK/ERK kinase (MEK), in particular, MEK1 or MEK2.

[0014] The kinase in the JNK signaling pathwaycan be a JNK.

[0015] In one embodiment, the inhibitor of at least one kinase in the ERK signaling pathway is selected from the group consisting of a chromone and a flavone. The ERK signaling pathway inhibitor can be selected from the group consisting of 2-(2-amino-3-methoxyphenyl)-4H-1-benzopyran-4-one (PD98059), 1,4-diamino-2,3-dicyano-1,4-bis(2-aminophenylthio)butadiene (U0126), Z-& E-a-(amino-((4-aminophenyl)thio)methylene)-2-(trifluoromethyl)benzeneacetonitrile (MEK1/2), PD0325901, AZD6244/ARRY-142886, and ARRY-438162. In a preferable embodiment, the inhibitor of at least one kinase in the ERK signaling pathway is PD98059.

[0016] In a further embodiment, the inhibitor of at least one kinase in the JNK signaling pathway can be an anthrapyrazolone. In a preferred embodiment, the anthrapyrazolone is anthra[1,9-cd]pyrazol-6(2H)-one (SP600125). The inhibitor of at least one kinase in the JNK signaling pathway can be CC-401.

[0017] In one aspect, treating a cardiomyopathy comprises improving cardiac function or preventing deterioration in cardiac function. Improving cardiac function or preventing deterioration in cardiac function can comprise increasing at least one of ejection fraction or fractional shortening. Improving cardiac function or preventing deterioration in cardiac function can also comprise decreasing at least one of left ventricular end systolic diameter or left ventricular end diastolic diameter.

[0018] For purposes of the present invention, treating or preventing cardiomyopathy can comprise reducing expression of at least one molecular marker of cardiomyopathy. In one embodiment, the molecular marker is selected from the group consisting of atrial natriuretic factor, brain natriuretic factor, Bcl-2, Elk-1, c-Jun, JunD, Vegf, Myl7, Sln, and Elk 4. The molecular marker can be a sarcomere structure protein, for example, myosin.

[0019] The disclosure also provides a method for identification of a compound or a combination of compounds that is/are useful in the treatment of cardiac disease, such as cardiomyopathy, and/or improvement of cardiac function, the method comprising administering the compound or combination of compounds to an animal that is a model of cardiac disease or cardiac malfunction, wherein the model is a knock-in mouse model of autosomal dominant Emery-Dreifuss muscular dystrophy (*Lmna*$^{H222P/H222P}$ mice), and determining whether the compound or combination of compounds improves cardiac function in the mouse, compared to a mouse model not so treated.

BRIEF DESCRIPTION OF THE DRAWINGS

[0020] **Figures 1A-1C** show RNA expression profiling in hearts of *Lmna* H222P mice. **(1A)** Hierarchical clustering analysis of differentially expressed genes in hearts from *Lmna*$^{+/+}$, *Lmna*$^{H222P/+}$ and *Lmna*$^{H222P/H222P}$ mice. Rows indicate the expression of individual genes and vertical lines indicate each sample. For each gene, the ratio of transcript abundance in the samples to its abundance in the control is represented by color intensities (red indicates higher expression and green indicates lower expression). Transcriptional profiles of hearts from *Lmna*$^{H222P/H222P}$ and *Lmna*$^{H222P/+}$ mice show a greater degree of similarity to each other

than to hearts from control *Lmna*$^{+/+}$ mice. (**1B**) Volcano plots of absolute expression values ($\log_2$[*q*-value]) determined by robust multichip analysis. For each probe set, expression in hearts from *Lmna*$^{H222P/H222P}$ and *Lmna*$^{H222P/+}$ mice is plotted. A two-fold threshold and $q<0.05$ was used to determine the probe sets significantly altered in the analysis (red dot squares). (**1C**) Validation of RNA expression profiling of selected genes in hearts from *Lmna*$^{+/+}$, *Lmna*$^{H222P/+}$ and *Lmna*$^{H222P/H222P}$ mice using real-time PCR. Bars indicate the fold overexpression of the indicated mRNA in hearts as calculated by the $\Delta\Delta C_T$ method. Values are means ± standard deviations for n=6 samples per group. The real-time PCR were performed in triplicate with the different RNA samples. Matrices visualizing Affymetrix GeneChip data of corresponding probe sets of RNAs are shown at right of bar graph. In these matrices, each probe set is visualized as a row of colored squares with one square for each sample. *Myh7*, *Myh4*, *Myl7*, *Acta2 and Sln* show higher expression and *Pttg* lower expression compared to controls.

[0021] **Figures 2A-2C** show histological analysis of heart muscle in *Lmna* H222P mice and expression of myosins and ANF. (**2A**) Histological analysis of hearts from 10-week old control *Lmna*$^{+/+}$ and *Lmna*$^{H222P/H222P}$ mice. Representative fixed sections of left ventricles stained with hematoxylin and eosin (upper panels) and Gomori's trichrome (lower panels) are shown. Bars: 50 μm. Note normal-appearing cardiomyocytes and absence of fibrosis. (**2B**) Expression of myosins and ANF in hearts of 10-week old *Lmna*$^{+/+}$, *Lmna*$^{H222P/+}$ and *Lmna*$^{H222P/H222P}$ mice. Representative immunoblots for ANF, β- MHC and MLC-2 are shown. β-tubulin Ab labeling is shown as a loading control. (**2C**) Data in bar graphs are means ± standard deviations of n=5 samples per group (*$p<0.05$).

[0022] **Figures 3A-3B** show MAPK signaling is activated in hearts and isolated cardiomyocytes from *Lmna* H222P mice. (**3A**) Detection of phosphorylated JNK and ERK1/2 in hearts and isolated cardiomyoctes from *Lmna*$^{+/+}$, *Lmna*$^{H222P/+}$ and *Lmna*$^{H222P/H222P}$ mice. JNK and ERK1/2 were measured by immunoblotting with Abs against total protein (JNK and ERK1/2) and phosphoprotein (pJNK and pERK1/2). Data in bar graphs are means ± standard deviations of n=5 samples per group (*$p<0.05$, ***$p<0.0005$). (**3B**) Effect of MAPK activation on downstream targets in *Lmna*$^{+/+}$, *Lmna*$^{H222P/+}$ and *Lmna*$^{H222P/H222P}$ mice. Representative immunoblots using Abs that recognize phosphorylated c-Jun (pc-Jun), elk-1, bcl-2 and β-tubulin loading control are shown for proteins extracted from heart tissue and isolated ventricular cardiomyocytes.

[0023] **Figures 4A-4C** show immunofluorescence microscopic analysis of pERK1/2 in heart sections from *Lmna*$^{H222P/H222P}$ mice. (**4A**) Sections of frozen heart from *Lmna*$^{+/+}$ (top panel) and *Lmna*$^{H222P/H222P}$ (bottom panel) mice were analyzed by immunofluorescence microscopy using Ab recognizing pERK1/2. Sections were counterstained with DAPI. Bars: 50 μm. (**4B**) Quantification of pERK1/2 labeling in cardiomyocytes from *Lmna*$^{+/+}$ mice and *Lmna*$^{H222P/H222P}$ mice. Cardiomyocytes are delimited by dotted line and intensity of emitted fluorescence is measured along the yellow line (a to b). Position of the nucleus and intensity of fluorescence using anti pERK1/2 Ab is shown in the diagram of a single cardiomyocyte. (**4C**) Bars indicate intensity of pERK1/2 fluorescence in the nucleus of the indicated hearts. Values are means ± standard deviations for the intensity of nuclear fluorescence from n=90 cardiomyocytes from two different hearts per group (*p<0.05).

[0024] **Figure 5** shows expression of Elk-1, c-Jun, JunD and Elk-4 in various tissues from 10 week old Lmna+/+ and LmnaH222P/H222P mice. Summary of real-time PCR results in heart, skeletal muscle, lung, spleen and bladder are shown. Bars indicate the fold overexpression of the indicated mRNA normalized to Gapdh as calculated by the ΔΔCT method. Values are means ± standard deviations for n=6 samples per group (*p<0.05, **p<0.005).

[0025] **Figure 6** shows time-course expression of genes activated by MAPK in hearts from LmnaH222P/H222P mice at 4, 7 and 10 weeks of age. Expression of Vegf, Myl7, Sln, c-Jun, Elk-1, JunD and Elk-4 in hearts of Lmna+/+ and LmnaH222P/H222P mice is shown. Bars indicate the fold overexpression of the indicated mRNA normalized to Gapdh as calculated by the ΔΔCT method. Values are means ± standard deviations for n=6 samples per group (*p<0.05, **p<0.005).

[0026] **Figures 7A-7F** show Expression of H222P lamin A in transfected Cos-7 and C2C12 cells leads to increased phosphorylation and enhanced nuclear translocation of ERK1/2. (**7A-7B**) Effect of H222P lamin A expression on levels of pERK1/2 in transfected Cos-7 (A) and C2C12 (B) cells. Immunoblotting with pERK1/2 Ab or total ERK1/2 Ab was performed. Data are shown as means ± standard deviations of n=11 (A) and n=7 (B) samples per group (*p<0.05). Significance of the results was determined using paired t-test (parametric) and a Wilcoxon test (non-parametric). Immunoblotting with GFP Ab are shown to demonstrate expression of proteins encoded by transfected plasmids. Immunoblottings

with β-actin Ab are shown as loading controls. (**7C-7D**) Effect of H222P lamin A on nuclear translocation of pERK1/2 in transfected Cos-7 (C) and C2C12 (D) cells. Representative photomicrographs are shown for non-transfected cells (NT), transfected cells expressing a GFP fusion of wild type lamin A (WT lamin A) and transfected cells expressing a GFP fusion of lamin A with the H222P amino acid substitution (H222P lamin A). Arrowheads show enhanced nuclear localization of pERK1/2 in cells expressing GFP-H222P lamin A. Bars: 10 μm. (**7E-7F**) Percentages of Cos-7 (E) and C2C12 (F) cells with pERK1/2 primarily in the nucleus. Non-transfected cells (NT), transfected cells expressing a GFP fusion of wild type lamin A (WT lamin A) and transfected cells expressing a GFP fusion of lamin A with the H222P aa substitution (H222P lamin A) were randomly counted and scored for nuclear pERK1/2 (see arrowheads in C for example). Transfected cells were determined by presence of GFP signal. Values are means ± standard deviations for n=200 cells per group (*$p<0.05$, **$p<0.005$). The person counting the cells was "blinded" as to which protein was expressed.

[0027] **Figure 8** shows activation of c-Jun and Elk-1 by expression of lamin A mutants. Cos-7 cells were transiently transfected with plasmids encoding wild type lamin A, lamin A with the indicated amino acid substitution and the associated phenotype to each mutation (e.g. EDMD or FPLD) or "empty vector" control. After 24h, luciferase activities induced by expression of c-Jun (upper panel) or Elk-1 (lower panel) were measured in cell lysates and normalized to β-gal activities obtained from a protein encoded by a co-transfected plasmid. Results are means ± standard deviations of n=5 experiments (*$p<0.05$, **$p<0.005$).

[0028] **Figure 9** shows a model of how abnormalities of A-type lamins in the nuclear lamina may lead to cardiomyopathy. Abnormalities of A-type lamins in the nuclear lamina activates MAPK cascades, possibly via heterotrimeric G-protein receptors or by inducing stress responses by unknown mechanisms (?). This leads to enhanced phosphorylation of ERK and JNK1/2 and their subsequent nuclear translocation. In the nucleus, pERK1/2 and pJNK activate transcription factors such as elk-1, bcl-2, JunD, elk-4 and c-Jun, leading to increased synthesis of these proteins. Increased amounts and activities of transcription factors activated by pJNK and pERK1/2 alter expression of other genes, some encoding components of muscle fibers and sarcomeres. Aberrant expression of these proteins leads to development of cardiomyopathy.

[0029] **Figures 10A-10D** show expression of H222P lamin A in transfected Cos-7 and C2C12 leads to enhanced nuclear translocation of phospho-JNK. (**10A-10B**) Effect of H222P lamin A on nuclear translocation of pJNK in transfected Cos-7 (A) and C2C12 (B) cells. Representative photomicrographs are shown for non-transfected cells (NT), transfected cells expressing a GFP fusion of wild type lamin A (WT lamin A) and transfected cells expressing a GFP fusion of lamin A with the H222P amino acid substitution (H222P lamin A). Arrowheads show enhanced nuclear localization of pJNK in cells expressing GFP-H222P lamin A. Bars: 10 μm. (**10C-10D**) Percentages of Cos-7 (C) and C2C12 (D) cells with pJNK primarily in the nucleus. Non-transfected cells (NT), transfected cells expressing a GFP fusion of wild type lamin A (WT lamin A) and transfected cells expressing a GFP fusion of lamin A with the H222P aa substitution (H222P lamin A) were randomly counted and scored for nuclear pJNK (see arrowheads in A for example). Transfected cells were determined by presence of GFP signal. Values are means ± standard deviations for n=200 cells per group (*p<0.05, **p<0.005).

[0030] **Figure 11** shows daily injection of inhibitors (PD98059, SP600125 or both altogether) in *Lmna*$^{H222P/H222P}$ mice inhibits phosphorylation of their specific targets in heart from mice. Immunoblots using anti-pERK1/2, anti-ERK1/2, anti-pJNK and anti-JNK antibodies on hearts from *Lmna*$^{H222P/H222P}$ mice treated or not with the different inhibitors. Hearts from *Lmna*$^{+/+}$ mice and *Lmna*$^{H222P/H222P}$ mice treated with the vehicle alone (DMSO) were used as controls.

[0031] **Figures 12A-12B** show treatment of *Lmna*$^{H222P/H222P}$ mice with MEK inhibitor PD98059 inhibits phosphorylation of ERK1/2 and activation of downstream target genes. (**12A**) Representative immunoblots using antibodies against phosphorylated ERK1/2 (pERK1/2) and antibodies against total ERK1/2 using proteins extracted from hearts from *Lmna*$^{H222P/H222P}$ mice treated with PD98059 or placebo (DMSO). Results in hearts from *Lmna*$^{+/+}$ mice and untreated *Lmna*$^{H222P/H222P}$ mice are shown for comparison. Data in bar graphs are the quantification of phosphorylated ERK1/2 compared to total ERK1/2 measured by scanning the immunoblots and using Scion image Software (Scion Corporation). Values are means ± standard deviations for n = 3 samples from different animals per group. Results were compared using a two-tailed *t* test (*p<0.05). (**12B**) Quantitative real-time RT-PCR showing expression of RNAs of selected downstream target genes (*Elk1*, *Elk4*, *Atf2*, *Atf4*) of ERK signaling cascade in hearts from *Lmna*$^{H222P/H222P}$ mice treated with PD98059 or placebo

(DMSO). Results from hearts from *Lmna*$^{+/+}$ mice and untreated *Lmna*$^{H222P/H222P}$ mice are shown for comparison. Bars indicate the fold overexpression of the indicated mRNA in hearts. Values are means ± standard deviations for n = 4 samples from different animals per group. Reactions were performed in triplicate for each different RNA sample. Results were compared using a two-tailed *t* test (*p<0.05, **p<0.005).

[0032] **Figures 13A-13B** show the effect of MEK inhibitor PD98059 on cardiac expression of natriuretic peptides and myosins in *Lmna*$^{H222P/H222P}$ mice. (**13A**) Immunoblot showing expression of natriuretic peptide precursor A (Nppa) in hearts from *Lmna*$^{H222P/H222P}$ mice treated with PD98059 or placebo (DMSO). Results using hearts from *Lmna*$^{+/+}$ mice and untreated *Lmna*$^{H222P/H222P}$ mice are shown for comparison. Labeling with antibody against Gapdh is shown as a loading control. (**13B**) Quantitative real-time RT-PCR showing expression of RNAs from *NppA* and *NppB* genes, respectively encoding natriuretic peptide precursors A and B, and *Myl4* and *Myl7* genes, encoding myosin light chains, in hearts from *Lmna*$^{H222P/H222P}$ mice treated with PD98059 or placebo (DMSO). Results from hearts from *Lmna*$^{+/+}$ mice and untreated *Lmna*$^{H222P/H222P}$ mice are shown for comparison. Bars indicate the fold overexpression of the indicated mRNA in hearts as calculated by the CT method. Values are means ± standard deviations for n = 4 samples from different animals per group. Reactions were performed in triplicate for each different RNA sample. Results were compared using a two-tailed *t* test (*p<0.05).

[0033] **Figures 14A-14B** show treatment with the MEK inhibitor PD98059 prevents dilation and deterioration of dynamics of the left ventricle in *Lmna*$^{H222P/H222P}$ mice. (**14A**) Histological analysis of heart sections stained with hematoxylin and eosin from *Lmna*$^{H222P/H222P}$ mice treated with PD98059 or placebo (DMSO). Hearts from *Lmna*$^{+/+}$ mice and untreated *Lmna*$^{H222P/H222P}$ mice are shown for comparison. The left ventricle is dilated in *Lmna*$^{H222P/H222P}$ mice that were untreated or that received DMSO placebo whereas hearts from *Lmna*$^{H222P/H222P}$ mice treated with PD98059 had a left ventricular chamber diameter is similar to *Lmna*$^{+/+}$ mice. Scale bar: 1 mm. (**14B**) Transthoracic M-mode echocardiographic tracings in *Lmna*$^{H222P/H222P}$ mice treated with PD98059 or placebo (DMSO). Tracings from *Lmna*$^{+/+}$ mice and untreated *Lmna*$^{H222P/H222P}$ mice are shown for comparison. Left ventricular end systolic diameter (LVESD) and left ventricular end diastolic diameter (LVEDD) are indicated. Note LVESD and LVEDD are similar in *Lmna*$^{H222P/H222P}$ mice treated with

PD98059 and decreased in *Lmna*$^{H222P/H222P}$ mice that were untreated or that received DMSO placebo.

[0034] **Figures 15A-15B** show that treatment with PD98059 prevents abnormal elongation of cardiomyocyte nuclei in *Lmna*$^{H222P/H222P}$ mice. (**15A**) Histological analysis of cross sections of hearts from *Lmna*$^{H222P/H222P}$ mice treated with PD98059 or placebo (DMSO). Hearts from *Lmna*+/+ mice and untreated *Lmna*$^{H222P/H222P}$ mice were used for comparisons. Sections are stained with hematoxylin and eosin. Inserts with yellow lines with arrowheads demonstrate measurement of nuclear length. Scale bar: 50 μm. (**15B**) Quantification of nuclear elongation in cardiomyocytes from mice. Cardiomyocyte nuclei are measured along the yellow lines with arrowheads as shown as examples in A. Bars indicate length of cardiomyocyte nuclei in the indicated hearts. Values are means ± standard deviations for n = 400 cardiomyocytes (*p<0.0005).

[0035] **Figure 16A** is an immunoblot showing expression of total ERK1/2 and phosphorylated ERK1/2 (pERK1/2) in hearts from control and *Lmna*$^{-/-}$ mice. Data in bar graphs are means ± standard deviations derived from scanned immunoblots of n=4 samples per group (*p<0.05). **Figure 16B** shows expression of mRNA encoded by *c-Jun, Elk1, Mef2c, c-Fos, Atf2, JunD, Atf4 and Elk4* in hearts from control (open bars) and *Lmna*$^{-/-}$ (dark bars) mice using real-time quantitative RT-PCR. Bars indicate fold overexpression of the indicated mRNA. Values are means ± standard deviations for n=4 samples (*p<0.05, **p<0.005).

[0036] **Figure 17A** shows expression of mRNA encoded by *Gapdh*, *Emd* and *Lmna* in HeLa cells transfected with siRNA duplexes against *Gapdh*, *Emd* and *Lmna*, using real-time quantitative RT-PCR. Bars indicate fold overexpression of the indicated mRNA. Values are means ± standard deviations for n=4 samples (*p<0.05). **Figure 17B** is an immunoblot showing expression of GAPDH, emerin and lamin A/C in HeLa cells transfected with siRNA duplexes against *Gapdh*, *Emd* and *Lmna*. Antibody against actin was used as a loading control. **Figure 17C** shows expression of mRNA encoded by *Gapdh*, *Emd* and *Lmna* in C2C12 cells transfected with siRNA duplexes against *Gapdh*, *Emd* and *Lmna*, using real-time quantitative RT-PCR. Bars indicate fold overexpression of the indicated mRNA. Values are means ± standard deviations for n=3 samples (*p<0.05). **Figure 17D** is an immunoblot showing expression of GAPDH, emerin and lamin A/C in C2C12 cells transfected with

siRNA duplexes against *Gapdh*, *Emd* and *Lmna*. Antibody against actin was used as a loading control.

[0037] **Figure 18A** is a representative immunoblot showing expression of total ERK1/2 and phosphorylated ERK1/2 (pERK1/2) in HeLa cells transfected with siRNA duplexes against *Gapdh*, *Lmna* and *Emd*. **Figure 18B** shows expression of downstream genes in ERK pathway in HeLa cells transfected with siRNA duplexes against *Gapdh*, *Lmna* and *Emd*. Real-time RT-PCR results for *c-Jun*, *Elk1* and *Elk4* are shown. Bars indicate the fold overexpression of the indicated mRNA normalized to *Gapdh*. Values are means ± standard deviations for n=4 samples per group (*$p < 0.05$). **Figure 18C** is a representative immunoblot showing expression of total ERK1/2 and phosphorylated ERK1/2 (pERK1/2) in C2C12 cells transfected with siRNA duplexes against *Gapdh*, *Lmna* and *Emd*. **Figure 18D** shows expression of downstream genes in ERK pathway in C2C12 cells transfected with siRNA duplexes against *Gapdh*, *Lmna* and *Emd*. Real-time RT-PCR results for *c-Jun*, *Elk1* and *Elk4* are shown. Bars indicate the fold overexpression of the indicated mRNA normalized to *Gapdh*. Values are means ± standard deviations for n=4 samples per group (*$p < 0.05$).

[0038] **Figure 19A** shows the effect of siRNAs on nuclear translocation of pERK in transfected HeLa cells. Representative photomicrographs are shown for mock transfected cells, cells transfected with siRNA against *Gapdh* (siRNA *Gapdh*), *Emd* (siRNA *Emd*) and *Lmna* (siRNA *Lmna*). Arrowheads show enhanced nuclear localization of pERK in cells transfected with *Emd* and *Lmna* siRNAs. Bars: 10 μm. Bar graph shows percentages of HeLa cells with pERK primarily in the nucleus (see arrowheads for example). Values are means ± standard deviations for n=200 cells per group (*$p<0.05$). **Figure 19B** shows the effect of siRNAs on nuclear translocation of pERK in transfected C2C12 cells. Representative photomicrographs are shown for mock transfected cells, cells transfected with siRNA against *Gapdh* (siRNA *Gapdh*), *Emd* (siRNA *Emd*) and *Lmna* (siRNA *Lmna*). Arrowheads show enhanced nuclear localization of pERK in cells transfected with *Emd* and *Lmna* siRNAs. Bars: 10 μm. Bar graph shows percentages of C2C12 cells with pERK primarily in the nucleus (see arrowheads for example). Values are means ± standard deviations for n=150 cells per group (*$p<0.05$).

[0039] **Figure 20A** shows an immunoblot showing the effect of the MEK inhibitor PD98059 on the expression of total ERK1/2 and phosphorylated ERK1/2 in HeLa cells transfected with siRNAs against *Gapdh*, *Lmna* and *Emd*. **Figure 20B** (upper part) is an immunoblot showing effect of the MEK inhibitor PD98059 on the expression of total ERK1/2 and phosphorylated ERK1/2 in C2C12 cells transfected with siRNAs against *Gapdh*, *Lmna* and *Emd*. Lower part shows results of ELISA showing effect of the MEK inhibitor PD98059 on the expression of total ERK1/2 and phosphorylated ERK1/2 in C2C12 cells transfected with siRNAs against *Gapdh*, *Lmna* and *Emd*. Bar graph shows the relative phosphorylation of ERK1/2. Values are means ± standard deviations for n=3 samples per group (*p<0.05 when compared to mock treatment, #p<0.05 when compared C2C12 cells with or without addition of PD98059).

DETAILED DESCRIPTION OF THE INVENTION

MAP Kinase Signaling

[0040] Mitogen-activated protein (MAP) kinases are serine/threonine-specific protein kinases that respond to extracellular stimuli (mitogens). MAP kinases are successively acting phosphorylases that function as regulators of cell growth, differentiation and transformation and have been implicated in many physiological and pathological processes (22, 28, 29). MAP kinase signaling cascades have been evolutionarily well-conserved from yeast to mammals. There are several types of MAP kinases, including, but not limited to the "extracellular signal-regulated kinases" or "ERKS" (such as ERK1 and ERK2), and the "c-jun N-terminal kinases" or "JNKs" (such as MAPK8, MAPK9, and MAPK10). Activation of the ERK subfamily of MAPKs is generally mediated by receptor protein tyrosine kinases or G-protein-coupled receptors (41). The JNK subfamily of MAPKs are generally activated by factors such as osmotic stress (42) and physical stress (43).

[0041] Several downstream target genes are activated by MAPKs including, but not limited to, *Elk-1*, *Bcl-2*, *JunD, Elk-4* and *c-Jun*. Activation of these targets can in turn regulate expression of additional genes, including those encoding proteins involved in sarcomere structure, cardiomyofiber organization and other aspects of heart function (30, 31). Abnormal expression of these proteins can lead to cardiomyopathy (See Figure 9). Examples of proteins in the ERK signaling pathway are Raf-1 and MAPK/ERK kinases (MEK).

Examples of proteins in the JNK signaling pathway are c-Jun, JNK kinase 1, JNK kinase 2, and JNK Interacting Proteins.

[0042] MAP kinase signaling pathways, such as the JNK and ERK type signaling pathways, are well known to those of skill in the art. Such pathways are described in, for example, Maosong & Elion (151), Chang & Karin (152), Chen *et al.* (153), Pearson *et al.* (154), Davis *et al.* (155), Roux & Blenis (156), and the web site of Cell Signaling.com, the contents of each of which are hereby incorporated by reference.

Inhibitors

[0043] The present invention provides methods for the treatment and/or prevention of cardiomyopathies which comprise administration of one or more inhibitors. The inhibitors of the invention include inhibitors of kinases in the extracellular signal-regulated kinase or "ERK" signaling pathway(s), and inhibitors of kinases in the c-jun N-terminal kinase or "JNK" signaling pathway(s). Any suitable inhibitor of a kinase in the ERK and/or JNK pathways may be used. Such inhibitors may be, for example, small molecule drugs, peptide agents, peptidomimetic agents, antibodies, inhibitory RNA molecules and the like. One of skill in the art will understand that these and other types of agents may be used to inhibit kinases in the ERK and/or JNK pathways.

[0044] In one embodiment, an inhibitor of the invention is a small molecule inhibitor of a kinase in an ERK signaling pathway. Such inhibitors include, but are not limited to, chromone and flavone type inhibitors. Other suitable small molecule inhibitors or ERK pathway kinases include, but are not limited to, 2-(2-amino-3-methoxyphenyl)-4H-1-benzopyran-4-one (PD98059) (see reference 168), PD0325901 (Pfizer), AZD6244/ARRY-142886 (AstraZeneca/Array BioPharma), ARRY-438162 (Array BioPharma), PD198306, PD0325901 (reference 172), AZD8330 (reference 172), CI-1040, PD184161, Z-& E-a-(Amino-((4-aminophenyl)thio)methylene)-2-(trifluoromethyl)benzeneacetonitrile (SL327) (see references 157-163), 1,4-Diamino-2,3-dicyano-1,4-bis(2-aminophenylthio)butadiene (see reference 164-166), U0126 (see reference 167 and 168), GW 5074 (reference 168), BAY 43-9006 (reference 168), PD184352 (reference 168), Wyeth-Ayerst Compound 14 (reference 168), Ro 09-2210 (reference 168), L-783.277 (reference 168), FR180204 (reference 169), 3-(2-aminoethyl)-5-))4-ethoxyphenyl)methylene)-2,4-thiazolidinedione (PKI-ERK-005) (references 170, 171), CAY10561 (CAS 933786-58-4; Cayman Chemical), GSK1120212

(reference 172), RDEA119 (Ardea Biosciences; reference 172), XL518 (reference 172), and ARRY-704 (AstraZeneca).

[0045] In another embodiment, an inhibitor of the invention is a small molecule inhibitor of a kinase in a JNK signaling pathway. Such inhibitors include, but are not limited to, anthrapyrazolone type inhibitors. Other suitable small molecule inhibitors of JNK pathway kinases include, but are not limited to, anthra[1,9-cd]pyrazol-6(2H)-one (SP600125), CC-401 (Celgene), CEP-1347 (Cephalon), BI-78D3 (reference 173), and AS601245 (reference 175). U.S. Patent No. 7,199,124 to Ohkawa et al. also describes JNK inhibitors suitable for use in this invention.

[0046] In other embodiments, the inhibitors of the invention are peptide or peptidomimetic inhibtors of a kinase in the ERK or JNK signaling pathways. Such inhibitors include, but are not limited to a peptide corresponding to the amino-terminal 13 amino acids of MEK1 (MPKKKPTPIQLNP) (see reference 168) and the JNK inhibitor XG-102, TAT-coupled dextrogyre peptide (reference 174).

[0047] In yet other embodiments, the inhibitors of the invention are antibody inhibtors of a kinase in the ERK or JNK signaling pathways. Such inhibitors include, but are not limited to humanized antibodies, fully human antibodies, and antibody fragments that bind to and inhibit the function of a kinase in the ERK or JNK signaling pathways.

[0048] In yet other embodiments, the inhibitors of the invention are nucleotide-based inhibtors of a kinase in the ERK or JNK signaling pathways. Such inhibitors include, but are not limited to siRNAs, shRNAs, dsRNAs, microRNAs, antisense RNA molecules, and ribozymes, that inhibit the expression or activity of a kinase in the ERK or JNK signaling pathways. Such nucleotide-based inhibtors may comprise ribonucleotides, deoxyribonucleotides, or various artificial nucleotide derivatives.

[0049] One of skill in the art will understand that other agents may be useful as inhibitors of kinases in the ERK and/or JNK signaling pathways and may be used in conjunction with the methods of the invention.

Administration

[0050] The inhibitors of the invention may be formulated into compositions for administration to subjects for the treatment and/or prevention of cardiomyopathies. Such

compositions may comprise the inhibitors of the invention in admixture with one or more pharmaceutically acceptable diluents and/or carriers and optionally one or more other pharmarceutically acceptable additives. The pharmaceutically-acceptable diluents and/or carriers and any other additives must be "acceptable" in the sense of being compatible with the other ingredients of the composition and not deleterious to the subject to whom the composition will be administered. One of skill in the art can readily formulate the inhibitors of the invention into compositions suitable for administration to subjects, such as human subjects, for example using the teaching a standard text such as Remington's Pharmaceutical Sciences, 18th ed, (Mack Publishing Company: Easton, Pa., 1990), pp. 1635-36), and by taking into account the selected route of delivery.

[0051] Examples of diluents and/or carriers and/or other additives that may be used include, but are not limited to, water, glycols, oils, alcohols, aqueous solvents, organic solvents, DMSO, saline solutions, physiological buffer solutions, peptide carriers, starches, sugars, preservatives, antioxidants, coloring agents, pH buffering agents, granulating agents, lubricants, binders, disintegrating agents, emulsifiers, binders, excipients, extenders, glidants, solubilizers, stabilizers, surface active agents, suspending agents, tonicity agents, viscosity-altering agents, carboxymethyl cellulose, crystalline cellulose, glycerin, gum arabic, lactose, magnesium stearate, methyl cellulose, powders, saline, sodium alginate. The combination of diluents and/or carriers and/or other additives used can be varied taking into account the nature of the active agents used (for example the solubility and stability of the active agents), the route of delivery (e.g. oral, parenteral, etc.), whether the agents are to be delivered over an extended period (such as from a controlled-release capsule), whether the agents are to be co-administered with other agents, and various other factors. One of skill in the art will readily be able to formulate the compounds for the desired use without undue experimentation.

[0052] The inhibitors of the invention may be administered to a subject in an amount effective to treat or prevent a cardiomyopathy. One of skill in the art can readily determine what would be an effective amount of the inhibitors of the invention to be administered to a subject, taking into account whether the inhibitor is being used prophylactically or therapeutically, and taking into account other factors such as the age, weight and sex of the subject, any other drugs that the subject may be taking, any allergies or contraindications that the subject may have, and the like. For example, an effective amount can be determined by the skilled artisan using known procedures, including analysis of titration curves established

in vitro or in vivo. Also, one of skill in the art can determine the effective dose from performing pilot experiments in suitable animal model species and scaling the doses up or down depending on the subjects weight etc. Effective amounts can also be determined by performing clinical trials in individuals of the same species as the subject, for example starting at a low dose and gradually increasing the dose and monitoring the effects on cardiopmyopathy. Appropriate dosing regimens can also be determined by one of skill in the art without undue experimentation, in order to determine, for example, whether to administer the agent in one single dose or in multiple doses, and in the case of multiple doses, to determine an effective interval between doses.

[0053] The inhibitors of the invention may be administered to a subject by any suitable method that allows the agent to exert its effect on the subject *in vivo*. For example, the compositions may be administered to the subject by known procedures including, but not limitated to, by oral administration, sublingual or buccal administration, parenteral administration, transdermal administration, via inhalation, via nasal delivery, vaginally, rectally, and intramuscularly. The compounds of the invention may be administered parenterally, or by epifascial, intracapsular, intracutaneous, subcutaneous, intradermal, intrathecal, intramuscular, intraperitoneal, intrasternal, intravascular, intravenous, parenchymatous, or sublingual delivery. Delivery may be by injection, infusion, catheter delivery, or some other means, such as by tablet or spray. In one embodiment, the inhibitors of the invention are adiminstered to the subject by way of delivery directly to the heart tissue, such as by way of a catheter inserted into, or in the proximity of the subject's heart, or by using delivery vehicles capable of targeting the drug to the heart. For example, the inhibitors of the invention may be conjugated to or administered in conjunction with an agent that is targeted to the heart, such as an antibody or antibody fragment.

[0054] For oral administration, a formulation of the inhibitors of the invention may be presented as capsules, tablets, powders, granules, or as a suspension or solution. The formulation may contain conventional additives, such as lactose, mannitol, cornstarch or potato starch, binders, crystalline cellulose, cellulose derivatives, acacia, cornstarch, gelatins, disintegrators, potato starch, sodium carboxymethylcellulose, dibasic calcium phosphate, anhydrous or sodium starch glycolate, lubricants, and/or or magnesium stearate.

[0055] For parenteral administration (*i.e.*, administration by through a route other than the alimentary canal), the inhibitors of the invention may be combined with a sterile aqueous solution that is isotonic with the blood of the subject. Such a formulation may be prepared by dissolving the active ingredient in water containing physiologically-compatible substances, such as sodium chloride, glycine and the like, and having a buffered pH compatible with physiological conditions, so as to produce an aqueous solution, then rendering the solution sterile. The formulation may be presented in unit or multi-dose containers, such as sealed ampoules or vials. The formulation may be delivered by injection, infusion, or other means known in the art.

[0056] For transdermal administration, the inhibitors of the invention may be combined with skin penetration enhancers, such as propylene glycol, polyethylene glycol, isopropanol, ethanol, oleic acid, *N*-methylpyrrolidone and the like, which increase the permeability of the skin to the compounds of the invention and permit the compounds to penetrate through the skin and into the bloodstream. The inhibitors of the invention also may be further combined with a polymeric substance, such as ethylcellulose, hydroxypropyl cellulose, ethylene/vinylacetate, polyvinyl pyrrolidone, and the like, to provide the composition in gel form, which are dissolved in a solvent, such as methylene chloride, evaporated to the desired viscosity and then applied to backing material to provide a patch.

[0057] In some embodiments, the inhibitors of the invention are provided in unit dose form such as a tablet, capsule or single-dose injection or infusion vial.

[0058] In certain embodiments, the inhibitors of the invention may be used in combination with other agents useful for the treatment of cardiomyopathies. For example, in one embodiment, the inhibitors of the invention may be delivered to a subject as part of a composition containing one or more additional active agents. In another embdodiment, the inhibitors of the invention may be delivered to a subject in a composition or formulation containing only that active agent, while one or more other agents useful for the treatment of a cardiomyopathy may be also be administered to the subject in one or more separate compositions or formulations.

[0059] The inhibitors of the invention and the other agents useful for the treatment of cardiomyopathies may be administered to the subject at the same time, or at different times. For example, the inhibitors of the invention and the other agents may be administered within

minutes, hours, days, weeks, or months of each other, for example as part of the overall treatment regimen of a subject. The inhibitors of the invention may also be used in combination with surgical or other interventional treatment regimens used for the treatment of cardiomyopathies.

Mouse Model of Cardiomyopathy

[0060] The present invention is a method of treating or preventing a MAPK-associated cardiomyopathy. A "MAPK-associated cardiomyopathy" is a cardiomyopathy that is characterized by activation of the MAPK signaling pathway in heart tissue. Cardiomyopathies can also be associated with activation of one or more members of the ERK signaling pathway. Cardiomyopathies can additionally be associated with activation of one or more members of the JNK signaling pathway.

[0061] The cardiomyopathy can be inherited, as in EDMD, or acquired. A cardiomyopathy that results from activation of MAPK signaling, particularly from activation of ERK signaling and/or activation of JNK signaling, can be treated or prevented by administration of an inhibitor of the ERK or JNK signaling pathways, regardless of whether the cardiomyopathy is inherited or acquired. The methods of the present invention are useful in the treatment of various types of cardiomyopathies, including dilated cardiomyopathy and hypertrophic cardiomyopathy.

[0062] It has not been known how certain mutations in LMNA encoding A-type lamins cause striated muscle disease. Therefore, it has been impossible to develop targeted treatments. To obtain information on the pathogenic abnormalities in cardiac tissue that may cause cardiomyopathy in autosomal dominant EDMD, we carried out a genome-wide RNA expression analysis in hearts from LmnaH222P/+ and LmnaH222P/H222P "knock in" mice, which serve as a model for the human disease. A detailed description of these mice has been published previously (14). In brief, male LmnaH222P/H222P mice develop cardiac chamber dilation, decreased left ventricle fractional shortening and hypokinesis detectable by echocardiography starting at 8 weeks of age. At 12 weeks of age, abnormalities of the conduction system become pronounced and are characterized primarily by an increased PR interval on electrocardiograms. Histological analysis shows pronounced left ventricular fibrosis and fiber degeneration by 16 weeks of age along with obvious atrial dilation. The male mice die between 4 and 9 months of age. In female mice, disease develops more slowly.

Both male and female mice also develop problems with locomotion secondary to skeletal muscle myopathy.

[0063] We have selected to study cardiac tissue and function rather than skeletal muscle, the most significant reason being that cardiomyopathy is the life-threatening problem in human patients with EDMD. Furthermore, cardiac tissue is homogenous and therefore easier to study biochemically than skeletal muscle, with is regionally and variably affected in EDMD as well as mouse models of the disease. Cardiac function is also easier to assess in LmnaH222P/H222P mice than skeletal muscle function. For example, left ventricular contraction can be readily measured by echocardiography and, as cardiac dysfunction is the cause of early death in these mice, survival can be easily assessed.

Linkage of LMNA Mutations to EDMD

[0064] Cellular mechanisms linking mutations in *LMNA* to cardiomyopathy are unknown. While several investigators have hypothesized that *LMNA* mutations lead to alterations in gene expression that could have tissue-selective pathogenic consequences (7), altered expression of functional groups of genes or activation of signal transduction pathways that can explain the development of disease have not been demonstrated in affected tissues. We addressed this issue by using genome-wide profiling in hearts from a mouse model of autosomal dominant EDMD. Our analysis lead us to focus on MAPK signaling because in a genome-wide expression analysis several genes related to this pathway had significantly altered expression in hearts of mice with the *Lmna* H222P mutation prior to development of significant cardiomyopathy.

[0065] In hearts of $Lmna^{H222P/H222P}$ mice, we found significantly increased expression of transcripts encoding several downstream components of MAPK cascades, such as *c-Jun* and *Elk-1*, only by using real-time PCR. Increased expression of these transcripts, which was approximately 2-fold, was not detected in our microarray analysis. Similar discrepancies between microarrays and real-time PCR have been reported (26, 27), especially when the absolute expression levels are low or when the differences between experimental and control are relatively small, which was the case for the transcripts we measured. In addition to increased expression of transcripts encoding several components, activation of MAPK cascades in hearts of *Lmna* H222P mice was also strongly supported by increased levels of

selected encoded proteins, increases in nuclear pERK1/2 and activation of ERK1/2 and JNK in cells transfected with constructs encoding Lamin A with aa substitutions causing EDMD.

[0066] MAPK activation occurred prior to significant cardiomyopathy in *Lmna*$^{H222P/H222P}$ mice and also in *Lmna*$^{H222P/+}$ mice, which do not develop clinical heart disease until 2 years of age. This is consistent with activation of MAPK signaling underlying development of disease rather than occurring as a consequence. The temporal differences to develop cardiomyopathy between heterozygous and homozygous mice may be a result of "dosage", as JNK activation and increased expression of its downstream targets bcl-2, and phosphorylated c-Jun, appeared to be more significant in hearts from *Lmna*$^{H222P/H222P}$ mice compared to hearts from *Lmna*$^{H222P/+}$ mice. Several genes were also activated or repressed in heterozygous mice compared to homozygous mice; however, how this is related to development of disease remains to be investigated.

[0067] Results from previous studies have implicated activation of MAPKs in development of cardiomyopathy. Petrich et al. (19, 20) generated transgenic mice expressing an activated mutant of MKK7, a kinase activating JNK, specifically in heart. These mice developed dilated cardiomyopathy. Similar results have been observed in transgenic mice overexpressing mutants of MKK3 and MKK6, kinases that also activate MAPKs (32). Nicol et al. (33) generated transgenic mice over expressing MEK5, which activates ERK, in hearts and these mice developed dilated cardiomyopathy. JNK is also activated in dilated human hearts (34, 35). Recently, Rodriguez-Viciana et al. demonstrated that mutations in *MEK1* and *MEK2*, which encode kinases that activate ERK1 and ERK2, cause cardio-facial-cutaneous syndrome in humans (36). The MEK mutants were more active than wild type in phosphorylating ERK. Transgenic mice expressing activated MEK1 similarly have enhanced ERK1/2 signaling and develop cardiomyopathy (37). Activation of the ERK cascade has also been reported in caveolin-3 (38), caveolin-1 (39) and p85 subunit of class I(A) PI3K (40) knockout mice, all of which develop cardiomyopathy at 2 months of age.

[0068] While it remains unclear how A-type lamins with aa substitutions activate MAPKs, our results show that they do so when expressed in transfected cells. Activation of the ERK subfamily of MAPKs is mediated by receptor protein tyrosine kinases or G-protein-coupled receptors (41). JNK subfamily of MAPK is activated by osmotic stress (42) and physical stress (43). It is possible that abnormalities in the nuclear lamina lead to activation of G-

protein coupled or other receptors via an unknown mechanism (Figure 9). Several investigators have hypothesized that alterations in response to stress may underlie the development of striated muscle diseases caused by *LMNA* mutations (7). Abnormal responses to stress in cells with abnormalities in A-type lamins could therefore potentially impact on activation of JNK (Figure 9). Fibroblasts from mice lacking A-type lamins have increased nuclear deformation and impaired viability under mechanical strain as well as attenuated NF- κB-regulated transcription in response to stress (14). In addition, we observed that expression of H222P lamin A in transfected cells lead to enhanced nuclear translocation of activated ERK and JNK. Smith et al. (44) have demonstrated that suppression of cell proliferation after retinoic acid–induced endoderm differentiation of embryonic stem and carcinoma cells is achieved by restricting nuclear entry of activated MAPK and an intact cytoskeleton is required for the restraint. Hence, interactions between the nuclear lamina and cytoskeletal components could potentially influence nuclear translocation of activated MAPKs, with abnormalities in the lamina enhancing their nuclear localization. Recently, Ivorra et al. (45) highlighted a direct interaction between A-type lamins and the transcription factor c-fos. This raises the possibility that A-type lamins may bind to component of MAPK cascades and that the H222P aa substitution may alter such an interaction.

[0069] Our results provide a foundation upon which pharmacological interventions for treatment or prevention of cardiomyopathy in EDMD can be based. If mutant A-type lamins activate JNK and ERK, which in turn lead to gene expression alterations responsible for the development of cardiomyopathy, MAPK inhibitors could potentially be used to treat or prevent disease. MAPK inhibitors have been studied as potential therapeutic agents for a wide range of diseases. JNK inhibitors have been shown to be beneficial in reducing myocardial ischemic injury (59), stroke (60), hearing impairment (61) and various neurodegenerative disorders (62). The availability of MAPK inhibitors with *in vivo* activities makes "clinical trials" to prevent or treat cardiomyopathy in $Lmna^{H222P/H222P}$ mice possible. In addition, knock-out mouse models of ERK1/2 and JNK have been generated (63). Crossing those mice with $Lmna^{H222P/H222P}$ mice could also establish if abolishing function of MAPKs can rescue cardiomyopathy.

[0070] Analysis of genome-wide expression changes in hearts from *Lmna* H222P mice revealed significant alterations in expression of genes involved in inflammation and fibrosis

prior to detectable abnormalities in hearts examined using conventional histological methods. Ultimately, fibrosis with minimal inflammation occurs in hearts from *Lmna*$^{H222P/H222P}$ mice (14) as well as *Lmna*$^{N195K/N195K}$ mice, another model of EDMD (64). This suggests that in addition to treatment with MAPK inhibitors, early treatment with anti-inflammatory or anti-fibrotic agents may benefit human subjects with EDMD.

Prevention and Treatment of MAPK-Associated Cardiomyopathies

[0071] "Treating" cardiomyopathy includes the improvement of cardiac function in a patient with cardiomyopathy, as measured by (1) an increase in ejection fraction (EF), and/or (2) an increase in fractional shortening (FS), and/or (3) a decrease in left ventricular end systolic diameter (LVESD), and/or (4) a decrease in left ventricular end diastolic diameter (LVEDD). "Treating" cardiomyopathy additionally includes the prevention of further deterioration of cardiac function, as measured by the above parameters.

[0072] "Preventing" cardiomyopathy includes arresting the onset of physiological and/or molecular indications of cardiomyopathy. Physiological indicators of cardiomyopathy include: (1) decreased ejection fraction (EF), and/or (2) decreased fractional shortening (FS), and/or (3) increased left ventricular end systolic diameter (LVESD), and/or (4) increased left ventricular end diastolic diameter (LVEDD). Molecular indicators of cardiomyopathy include increased expression of certain markers, including, but not limited to: sarcomere structure proteins (including β-myosin heavy chain and myosin light chain 2), atrial natriuretic factor, brain natriuretic factor, phosphorylated JNK, phosphorylated ERK1/2, Bcl-2, Elk-1, phosphorylated c-Jun, *JunD*, *Vegf*, *Myl7*, *Sln*, and *Elk 4*.

[0073] Our work demonstrates that ERK and JNK inhibitors improve the cardiac phenotype in a mouse model of EDMD. Our work showed that the cardiac function was in part or totally recovered, following 8 weeks treatment using PD98059 and/or SP600125 or U0126 or MEK1/2. In Example 2, we administered the inhibitors before the appearance of cardiac symptoms in *Lmna*$^{H222P/H222P}$ mice. In Example 3, we show that the inhibitors can also be administered when the cardiomyopathy is evident in *Lmna*$^{H222P/H222P}$ mice (after 12 weeks), to demonstrate that the inhibitors can also reverse the existing cardiac phenotype.

[0074] PD98059 shows high specificity for MEK over other serine/threonine kinases (83, 136). However, it also has activity against cyclooxygenase-1 and cyclooxygenase-2 (137). It is therefore possible that the beneficial effects of PD98059 in *Lmna*$^{H222P/H222P}$ mice could in

part be due to cyclooxygenase inhibition. We do not however consider cyclooxygenase inhibition to be a major mechanism of action given the widespread use of non-steroidal anti-inflammatory drugs in clinical practice and absence of data showing any utility in preventing heart failure. In fact, retrospective populations cohort studies suggest that use of both cyclooxygenase-2 inhibitors and non-selective cyclooxygenase inhibitors are associated with exacerbation of heart failure in humans (138, 139). Nonetheless, future controlled experimental testing of cyclooxygenase inhibition in *Lmna*$^{H222P/H222P}$ mice would be useful in determining if it also has any beneficial effect in delaying or preventing cardiomyopathy.

[0075] Similar to *Lmna*$^{H222P/H222P}$ mice, we have shown abnormal activation of ERK signaling in hearts of *Emd*$^{-/y}$ mice lacking the integral inner nuclear membrane protein emerin that binds to A-type lamins (69). In humans, *EMD* mutations resulting in lack of or reduced emerin in the nuclear envelope cause X-linked Emery-Dreifuss muscular dystrophy (2, 4, 140). Like the autosomally inherited form of the disease caused by *LMNA* mutations, dilated cardiomyopathy is a major feature of X-linked Emery-Dreifuss muscular dystrophy. Therefore, the present results in *Lmna*$^{H222P/H222P}$ mice are likely to be relevant to cardiomyopathy caused by emerin deficiency. However, because the clinical phenotype of first-degree heart block in *Emd*$^{-/y}$ mice greater than 40 weeks of age is very subtle and not readily measurable without intensive electrophysiologically monitoring (106, 107), we have deferred a trial of an ERK inhibitor in this animal model.

[0076] Our results provide initial proof of principle for ERK and/or JNK inhibition as a therapeutic option to prevent or delay the onset of heart failure in cardiomyopathy caused by *LMNA* mutation. The only other demonstration of improving an abnormal phenotype caused by mutations in the gene encoding A-type lamins in mammals is the use of a protein farnesyltransferase inhibitor to block prenylation of truncated prelamin A in mice carrying a mutation that causes Hutchinson-Gilford progeria syndrome (141, 142). In the present invention, treatment with a MEK inhibitor at an age when *Lmna*$^{H222P/H222P}$ mice first begin to develop cardiac abnormalities maintained LV function at normal levels while untreated mice had approximately a 30% reduction in ejection fraction over a time period of 8 weeks. (See Example 2.)

[0077] In humans, the progression of cardiomyopathy caused by *LMNA* mutations in often rapid compared to other primary cardiomyopathies (129). Therefore, pharmacological

interventions to slow progression should be clinically beneficial. Further preclinical investigation, including for example an analysis of effects on different tissues, skeletal myopathy and overall activity, will determine the safety and efficacy of ERK or JNK inhibition as a therapeutic intervention for dilated cardiomyopathy. It is worth noting that oral MEK inhibitors have already been safely administered to humans (99, 143). In sum, for treatment of cardiomyopathy, for example in EDMD patients, it appears important to identify a MAPK inhibitor that inhibits specifically the ERK branch or the JNK branch, which inhibitor is tolerated over the long-term.

Activation of ERK Signaling by Reduced Expression of A-type Lamins and Emerin

[0078] Our studies have shown that abnormalities in A-type lamins and emerin activated MAP kinases in the hearts of mouse models of X-linked and autosomal EDMD [69, 89]. We have analyzed affected and unaffected tissues in *Lmna*$^{H222P/H222P}$ mice and found abnormal activation of genes downstream of ERK only in cardiac and to a more limited extent skeletal muscle [89]. We have similarly demonstrated abnormal activation of ERK and downstream genes in hearts of emerin-deficient mice [69]. Although the exact mechanism of activation remains unclear, these findings provide the basis for pharmacological therapies that can prevent or improve cardiac function in cardiomyopathies, such as those associated with EDMD. In the present invention, we describe activation of ERK in a third mouse model of EDMD and established a cellular model of activation of induced by siRNA-mediated knockdown of emerin and A-type lamins. (See Example 4.) We show that loss of A-type lamins in mouse heart and partial loss of A-type lamins and emerin in cultured cells leads to activation.

[0079] Loss of emerin leads to EDMD in humans [2, 4] but it induces only a first-degree heart block in *Emd*$^{y/-}$ mice [106, 107]. Haploinsufficiency and point mutations in *LMNA* lead to EDMD in humans [5] and *Lmna*$^{-/-}$ mice have severe abnormalities of both skeletal and cardiac muscles [101]. We show in the present invention that ERK is activated in hearts from *Lmna*$^{-/-}$ mice compared to control mice. However, this appears to be a less pronounced activation than in hearts from *Emd*$^{-/y}$ and *Lmna*$^{H222P/H222P}$ mice [69, 89]. The cardiac phenotype in these three mouse models of EDMD is different. The *Emd*$^{-/y}$ mice we analyzed have only minimal cardiac dysfunction characterized by first-degree heart block and vacuolization of cardiomyocytes and have normal life spans [106]. *Lmna*$^{H222P/H222P}$ mice develop cardiac chamber dilation associated with decreased left ventricle fractional

shortening starting at about 8 weeks of age and subsequently develop more severe conduction system abnormalities and dilated cardiomyopathy, dying at an average age of 36 weeks [14]. *Lmna*$^{-/-}$ mice develop cardiac disease at 4 weeks of age with atrophic and degenerated myocytes and die at an average age of 8 weeks [101, 108]. We hypothesized a relationship between the degree of MAP kinase cascade activation and the severity of the heart disease [69]. Our present results suggest that this might not be the case. ERK activation in the heart is related to the development of cardiac dysfunction but other factors or signaling pathways could determine its progression or severity. This could explain why *Emd*$^{-/y}$ mice have an apparently greater activation of ERK than *Lmna*$^{-/-}$ mice. We have reported that other signaling cascades may be altered in hearts from *Emd*$^{-/y}$ and male *Lmna*$^{H222P/H222P}$ mice [69]. Among them are Wnt signaling pathway, I-κB /NF-κB cascade and Tgf-β receptor signaling pathway. These pathways may not be viewed as unique cascades, as crosstalks between Wnt, Tgf- β and MAP kinase pathways occur [109-112]. Hence, other signaling pathways could interact with ERK activation in the development of cardiac disease in X-linked and autosomal EDMD.

[0080] We detected ERK activation in hearts of *Lmna*$^{-/-}$ mice at 5 weeks of age, which mice develop cardiomyopathy at 4 weeks of age [108]. A recent publication by Wolf et al. [113] described cardiac abnormalities in *Lmna*$^{+/-}$ mice. These heterozygous null mice develop cardiac conduction defects at 10 weeks of age and dilated cardiomyopathy at approximately 50 weeks of age. The authors apparently did not observe an abnormal activation of MAP kinases and downstream targets in hearts from *Lmna*$^{+/-}$ mice at 20 weeks [113]. They concluded that lamin haploinsufficiency does not cause activation of the ERK or JNK branches of the MAP kinase pathway. These results are not incompatible with those in our current or previous [69, 89] studies. Firstly, *Lmna*$^{+/-}$ mice at 20 weeks do not have left ventricular dilation and do not develop it for another 30 weeks. It is therefore possible that ERK activation occurs sometime between 20 and 50 weeks of age prior to the onset of cardiomyopathy, as in *Lmna* H222P mice [89]. Secondly, Wolf et al. [113] showed an unchanged expression of ERK1/2 and JNK1 but did not clearly report data on levels of the phosphorylated (activated) forms of the proteins. It is therefore possible that their methods missed to detect activation of ERK and JNK. Finally, Wolf et al. [113] examined MAP kinase activities only in two wild type mice, giving their reported negative result low, if any, statistical power. Differences and similarities in MAP kinase activities in hearts from various

mouse models of EDMD and cultured cells with similar genetic alterations remain to be further examined.

[0081] We have demonstrated that activation of MAP kinase pathway is related to abnormalities in nuclear envelope in transfected cultured cells expressing lamin A variants found in subjects with EDMD [89]. While most of the human *LMNA* mutations causing EDMD are missense, some patients carry nonsense mutations leading to haploinsufficiency [5] . Mutations in *EMD* on the other hand lead in most cases to a loss of emerin [2, 4]. Here we show an aberrant increase of ERK activation and downstream transcription factors in siRNA-treated HeLa and C2C12 cells with decreased emerin and A-type lamin expression. These results reproducibly show that altering the expression of A-type lamins and emerin activates MAP kinases [69. 89]. The MAP kinase cascade is a signal transduction pathway that transmits signals from extracellular stimuli such as growth factors and hormones [114] and from intracellular stimuli such as redox state [115]. In the cardiac cells, MAP kinases are stimulated by G-protein-coupled receptors (endothelin-1, α-adrenoreceptor agonists, angiotensin II), as well as mechanical stretch (structural stress and electrical pacing), H_2O_2 and osmotic shock [116]. Recent studies have identified a physical link between the nuclear envelope and the cytoplasm; the LINC complex [117]. The LINC complex provides a potential mechanical network from the cell surface to the nucleus. Reduced expression of A-type lamins and emerin could weaken the LINC complex and make cells more susceptible to mechanical stress, in turn more readily leading to MAP kinase activation. However, the mechanisms that activate MAP kinases in cells with abnormalities in A-type lamins and emerin remain to be determined experimentally.

[0082] Our results have practical implications because small molecule drugs can be used to inhibit ERK [118]. Several ERK and JNK inhibitors, including PD98059 and SP600125 are commercially available, potent and selective inhibitors. PD98059 mediates its inhibitory properties by binding to MEK, therefore preventing phosphorylation of ERK. We show that PD98059 reduces ERK1/2 activity in HeLa and C2C12 cells with reduced A-type lamins and emerin. This opens the road for other similar studies on cultured cells committed to striated muscle lineages such as differentiated myotubes, mouse muscle satellite cells, mouse cardiac muscle cells and primary cardiomyocytes. Such studies could determine if activation of ERK due to reduced expression of A-type lamins and emerin is related to changes in the expression of downstream genes in muscle development or function *in vitro*. Furthermore, our results

provide the basis for a "clinical trial" of an ERK inhibitor in a mouse model of cardiomyopathy.

EXAMPLES

[0083] The following examples are meant to illustrate the methods and materials of the present invention and are not intended to limit the invention in any way.

Example 1: Activation of MAPK Pathways Links LMNA Mutations to Cardiomyopathy in Emery-Dreifuss Muscular Dystrophy

Methods

Mice

[0084] *Lmna* H222P knock-in mice were generated and genotyped as described (14). Hearts were isolated from male $Lmna^{H222P/H222P}$, $Lmna^{H222P/+}$ and $Lmna^{+/+}$ mice at 4, 7 or 10 weeks of age. For all immunoblotting and real-time PCR experiments, $Lmna^{H222P/H222P}$ and $Lmna^{H222P/+}$ mice were compared directly to $Lmna^{+/+}$ littermates. For microarray analysis, mice were combined from 5 different litters of crosses between $Lmna^{H222P/+}$ mice; control $Lmna^{+/+}$ mice were included from each of the litters from which $Lmna^{H222P/H222P}$ and $Lmna^{H222P/+}$ were used.

RNAi Isolation

[0085] Total RNA was extracted using the Rneasy isolation kit (Qiagen) according to the manufacturer's instructions. Adequacy and integrity of extracted RNA were determined by gel electrophoresis and concentrations measured by ultraviolet absorbance spectroscopy.

Microarray Processing

[0086] We used Mouse Genome 430 2.0 GeneChip Arrays (Affymetrix), which contain 45,101 probes sets corresponding to known genes and expressed sequence tags. Complimentary DNA synthesis, cRNA synthesis and labeling were performed as described in the Affymetrix GeneChip Technical Manual. Hybridization, washing, staining and scanning of arrays were performed at the Gene Chip Core Facility of the Columbia University Genome Center.

Microarray Data Analysis

[0087] Image files were obtained through Affymetrix GeneChip software and analyzed by robust multichip analysis using Affymetrix microarray ".cel" image file and GeneTraffic

(Iobion Informatics) software. Robust multichip analysis is composed of three steps: background correction, quantile normalization and robust probe set summary. Genes were identified as differentially expressed if they met a false discovery rate threshold of 0.05 in a two-sample t-test (*q*-value) and showed at least a two-fold difference in expression independent of absolute signal intensity. We have made the gene expression data available in the National Center for Biotechnology Information's Gene Expression Omnibus (GEO, http://www.ncbi.nlm.nih.gov/geo/), accessible through GEO Series accession number GSE6397 and GSE6398.

Analysis of Functional Groups of Genes

[0088] Gene expression changes related to functional groups were analyzed using the Class Score method in ermineJ to provide a statistical confidence to functional groupings (65). The algorithm takes as input the log-transformed t-test *p*-values of genes that are members of a single Gene Ontology class and estimates the probability that the set of *q*-values would occur by chance. Significant Gene Ontology terms were identified using a false discovery rate of 0.05. For automated functional annotation and classification of genes of interest based on GO terms we used the Database for Annotation, Visualization and Integrated Discovery (DAVID) (http://david.abcc.ncifcrf.gov/) (66).

Real-Time PCR Analysis

[0089] We synthesized cDNA using Omniscript Reverse Transcriptase (Qiagen) on total cellular RNA. For each replicate in each experiment, RNA from tissue samples of different animals was used. Primers were designed correspond to mouse RNA sequences using Primer3 (http://frodo.wi.mit.edu/cgi-bin/primer3/primer3_www.cgi). The Real-time PCR reaction contained iQ SYBR green super mix (Bio-Rad), 200 nM of each primer and 0.2 μl of template in a 25-μl reaction volume. Amplification was carried out using the MyiQ Single-Color Real-Time PCR Detection System (Bio-Rad) with an initial denaturation at 95°C for 2 min followed by 50 cycles at 95°C for 30 s and 62°C for 30 s. Relative levels of mRNA expression were calculated according to the $\Delta\Delta C_T$ method (67). Individual expression values were normalized by comparison with *Gapdh* mRNA.

Extraction of Proteins from Hearts and Immunoblotting

[0090] Hearts were excised from mice and snap-frozen in liquid nitrogen-cooled isopentane. To obtain protein extracts, both ventricles were homogenized in extraction buffer

(25 mM Tris [pH 7.4], 150 mM NaCl, 5 mM EDTA, 10 mM sodium pyrophosphate, 1 mM Na_3VO_4, 1% SDS, 1 mM dithiothreitol) containing protease inhibitors (25 mg/ml aprotinin and 10 mg/ml leupeptin). Protein samples were subjected to SDS-PAGE, transferred to nitrocellulose membranes and blotted with primary Abs against elk-1 (Santa-Cruz), ERK1/2 (Santa-Cruz), pERK1/2 (Cell Signaling), JNK1 (Santa-Cruz), pJNK (Cell Signaling), bcl-2 (Santa-Cruz), pc-Jun (Santa-Cruz), β-MHC (Santa-Cruz), MLC-2 (Santa-Cruz), ANF (Santa-Cruz), β- actin (Santa-Cruz) and β-tubulin (Santa-Cruz). Secondary Abs were HRP–conjugated (Amersham). Recognized proteins were visualized by enhanced chemiluminescence (ECL- Amersham). Antibodies against β-tubulin and β-actin were used as internal controls to normalize the amounts of protein between immunoblots. Band densities were calculated using Scion Image software (Scion Corporation) and normalized to the appropriate total extract to control for protein loading. Data are reported as means ± standard deviations and are compared with respective controls using a two-tailed *t* test.

Immunohistochemistry

[0091] Immunofluorescence staining for pERK1/2 was performed on Frozen sections (8 μm) of transversal cardiac muscles by fixing them in 3.7% formaldehyde in PBS for 15 minutes, then blocked in 5% fetal goat serum in PBS/triton for 1 hour. Cells were incubated in blocking solution with anti-pERK1/2 monoclonal antibody (Cell Signaling) overnight at 4°C followed by PBS washing and incubation with Texas red–conjugated goat anti-mouse IgG secondary antibody (Invitrogen) and counterstained with 0.1 μg/ml DAPI (Sigma-Aldrich). Intensity of pERK1/2 in cardiocytes was measured using Scion Image software (Scion Corporation). Data are reported as means ± standard deviations and are compared with respective controls using a two-tailed *t* test.

Primary Culture and Isolation of Ventricular Myocytes

[0092] *Lmna*$^{+/+}$ and *Lmna*$^{H222P/H222P}$ knock-in mice (10 weeks of age) were anesthetized with pentofurane. Ventricular cardiomyocytes were isolated as described in the Alliance for Cellular Signaling procedure protocol PP00000125 (http://www.signaling-gateway.org). For immunoblotting, cells were washed in ice cold PBS and lysed in extraction buffer. Lysates were centrifuged at 16,000×g and the supernatants collected. Immunoblotting was performed as described above.

Plasmid Construction

[0093] To generate constructs to express lamins in transfected cells, cDNAs encoding wild type lamin A and lamin A with H222P, N195K, R298C, R482W, N456I and T528K aa substitutions were cloned in pegfp-C1 plasmid (Clontech) between XhoI and BamHI restriction endonuclease sites.

Cell Culture and Transfection to Examiner MAPK Activation and Localization

[0094] Cos-7 and C2C12 cells were maintained in Dulbecco's modified Eagle's medium supplemented with 10% fetal calf serum and 0.5% gentamycin at 37°C in a humidified atmosphere of 95% air and 5% CO_2. Cells were transfected with plasmids encoding GFP-wild type lamin A and GFP-H222P lamin A using Lipofectamine 2000 according to the manufacturer's instructions (Invitrogen). Cells were analyzed 48 hours after transfection. Cells were either fixed for 10 min in methanol at -20°C or lysed in extraction buffer for subsequent immunoblotting.

Immunofluorescence Microscopy

[0095] For immunofluorescence staining, fixed cells were incubated with rabbit Abs that recognize pERK1/2 (Cell Signaling) or pJNK (Cell Signaling). Cells were then washed and incubated with Texas Red conjugated goat anti-rabbit secondary Abs (Molecular Probes). For immunohistochemistry, frozen sections (8 μm) of transversal cardiac muscles were fixed in 3.7% formaldehyde in PBS for 15 minutes and then blocked in 5% fetal goat serum in PBS/Triton X-100 for 1 hour. Abs used for immunohistochemistry were primary rabbit anti-pERK1/2 (Cell Signaling) and secondary Texas Red conjugated goat anti-rabbit (Molecular Probes). Sections were counterstained with 0.1 μg/ml DAPI (Sigma-Aldrich). Immunofluorescence microscopy was performed on a Microphot SA (Nikon) microscope attached to a Spot RT Slide camera (Diagnostic Instruments). Images were processed using Adobe Photoshop 6.0 (Adobe Systems). Fluorescence intensity in cardiocytes was measured using Scion Image software (Scion Corporation). Data are reported as means ± standard deviations and are compared with respective controls using a two-tailed *t* test.

Luciferase Reporter Gene Assays

[0096] Luciferase reporter assays for *c-Jun* and *Elk-1* activation were carried out using Path Detect In Vivo Signal Transduction Pathway Trans-Reporting System (Stratagene). Cos-7 cells were plated in 12 well plates. The following day, cells were transfected with pegfp-

N1 constructs encoding wild type and mutant lamin A proteins, pFA2-cJun or pFA2-Elk-1 (Stratagene) and pFR-Luc (Stratagene) using Lipofectamine 2000. To correct for transfection efficiency, a plasmid encoding β-gal was co-transfected. After 24 h, cells were trypsinized and protein lysates obtained and extracted according to the manufacturer's instructions (Promega). Luciferase activity was measured with a luminometer.

Gene Expression Profiling in Hearts from Mice with Lmna H222P Mutation

[0097] To identify abnormal expression of genes involved in development of cardiomyopathy caused by *Lmna* mutation, we carried out a genome-wide RNA expression analysis in hearts from $Lmna^{H222P/+}$ and $Lmna^{H222P/H222P}$ mice. A detailed description of these mice has been previously published (14). Male $Lmna^{H222P/H222P}$ mice develop cardiac chamber dilation, decreased left ventricle fractional shortening and hypokinesis detectable by echocardiography at 8 weeks of age. At 12 weeks of age, conduction system abnormalities become pronounced, characterized primarily by an increased PR interval on electrocardiograms. Histological analysis shows left ventricular fibrosis and fiber degeneration by 16 weeks of age along with atrial dilation. Male mice die between 4 and 9 months of age. To focus on primary events and avoid interference caused by fibrotic cells and non-specific tissue damage in hearts from older $Lmna^{H222P/H222P}$ mice, we analyzed samples from mice at 10 weeks of age. There are no histological detectable abnormalities in hearts of mice at this age (see below). We also used hearts from heterozygous $Lmna^{H222P/+}$ mice, which do not develop signs of cardiomyopathy until 24 months of age (Bonne et al., unpublished observation) and have normal life spans.

[0098] Hearts were isolated and transcription profiles determined using amplified RNA for microarray analyses. We used Affymetrix Mouse Genome 430 2.0 Arrays, which contain 45,101 probes sets for known and predicted genes. We examined similarities in transcription profiles between hearts from control $Lmna^{+/+}$, $Lmna^{H222P/+}$ and $Lmna^{H222P/H222P}$ mice by hierarchical cluster analysis. Using hearts from control mice (n=8) as a baseline, this analysis revealed a strong consistency between replicates and distinct patterns of gene expression (Figure 1A). Compared to the mean value of expression in controls, hearts from $Lmna^{H222P/H222P}$ (n=6) and $Lmna^{H222P/+}$ (n=7) mice exhibited a large cluster of genes with increased expression and a small cluster with decreased expression.

[0099] We used a supervised learning method to distinguish probe sets representing genes with significant differences in expression between hearts from control and mutant mice. Probe sets were selected using sufficiently high absolute changes measured by *q*-values ($q<0.05$), which were determined using gene-wise t-tests. The analysis was tuned such that the false discovery rate among probe sets identified as significant was 5% and expression was more than 2-fold different than control. This analysis yielded 104 probe sets in hearts from *Lmna*$^{H222P/+}$ mice and 114 in hearts from *Lmna*$^{H222P/H222P}$ mice (Figure 1B). The 104 probes sets identified in hearts from *Lmna*$^{H222P/+}$ mice corresponded to 92 up-regulated genes, 69 known ones and 23 cDNAs with unknown functions (Table 1). The 12 down-regulated genes included 6 known ones and 6 uncharacterized cDNAs. The number of up-regulated genes corresponding to the probe sets identified in hearts from *Lmna*$^{H222P/H222P}$ mice was 94, 73 known genes and 21 cDNAs of unknown function (Table 2). The number of down-regulated genes was 20, 8 known genes and 12 cDNAs with unknown functions. There were 57 similar probes sets between hearts from *Lmna*$^{H222P/H222P}$ and *Lmna*$^{H222P/+}$ mice (Table 3).

[00100] To validate expression of selected transcripts identified by microarray analysis, we performed real-time PCR using RNA extracted from mouse hearts (Figure 1C). Genes encoding heavy and light chains of myosins (*Myl7*, *Myl4*, *Myh7)*, actin-α2 (*Acta2*), sarcolipin (*Sln*) and pituitary tumor-transforming 1 (*Pttg)* were selected as representative. There was a correlation between real-time PCR results and altered expression detected by microarrays for these genes with greater than 2-fold differences in expression in hearts from both *Lmna*$^{H222P/+}$ and *Lmna*$^{H222P/H222P}$ mice (Figure 1C).

[00101] Many genes, including some muscle-specific genes, with significantly altered expression compared to controls in hearts from *Lmna*$^{H222P/+}$ and *Lmna*$^{H222P/H222P}$ mice were identical (Table 3). *Myl4*, *Myl7*, *Myh7* and *Sln* were up-regulated in hearts from both *Lmna*$^{H222P/H222P}$ and *Lmna*$^{H222P/+}$ mice. There was also increased expression of genes encoding LIM domain family members, including *Pdlim3* and *Fhl1*. However, it appeared that increased expression of muscle-specific genes was greater in hearts of *Lmna*$^{H222P/H222P}$ mice than from *Lmna*$^{H222P/+}$ mice (Table 2 and Table 1, respectively). Statistically significant increases in RNA transcripts encoding atrial natriuretic factor and actin-α2 were observed only in hearts from *Lmna*$^{H222P/H222P}$ mice (Table 2).

[00102] We used ermineJ software, which analyzes Gene Ontology terms applied to genes, to identify functional classes of genes differentially expressed in hearts from *Lmna*$^{H222P/+}$ and *Lmna*$^{H222P/H222P}$ mice compared to controls. Analysis using functional class scoring improves sensitivity by statistically evaluating genes in biologically meaningful groups. In hearts from *Lmna*$^{H222P/H222P}$ mice, the highest scoring Gene Ontology classes were genes encoding proteins involved in inflammation and fibrosis (Table 4). However, these classes were not significantly altered in hearts from *Lmna*$^{H222P/+}$ mice. Differential expression of genes encoding muscle components, including myosins and sarcomeric proteins, achieved statistical significance in hearts from *Lmna*$^{H222P/H222P}$ and *Lmna*$^{H222P/+}$ mice. Genes encoding various proteins involved in transcription and translation also demonstrated significant differences in expression, some only in hearts of *Lmna*$^{H222P/H222P}$ and others in heterozygotes. Genes encoding proteins in the Wnt receptor signaling pathway, in heterotrimeric G-protein complexes, in the JNK cascade branch of the MAPK pathway, with protein phosphatase type 2A activities and with transmembrane receptor protein kinase activities demonstrated significantly altered expression in hearts from *Lmna*$^{H222P/+}$ and *Lmna*$^{H222P/H222P}$ mice (Table 4).

Analysis of Markers of Cardiomyopathy in Hearts from Mice with Lmna H222P Mutation

[00103] Several genes discovered to be differentially expressed in hearts of *Lmna* H222P knock-in mice using microarray analysis appeared to be involved in pathological changes of cardiomyopathy. Activation of genes encoding proteins involved in inflammation and fibrosis has been reported in previous studies of cardiomyopathies in humans and mice (15, 16) and agrees with pathological changes that develop in hearts of *Lmna*$^{H222P/H222P}$ mice (14). However, histological examination did not reveal inflammation or fibrosis in hearts from *Lmna*$^{H222P/H222P}$ mice at 10 weeks (Figure 2A). This suggests that detection of "molecular signatures" using microarrays is more sensitive than conventional histology in detecting inflammation and fibrosis.

[00104] Deregulation of genes encoding muscle components and involved in "muscle organization" has been described in other studies of dilated cardiomyopathies (17, 18). We therefore used immunoblotting to analyze expression of β-myosin heavy chain (β-MHC) and myosin light chain 2 (MLC-2) polypeptides, as their genes showed significantly increased expression in hearts from mutant mice. Hearts from *Lmna*$^{H222P/+}$ and *Lmna*$^{H222P/H222P}$ mice respectively had 5.3-fold and 6.1-fold increases in β-MHC and 7.1-fold and 6.8-fold

increases in MLC-2 expression compared to controls (Figure 2B). We also measured expression of atrial natriuretic factor (ANF), which is up-regulated in heart failure, and its expression was increased in hearts from *Lmna*$^{H222P/H222P}$ mice by approximately 6-fold compared to controls (Figure 2B). However, the increase of ANF was not statistically significant in hearts from *Lmna*$^{H222P/+}$ mice. This is consistent with results of microarray analysis and also cardiac chamber dilation in hearts of *Lmna*$^{H222P/H222P}$ mice at 8 weeks of age (14).

MAPK Pathways Involved in Development of Cardiomyopathy Are Activated in Hearts of Lmna H2222P Mice

[00105] Our Functional Class Scoring analysis revealed significant differences in expression of genes encoding proteins in MAPK pathways in *Lmna* H222P mouse hearts (Table 4). Individual genes in MAPK pathways with significantly different expressions ($q<0.05$) in hearts from *Lmna*$^{H222P+}$ and *Lmna*$^{H222P/H222P}$ mice, as identified using DAVID (http://david.abcc.ncifcrf.gov/), are listed in Table 5 and Table 6. Because enhanced JNK cascade activity, a branch of MAPK pathways, has been shown to cause cardiomyopathy and conduction defects (19, 20), we focused our attention on the MAPK pathways. We first evaluated phosphorylation of two MAPKs, JNK and ERK1/2 (pJNK and pERK1/2, respectively), in hearts from *Lmna*$^{+/+}$, *Lmna*$^{H222P/+}$ and *Lmna*$^{H222P/H222P}$ mice. These kinases are activated by phosphorylation. Immunoblotting with anti-pJNK Ab demonstrated 5-fold and 9-fold increases in pJNK in hearts from *Lmna*$^{H222P/+}$ and *Lmna*$^{H222P/H222P}$, respectively (Figure 3A). Phosphorylated ERK1/2 was also significantly increased in hearts from *Lmna*$^{H222P/+}$ and *Lmna*$^{H222P/H222P}$ mice (2.3-fold and 2.1-fold, respectively) (Figure 3A). Infiltration of cells other than cardiomyocytes could be a potential confounding variable accounting for detection of activated MAPKs in heart tissue. To remove the influence of such cells, we tested whether JNK and ERK1/2 kinases were activated in isolated ventricular cardiomyocytes from *Lmna*$^{H222P/H222P}$. Expressions of pERK1/2 and pJNK were increased 4-fold and 12-fold, respectively, in cardiomyocytes from *Lmna*$^{H222P/H222P}$ mice compared to those from *Lmna*$^{+/+}$ mice (Figure 3A).

[00106] Phosphorylated JNK and pERK1/2 activate a series of downstream target genes, including those encoding bcl-2, elk-1 and c-Jun (21, 22, 23). Immunoblotting with Abs against bcl-2 and elk-1 demonstrated increased expression of these proteins in hearts from both *Lmna*$^{H222P/H222P}$ and *Lmna*$^{H222P/+}$ mice compared to *Lmna*$^{+/+}$ mice (Figure 3B). Pc-Jun

was also increased in hearts from *Lmna*$^{H222P/H222P}$ but not *Lmna*$^{H222P/+}$ mice (Figure 3B). Increases in elk-1, bcl-2 and pc-Jun were also detected in isolated ventricular cardiomyocytes from *Lmna*$^{H222P/H222P}$ mice compared to controls (Figure 3B). These data indicate aberrant activation of MAPK signaling in hearts from both *Lmna*$^{H222P/H222P}$ and *Lmna*$^{H222P/+}$ mice. However, the degree of enhanced signaling appeared to be greater in hearts from homozygous mutant mice.

[00107] To analyze *in vivo* activation of MAPK, we used an Ab that recognized pERK1/2 in sections of heart tissue. Immunofluorescence staining of heart sections from *Lmna*$^{+/+}$ mice with these antibodies revealed a faint, rather diffuse pattern whereas fluorescence in hearts from *Lmna*$^{H222P/H222P}$ mice was more intense and predominantly nuclear (Figure 4A). Quantitative analysis of individual cardiomyocytes in the sections confirmed that anti-pERK Ab labeled both cytoplasm and nucleus in hearts from *Lmna*$^{+/+}$ mice but essentially only the nucleus in hearts from *Lmna*$^{H222P/H222P}$ mice (Figure 4B). Fluorescence intensity of nuclear labeling was significantly higher in heart cells in *Lmna*$^{H222P/H222P}$ mice compare to *Lmna*$^{+/+}$ mice (Figure 4C). These results demonstrate greater activation and nuclear translocation of a MAPK in hearts from *Lmna*$^{H222P/H222P}$ mice compared to control.

[00108] To determine if MAPK activation is observed only in heart, we measured expression of downstream target genes *Elk-1*, *JunD*, *c-Jun* and *Elk-4* in different tissues. Real-time PCR showed significantly increased expression mostly in hearts from *Lmna*$^{H222P/H222P}$ mice (Figure 5). There was also increased expression of *Elk-4* in skeletal muscle of *Lmna*$^{H222P/H222P}$ mice.

[00109] Our initial analyses used hearts from mice 10 weeks of age, when *Lmna*$^{H222P/H222P}$ mice already have slight ventricular dilatation of the ventricles (14). Activation of fibrosis genes was also detected at this time. These alterations could affect cardiac cells and secondarily stimulate MAPK cascades. We therefore use real-time PCR to analyze expression of *c-Jun*, *Elk-1*, *JunD* and *Elk-4* in hearts from *Lmna*$^{+/+}$ and *Lmna*$^{H222P/H222P}$ mice at 4, 7 and 10 weeks of age. In hearts from 10-week old *Lmna*$^{H222P/H222P}$ mice, there was activation of *Vegf*, a marker of fibrosis, as well as *Myl7* and *Sln*. Expression of *c-Jun*, *Elk-1*, *JunD* and *Elk-4* was also significantly increased (Figure 6). In 7-week old *Lmna*$^{H222P/H222P}$ mice, there was increased cardiac expression of *Myl7* but not *Vegf* or *Sln* and expression of *c-Jun*, *Elk-1*, *JunD* and *Elk-4* was still increased (Figure 6). At 4 weeks of age, there was only

increased cardiac *JunD* expression in *Lmna*$^{H222P/H222P}$ mice (Figure 6). These results show that MAPK activation precedes increased expression of a fibrosis marker and two muscle-specific genes in hearts from *Lmna*$^{H222P/H222P}$ mice.

[00110] A fetal-like gene expression program of genes encoding cytoskeletal proteins is characteristic of many types of cardiomyopathy (17, 18, 46-49) and is similarly initiated during cardiac remodeling due to mechanical strain, such in hypertensive cardiomyopathy (50, 51). Increases in ventricular expression of ANF have been documented in experimental models of heart failure and cardiomyopathy (29, 38, 52-55) as well as in human heart failure (56). Our analysis identified 104 and 114 genes that were differentially expressed in hearts from *Lmna*$^{H222P/+}$ and *Lmna*$^{H222P/H222P}$ mice, respectively. These included several in the cardiac fetal gene expression program, such as those encoding β-MHC (*Myh7)*, MLC-2 (*Myl4*, *Myl7)* and ANF (*Anf)*. However, levels in the changes in expression of these genes were different in hearts from *Lmna*$^{H222P/+}$ and *Lmna*$^{H222P/H222P}$ mice. For example, the $\log_2$-fold changes in expression of *Myh7* were 2.38 in hearts from *Lmna*$^{H222P/+}$ mice and 3.49 in hearts from *Lmna*$^{H222P/H222P}$. Log_2-fold changes in expression of *Myl4* were 3.84 in hearts from *Lmna*$^{H222P/+}$ and 4.66 in hearts from *Lmna*$^{H222P/H222P}$ mice. *Anf* was not differentially expressed in hearts from *Lmna*$^{H222P/+}$ mice compared to wild type mice but was up-regulated significantly in hearts from *Lmna*$^{H222P/H222P}$ mice. These different degrees of gene expression changes may reflect the early onset of heart failure in *Lmna*$^{H222P/H222P}$ mice, which develop symptoms at approximately 2 months of age. In contrast, *Lmna*$^{H222P/+}$ mice exhibit a decrease in left ventricular fractional shortening only at 2 years of age (Bonne et al., unpublished observation).

[00111] Expression of genes encoding skeletal muscle α-actin (57) and c-myc (58), which re-express during cardiac remodeling, was not increased in hearts from *Lmna*$^{H222P/+}$ and *Lmna*$^{H222P/H222P}$ mice. These genes are activated in an early-response against passive tension, for example in cardiac hypertrophy secondary to pressure overload. Lack of activation of these genes is consistent with dilated cardiomyopathy without cellular hypertrophy and disarray in hearts from *Lmna*$^{H222P/H222P}$ mice (14). The observed up-regulation of genes encoding extracellular matrix-proteins, such as those encoding collagen Iα2 (*Col1a2*), decorin (*Dcn*) and matrix metalloproteinase 14 (*Mmp14*), may underlie the development of fibrosis in hearts from *Lmna*$^{H222P/H222P}$ mice.

Expression of Lamin A with the H222P aa Substitution Activates JNK and ERK and Alters Subcellular Localization

[00112] To determine if expression of lamin A with the H222P aa substitution is responsible for activation of MAPK signaling, we measured pERK1/2 and pJNK in transiently transfected Cos-7 and C2C12 cells expressing GFP fusions of wild type and H222P lamin A. Immunoblotting with Abs against total ERK1/2 and pERK1/2 demonstrated that expression of H222P lamin A increased the amount of phosphorylated protein (Figure 7A and Figure 7B). The increase was significant compared to non-transfected cells and cells expressing the GFP fusion of wild type lamin A.

[00113] Translocation of pERK1/2 and pJNK from cytoplasm to nucleus is required for activation of downstream targets (24, 25). In non-transfected Cos-7 and C2C12 cells, pERK1/2 was mainly distributed in the cytoplasm (Figure 7C and Figure 7D). When transfected with a plasmid expressing the GFP fusion of wild type lamin A, pERK1/2 was also mainly distributed in cytoplasm (Figure 7C and 7D). In contrast, expression of a GFP fusion of H222P lamin A induced translocation of pERK1/2 into the nucleus (Figure 7C and Figure 7D). Approximately 80% of Cos-7 and C2C12 cells expressing H222P lamin A showed a nuclear localization of pERK1/2. Nuclear localization of pERK1/2 was observed in only 15% of Cos-7 cells and 30% of C2C12 cells expressing wild type lamin A and was not observed in untransfected cells (Figure 7E and Figure 7F). Similar results were obtained for pJNK (Figure 10). Hence, expression of H222P lamin A stimulates phosphorylation and nuclear translocation of JNK and ERK1/2. While MAPKs were activated in C2C12 myoblasts transfected with H222P Lamin A, activated MAPK was not detected in skeletal muscle from *Lmna*$^{H222P/H222P}$ mice. However, myoblasts are only a small component of heterogeneous skeletal muscle sections. Furthermore, in humans with EDMD as well as *Lmna*$^{H222P/H222P}$ mice, skeletal muscle is variably affected.

Expression of Lamin A with aa Substitutions Identified in EDMD Associated with Cardiomyopathy Activates JNK and ERK

[00114] To further evaluate the effects of lamin A mutants on activation of MAPK pathways, we examined expression of *c-Jun* and *Elk-1* reporter genes. We transiently transfected Cos-7 cells with plasmids encoding GFP fusions of H222P lamin A as well as wild type lamin A and 5 other lamin A mutants. Cells were simultaneously transfected with plasmids encoding a reporter system to detect *c-Jun* or *Elk-1* promoter activities. Expression

of H222P lamin A and lamin A with N195K, R298C, and N456I aa substitutions found in EDMD significantly increased activity of the *c-Jun* and *Elk-1* promoters (Figure 8). Overexpression of wild type lamin A and lamin A with a R482W mutation found in subjects with Dunnigan-type partial lipodystrophy did not significantly increase their activity. However, expression of one lamin A with an aa substitution that causes EDMD (T528K) did not significantly increase *c-Jun* and *Elk-1* promoters activities in this assay. A possible explanation of this observation may be that a GFP-fusion of this mutant folds abnormally or is not as stable as the others when overexpressed in transfected cells. These results show that expression of A-type lamins with aa substitutions encoded by *LMNA* mutations causing cardiomyopathy leads to stimulation of downstream target genes in MAPK cascades in cultured cells.

Table 1. Genes with altered expression as defined by $q<0.05$ and >1 $\log_2$-fold change in hearts from *Lmna*$^{H222P/+}$ mice.

Probe set name	Gene symbol	Gene name	Fold	*q*-value
1449071_at	*Myl7*	myosin, light polypeptide 7, regulatory	4.91	0.003262303
1420884_at	*Sln*	sarcolipin	4.14	0.009783776
1422580_at	*Myl4*	myosin, light polypeptide 4, alkali; atrial, embryonic	3.84	0.004778844
1425521_at	*Paip1*	polyadenylate binding protein-interacting protein 1	3.32	0.000279415
1448553_at	*Myh7*	myosin, heavy polypeptide 7, cardiac muscle, beta	2.38	0.029672983
1449824_at	*Prg4*	proteoglycan 4	2.25	0.01330861
1441679_at	*Cacna1c*	calcium channel, voltage-dependent, L type, alpha 1C subunit	2.04	0.041791634
1449434_at	*Car3*	carbonic anhydrase 3	2.03	0.019735505
1419100_at	*Serpina3n*	serine (or cysteine) proteinase inhibitor, clade A, member 3N	1.92	0.041583562
1426260_a_at	*Ugt1a6*	UDP glycosyltransferase 1 family, polypeptide A6	1.86	0.006793397
1424749_at	*Wdfy1*	WD repeat and FYVE domain containing 1	1.79	0.006916706
1449178_at	*Pdlim3*	PDZ and LIM domain 3	1.70	0.002607879
1448595_a_at	*Rex3*	reduced expression 3	1.65	0.006428347
1428484_at	*Osbpl3*	oxysterol binding protein-like 3	1.61	0.008837797
1453232_at	*Calr3*	calreticulin 3	1.58	0.007966835
1424454_at	*A930025J12RIK*	RIKEN cDNA A930025J12 gene	1.55	0.019735505
1453145_at	*4933439C20RIK*	RIKEN cDNA 4933439C20 gene	1.53	0.006361691
1417462_at	*Cap1*	CAP, adenylate cyclase-associated protein 1 (yeast)	1.50	0.020072033
1435176_a_at	*Idb2*	inhibitor of DNA binding 2	1.49	0.006407563
1430519_a_at	*Cnot7*	CCR4-NOT transcription complex, subunit 7	1.47	0.0039589
1433184_at	*6720477C19RIK*	RIKEN cDNA 6720477C19 gene	1.45	0.035675657
1454959_s_at	*Gnai1*	guanine nucleotide binding protein, alpha inhibiting 1	1.45	0.015512236
1423915_at	*4832415H08RIK*	RIKEN cDNA 4832415H08 gene	1.45	0.002607879
1417867_at	*I*	adipsin	1.45	0.023285335
1423954_at	*C3*	complement component 3	1.39	0.024131569
1449461_at	*Rbp7*	retinol binding protein 7, cellular	1.39	0.042288878
1455136_at	*Atp1a2*	ATPase, Na+/K+ transporting, alpha 2 polypeptide	1.38	0.006428347
1452417_x_at	*AV057155*	AV057155 Mus musculus pancreas C57BL/6J adult Mus musculus	1.35	0.040758652
1443799_at	*AV348753*	AV348753 RIKEN full-length enriched, adult male olfactory	1.35	0.029103142
1421551_s_at	***Ifi202b***	interferon activated gene 202B	1.34	0.011539146
1449514_at	*Gprk5*	G protein-coupled receptor kinase 5	1.32	0.023285335
1419527_at	*Comp*	cartilage oligomeric matrix protein	1.31	0.032455373
1432205_a_at	*C130038G02RIK*	RIKEN cDNA C130038G02 gene	1.30	0.00705383
1422651_at	*Acdc*	adipocyte, C1Q and collagen domain containing	1.27	0.028936401
1447640_s_at	*Pbx3*	pre B-cell leukemia transcription factor 3	1.27	0.027186297
1427183_at	*Efemp1*	epidermal growth factor-containing	1.26	0.012371525

Probe set name	Gene symbol	Gene name	Fold	*q*-value
		fibulin-like extracellular matrix protein 1		
1448823_at	*Cxcl12*	chemokine (C-X-C motif) ligand 12	1.25	0.006196772
1421855_at	*Fgl2*	fibrinogen-like protein 2	1.24	0.012386508
1420731_a_at	*Csrp2*	cysteine and glycine-rich protein 2	1.24	0.011179832
1454966_at	*AK031326*	unknown	1.23	0.042632665
1427038_at	*BC049766*	unknown	1.22	0.007548482
1437123_at	***Mmrn2***	multimerin 2	1.21	0.000313227
1418674_at	*Osmr*	oncostatin M receptor	1.20	0.026645199
		cytochrome P450, family 2, subfamily e,		
1415994_at	*Cyp2e1*	polypeptide 1	1.19	0.044394162
1428343_at	*C730034d20rik*	RIKEN cDNA C730034D20 gene	1.19	0.018171429
1420930_s_at	*Catnal1*	catenin alpha-like 1	1.19	0.03182764
1455812_x_at	*Slitl2*	Slit-like 2 (Drosophila)	1.18	0.023909901
1421163_a_at	*Nfia*	nuclear factor I/A	1.18	0.034980094
1423854_a_at	*BC008101*	unknown	1.17	0.009795877
		DNA segment, Chr 6, Massachusetts		
1427660_x_at	*D6MIT97*	Institute of Technology 97	1.17	0.038499517
1424383_at	*BC003277*	cDNA sequence BC003277	1.16	0.009154495
1420952_at	*Son*	Son cell proliferation protein	1.16	0.046071596
1417126_a_at	*3110001N18RIK*	RIKEN cDNA 3110001N18 gene	1.15	0.009282894
		AV020525 Mus musculus 18-day embryo		
1440335_at	*AV020525*	C57BL/6J Mus musculus	1.13	0.046559367
		serine (or cysteine) proteinase inhibitor,		
1416666_at	*Serpine2*	clade E, member 2	1.13	0.013133867
1451447_at	*C330016O16RIK*	RIKEN cDNA C330016O16 gene	1.13	0.012386508
1426208_x_at	***Plagl1***	pleiomorphic adenoma gene-like 1	1.12	0.022034481
1448669_at	*Dkk3*	dickkopf homolog 3 (Xenopus laevis)	1.12	0.032901376
1429197_s_at	*BC038651*	unknown	1.12	0.006916706
		BB766329 RIKEN full-length enriched,		
1436672_at	*BB766329*	B16 F10Y cells Mus	1.12	0.017740892
1448734_at	*Cp*	ceruloplasmin	1.11	0.021961097
1418021_at	*Slp*	sex-limited protein	1.11	0.034532714
1434975_x_at	*9030221M09RIK*	RIKEN cDNA 9030221M09 gene	1.11	0.019735505
1426851_a_at	*Nov*	nephroblastoma overexpressed gene	1.11	0.033160989
1450876_at	*Cfh*	complement component factor h	1.10	0.035303157
1449556_at	*H2-T23*	histocompatibility 2, T region locus 23	1.10	0.027018405
1422631_at	*Ahr*	aryl-hydrocarbon receptor	1.09	0.006196772
1433647_s_at	*Rhobtb3*	Rho-related BTB domain containing 3	1.09	0.017793681
1433525_at	*Ednra*	endothelin receptor type A	1.09	0.02333671
1419155_a_at	*Sox4*	SRY-box containing gene 4	1.09	0.027469092
1419130_at	*Deadc1*	deaminase domain containing 1	1.09	0.006602357
1453435_a_at	*Fmo2*	flavin containing monooxygenase 2	1.09	0.020289251
1417065_at	*Egr1*	early growth response 1	1.08	0.021448558
1449106_at	***Gpx3***	glutathione peroxidase 3	1.08	0.030677188
1448162_at	*Vcam1*	vascular cell adhesion molecule 1	1.08	0.026413922
1422715_s_at	*Acp1*	acid phosphatase 1, soluble	1.07	0.023907748
		BMP and activin membrane-bound		
1423753_at	*Bambi*	inhibitor, homolog (Xenopus laevis)	1.06	0.011539146
1430637_at	*2210016H18RIK*	RIKEN cDNA 2210016H18 gene	1.06	0.047172391
1434990_at	*Ak122434*	unknown	1.06	0.006916706
1451240_a_at	*Glo1*	glyoxalase 1	1.05	0.042857264
		neural precursor cell expressed,		
1421955_a_at	*Nedd4*	developmentally down-regulated gene 4	1.05	0.035645582

Probe set name	Gene symbol	Gene name	Fold	*q*-value
1436431_at	*1700025G04RIK*	RIKEN cDNA 1700025G04 gene	1.05	0.011155847
1418536_at	*H2-Q7*	histocompatibility 2, Q region locus 7	1.04	0.033908679
1451285_at	*Fus*	fusion, derived from t(12;16) malignant liposarcoma (human)	1.04	0.022761224
1435943_at	*Dpep1*	dipeptidase 1 (renal)	1.03	0.010803727
1448705_at	*Zfp297*	zinc finger protein 297	1.03	0.014276303
1438631_x_at	*BC017545*	unknown	1.03	0.021575905
1456226_x_at	*Ddr1*	discoidin domain receptor family, member 1	1.03	0.021976404
1417872_at	*Fhl1*	four and a half LIM domains 1	1.03	0.009154583
1455940_x_at	*Wdr6*	WD repeat domain 6	1.03	0.01925172
1434328_at	*Loc380747*	similar to 60S ribosomal protein L15	1.02	0.02321354
1419103_a_at	*Abhd6*	abhydrolase domain containing 6	1.02	0.00503353
1438754_at	*Av372127*	AV372127 RIKEN full-length enriched, adult male colon Mus	-1.02	0.043783361
1447802_x_at	*AV099323*	expressed sequence AV099323	-1.03	0.012371525
1452590_a_at	*BC032982*	unknown	-1.08	0.015451729
1434008_at	*Loc384934*	similar to sodium channel beta 4 subunit	-1.08	0.023285335
1451675_a_at	*Alas2*	aminolevulinic acid synthase 2, erythroid	-1.10	0.002607879
1452318_a_at	*M12573*	unknown	-1.51	0.043962944
1426607_at	*3110070M22RIK*	RIKEN cDNA 3110070M22 gene	-1.51	0.028191889
1418480_at	*Cxcl7*	chemokine (C-X-C motif) ligand 7	-1.78	0.002607879
1437721_at	*BB543398*	BB543398 RIKEN full-length enriched, 0 day neonate eyeball	-1.80	0.018132165
1422919_at	***Hrasls***	HRAS-like suppressor	-2.02	0.037734414
1438390_s_at	*Pttg1*	pituitary tumor-transforming 1	-2.05	0.049414848
1428347_at	*Cyfip2*	cytoplasmic FMR1 interacting protein 2	-2.22	0.04909376

Table 2. Genes with altered expression as defined by $q<0.05$ and >1 $\log_2$-fold change in hearts from *Lmna*$^{H222P/H222P}$ mice.

Probe set name	Gene symbol	Gene name	Fold	*q*-value
1449071_at	*Myl7*	myosin, light polypeptide 7, regulatory	6.02	4.16256E-05
1420884_at	*Sln*	sarcolipin	5.13	0.000169726
1422580_at	*Myl4*	myosin, light polypeptide 4, alkali; atrial, embryonic	4.66	0.000256675
1448553_at	*Myh7*	myosin, heavy polypeptide 7, cardiac muscle, beta	3.49	0.001102336
1453898_at	*AK009352*	unknown	2.50	0.001402809
1449434_at	*Car3*	carbonic anhydrase 3	2.17	0.012439184
1457666_s_at	*Ifi202b*	interferon activated gene 202B	2.11	0.000846853
1448595_a_at	*Rex3*	reduced expression 3	2.10	0.000715362
1425521_at	*Paip1*	polyadenylate binding protein-interacting protein 1	1.89	0.023572154
1449824_at	*Prg4*	proteoglycan 4	1.85	0.003308574
1456062_at	*Anf*	atrial natriuretic factor	1.84	0.001119551
1418701_at	*Arvcf*	armadillo repeat gene deleted in velo-cardio-facial syndrome	1.83	0.012252465
1419100_at	*Serpina3n*	serine (or cysteine) proteinase inhibitor, clade A, member 3N	1.77	0.005743576
1454959_s_at	*Gnai1*	guanine nucleotide binding protein, alpha inhibiting 1	1.74	0.003649336
1429196_at	*BC038651*	unknown	1.73	0.003065936
1437358_at	*Wdfy1*	WD repeat and FYVE domain containing 1	1.65	0.001337287
1419155_a_at	*Sox4*	SRY-box containing gene 4	1.63	0.001102336
1448669_at	*Dkk3*	dickkopf homolog 3 (Xenopus laevis)	1.57	0.00096279
1455136_at	*Atp1a2*	ATPase, Na+/K+ transporting, alpha 2 polypeptide	1.57	0.001402809
1450857_a_at	*Col1a2*	procollagen, type I, alpha 2	1.55	0.026789241
1428484_at	*Osbpl3*	oxysterol binding protein-like 3	1.48	0.020741743
1425394_at	*BC023105*	cDNA sequence BC023105	1.45	0.006458272
1430519_a_at	*Cnot7*	CCR4-NOT transcription complex, subunit 7	1.45	0.004940192
1420731_a_at	*Csrp2*	cysteine and glycine-rich protein 2	1.44	0.000911703
1432205_a_at	*C130038G02RIK*	RIKEN cDNA C130038G02 gene	1.42	0.000671074
1424383_at	*BC003277*	cDNA sequence BC003277	1.41	0.000846853
1448823_at	*Cxcl12*	chemokine (C-X-C motif) ligand 12	1.39	0.000715362
1435290_x_at	*H2-Aa*	histocompatibility 2, class II antigen A, alpha	1.39	0.003976722
1449178_at	*Pdlim3*	PDZ and LIM domain 3	1.37	0.005362642
1429060_at	*D830013H23RIK*	RIKEN cDNA D830013H23 gene	1.37	0.004876867
1421855_at	*Fgl2*	fibrinogen-like protein 2	1.33	0.005743576
1425425_a_at	*Wif1*	Wnt inhibitory factor 1	1.33	0.040656125
1428343_at	*C730034D20RIK*	RIKEN cDNA C730034D20 gene	1.32	0.001873588
1437401_at	*Igf1*	insulin-like growth factor 1	1.32	0.001699794
1435176_a_at	*Idb2*	inhibitor of DNA binding 2	1.30	0.001735733
1417065_at	*Egr1*	early growth response 1	1.29	0.012103309
1419527_at	*Comp*	cartilage oligomeric matrix protein	1.28	0.015363433
1416666_at	*Serpine2*	serine (or cysteine) proteinase inhibitor, clade E, member 2	1.28	0.016566752

Probe set name	Gene symbol	Gene name	Fold	*q*-value
1426208_x_at	*Plagl1*	pleiomorphic adenoma gene-like 1	1.28	0.013612184
1449106_at	*Gpx3*	glutathione peroxidase 3	1.27	0.001946526
1449368_at	*Dcn*	decorin	1.25	0.012103309
1418174_at	*Dbp*	D site albumin promoter binding protein	1.25	0.005860191
1423753_at	*Bambi*	BMP and activin membrane-bound inhibitor, homolog (Xenopus laevis)	1.23	0.001119551
1425519_a_at	*Ii*	Ia-associated invariant chain	1.22	0.005689275
1453145_at	*4933439C20RIK*	RIKEN cDNA 4933439C20 gene	1.22	0.020741743
1423854_a_at	*BC008101*	unknown	1.21	0.004003416
1427038_at	*BC049766*	unknown	1.21	0.024041634
1448162_at	*Vcam1*	vascular cell adhesion molecule 1	1.19	0.017776185
1439766_x_at	*Vegfc*	vascular endothelial growth factor C	1.19	0.000846853
1451447_at	*C330016O16RIK*	RIKEN cDNA C330016O16 gene	1.18	0.017776185
1419130_at	*Deadc1*	deaminase domain containing 1	1.18	0.013925793
1437224_at	*Rtn4*	reticulon 4	1.18	0.006437433
1420952_at	*Son*	Son cell proliferation protein	1.17	0.002274827
1416454_s_at	*Acta2*	actin, alpha 2, smooth muscle, aorta	1.17	0.001385314
1437056_x_at	*1810049K24RIK*	RIKEN cDNA 1810049K24 gene	1.17	0.041776172
1448416_at	*Mglap*	matrix gamma-carboxyglutamate (gla) protein	1.16	0.004940192
1448383_at	*Mmp14*	matrix metalloproteinase 14 (membrane-inserted)	1.16	0.045912269
1447640_s_at	*Pbx3*	pre B-cell leukemia transcription factor 3	1.15	0.035771251
1415859_at	*3230401O13RIK*	RIKEN cDNA 3230401O13 gene	1.15	0.023410072
1418532_at	*Fzd2*	frizzled homolog 2 (Drosophila)	1.15	0.007687062
1460049_s_at	*1500015O10RIK*	RIKEN cDNA 1500015O10 gene	1.15	0.045369376
1449461_at	*Rbp7*	retinol binding protein 7, cellular	1.12	0.022192646
1451567_a_at	*Ifi203*	interferon activated gene 203	1.11	0.017776185
1422607_at	*Etv1*	ets variant gene 1	1.11	0.004940192
1424186_at	*2610001E17RIK*	RIKEN cDNA 2610001E17 gene	1.11	0.049669589
1426851_a_at	*Nov*	nephroblastoma overexpressed gene	1.11	0.023572154
1417462_at	*Cap1*	CAP, adenylate cyclase-associated protein 1 (yeast)	1.10	0.033983868
1426510_at	*C330023F11RIK*	RIKEN cDNA C330023F11 gene	1.10	0.036018704
1419042_at	*AW111922*	expressed sequence AW111922	1.10	0.000756273
1437123_at	*Mmrn2*	multimerin 2	1.10	0.000871383
1455346_at	*Masp1*	mannan-binding lectin serine protease 1	1.10	0.007687062
1448288_at	*E030026I10RIK*	RIKEN cDNA E030026I10 gene	1.09	0.004940192
1422631_at	*Ahr*	aryl-hydrocarbon receptor	1.09	0.018968038
1433924_at	*Peg3*	paternally expressed 3	1.08	0.035287641
1421917_at	*Pdgfra*	platelet derived growth factor receptor, alpha polypeptide	1.08	0.012633389
1422476_at	*Ifi30*	interferon gamma inducible protein 30	1.08	0.022192646
1450648_s_at	*H2-Ab1*	histocompatibility 2, class II antigen A, beta 1	1.08	0.001119551
1441137_at	*AK015956*	unknown	1.08	0.035122609
1449514_at	*Gprk5*	G protein-coupled receptor kinase 5	1.05	0.049669589
1417872_at	*Fhl1*	four and a half LIM domains 1	1.05	0.001337287
1417025_at	*H2-Eb1*	histocompatibility 2, class II antigen E beta	1.05	0.004603993
1443621_at	*BG092359*	mac09f12.x1 Soares mouse 3NbMS Mus musculus cDNA clone	1.04	0.001224434

Probe set name	Gene symbol	Gene name	Fold	*q*-value
1426083_a_at	*Btg1*	B-cell translocation gene 1, anti-proliferative	1.04	0.016940974
1449556_at	*H2-T23*	histocompatibility 2, T region locus 23	1.03	0.02194224
1454696_at	*BC003294*	unknown	1.02	0.023314255
1456226_x_at	*Ddr1*	discoidin domain receptor family, member 1	1.02	0.024041634
1454764_s_at	*Slc38a1*	solute carrier family 38, member 1	1.02	0.04708546
1418929_at	*Esrrbl1*	estrogen-related receptor beta like 1	1.02	0.011056089
1455393_at	*Cp*	ceruloplasmin	1.02	0.019001003
1448754_at	*Rbp1*	retinol binding protein 1, cellular	1.02	0.041776172
1439381_x_at	*Mrvldc1*	MARVEL (membrane-associating) domain containing 1	1.01	0.020452219
1447903_x_at	*Ap1s2*	adaptor-related protein complex 1, sigma 2 subunit	1.01	0.031364482
1434141_at	*Gucy1a3*	guanylate cyclase 1, soluble, alpha 3	1.01	0.046340908
1417253_at	*Frg1*	FSHD region gene 1	1.01	0.013925793
1424505_at	*0610042C05RIK*	RIKEN cDNA 0610042C05 gene	-1.02	0.018968038
1434008_at	*Loc384934*	similar to sodium channel beta 4 subunit	-1.07	0.017776185
1456397_at	*BB210819*	BB210819 RIKEN full-length enriched, 0 day neonate thymus	-1.08	0.013489859
1434893_at	*AI845177*	UI-M-BG0-aht-a-04-0-UI.s1 NIH_BMAP_MSC Mus musculus cDNA	-1.09	0.023572154
1451371_at	*1110025G12RIK*	RIKEN cDNA 1110025G12 gene	-1.10	0.027434576
1452590_a_at	*BC032982*	unknown	-1.11	0.005944427
1421278_s_at	*Spna1*	spectrin alpha 1	-1.12	0.033541643
1455208_at	*Pex19*	peroxisome biogenesis factor 19	-1.14	0.008107383
1452388_at	*BC054782*	unknown	-1.15	0.035755727
1424077_at	*2610020H15RIK*	RIKEN cDNA 2610020H15 gene	-1.23	0.002678732
1417680_at	*Kcna5*	potassium voltage-gated channel, shaker-related subfamily, member 5	-1.24	0.040656125
1438511_a_at	*1190002H23RIK*	RIKEN cDNA 1190002H23 gene	-1.25	0.000463385
1447802_x_at	*AV099323*	expressed sequence AV099323	-1.31	0.004421495
1457282_x_at	*Tubgcp5*	tubulin, gamma complex associated protein 5	-1.45	0.007899515
1427126_at	*M12573*	unknown	-1.91	0.046946097
1428991_at	*Hrasls*	HRAS-like suppressor	-2.07	0.003308574
1437721_at	*BB543398*	BB543398 RIKEN full-length enriched, 0 day neonate eyeball	-2.08	0.036438465
1424105_a_at	*Pttg1*	pituitary tumor-transforming 1	-2.69	0.013852722
1428347_at	*Cyfip2*	cytoplasmic FMR1 interacting protein 2	-2.84	0.007687062
1432198_at	*6330414G02RIK*	RIKEN cDNA 6330414G02 gene	-4.12	0.015578517

Table 3. Genes commonly affected as defined by $q<0.05$ and >1 $\log_2$-fold change in hearts from *Lmna*$^{H222P/H222P}$ and *Lmna*$^{H222P/+}$ mice.

Probe set name	Gene symbol	Gene name	*Lmna*$^{H222P/H222P}$ Fold	*Lmna*$^{H222P/H222P}$ *q*-value	*Lmna*$^{H222P/+}$ Fold	*Lmna*$^{H222P/+}$ *q*-value
1449071_at	*Myl7*	myosin, light polypeptide 7, regulatory	6.02	4.16256E-05	4.91	0.003262303
1420884_at	*Sln*	sarcolipin	5.13	0.000169726	4.14	0.009783776
1422580_at	*Myl4*	myosin, light polypeptide 4, alkali; atrial, embryonic	4.66	0.000256675	3.84	0.004778844
1448553_at	*Myh7*	myosin, heavy polypeptide 7, cardiac muscle, beta	3.49	0.001102336	2.38	0.029672983
1449434_at	*Car3*	carbonic anhydrase 3	2.17	0.012439184	2.03	0.019735505
1457666_s_at	*Ifi202b*	interferon activated gene 202B	2.11	0.000846853	1.34	0.011539146
1448595_a_at	*Rex3*	reduced expression 3	2.10	0.000715362	1.65	0.006428347
1425521_at	*Paip1*	polyadenylate binding protein-interacting protein 1	1.89	0.023572154	3.32	0.000279415
1449824_at	*Prg4*	proteoglycan 4	1.85	0.003308574	2.25	0.01330861
1454959_s_at	*Gnai1*	guanine nucleotide binding protein, alpha inhibiting 1	1.74	0.003649336	1.45	0.015512236
1429196_at	*BC038651*	unknown	1.73	0.003065936	1.12	0.006916706
1437358_at	*Wdfy1*	WD repeat and FYVE domain containing 1	1.65	0.001337287	1.79	0.006916706
1419155_a_at	*Sox4*	SRY-box containing gene 4	1.63	0.001102336	1.09	0.027469092
1448669_at	*Dkk3*	dickkopf homolog 3 (Xenopus laevis)	1.57	0.00096279	1.12	0.032901376
1455136_at	*Atp1a2*	ATPase, Na+/K+ transporting, alpha 2 polypeptide	1.57	0.001402809	1.38	0.006428347
1428484_at	*Osbpl3*	oxysterol binding protein-like 3	1.48	0.020741743	1.61	0.008837797
1430519_a_at	*Cnot7*	CCR4-NOT transcription complex, subunit 7	1.45	0.004940192	1.47	0.0039589
1420731_a_at	*Csrp2*	cysteine and glycine-rich protein 2	1.44	0.000911703	1.24	0.011179832
1432205_a_at	*C130038G02RIK*	RIKEN cDNA C130038G02 gene	1.42	0.000671074	1.30	0.00705383
1424383_at	*BC003277*	cDNA sequence BC003277	1.41	0.000846853	1.16	0.009154495
1448823_at	*Cxcl12*	chemokine (C-X-C motif) ligand 12	1.39	0.000715362	1.25	0.006196772
1449178_at	*Pdlim3*	PDZ and LIM domain 3	1.37	0.005362642	1.70	0.002607879
1421855_at	*Fgl2*	fibrinogen-like protein 2	1.33	0.005743576	1.24	0.012386508
1428343_at	*C730034D20RIK*	RIKEN cDNA C730034D20 gene	1.32	0.001873588	1.19	0.018171429
1435176_a_at	*Idb2*	inhibitor of DNA binding 2	1.30	0.001735733	1.49	0.006407563
1417065_at	*Egr1*	early growth response 1	1.29	0.012103309	1.08	0.021448558
1419527_at	*Comp*	cartilage oligomeric matrix protein	1.28	0.015363433	1.31	0.032455373
1416666_at	*Serpine2*	serine (or cysteine) proteinase inhibitor, clade E, member 2	1.28	0.016566752	1.13	0.013133867
1426208_x_at	*Plagl1*	pleiomorphic adenoma gene-like 1	1.28	0.013612184	1.12	0.022034481
1449106_at	*Gpx3*	glutathione peroxidase 3	1.27	0.001946526	1.08	0.030677188
1423753_at	*Bambi*	BMP and activin membrane-bound inhibitor, homolog (Xenopus laevis)	1.23	0.001119551	1.06	0.011539146
1453145_at	*4933439C20RIK*	RIKEN cDNA 4933439C20 gene	1.22	0.020741743	1.53	0.006361691
1423854_a_	*BC008101*	unknown	1.21	0.004003416	1.17	0.009795877

Probe set name	Gene symbol	Gene name	$Lmna^{H222P/H222P}$ Fold	$Lmna^{H222P/H222P}$ *q*-value	$Lmna^{H222P/+}$ Fold	$Lmna^{H222P/+}$ *q*-value
at						
1427038_at	*BC049766*	unknown	1.21	0.024041634	1.22	0.007548482
1448162_at	*Vcam1*	vascular cell adhesion molecule 1	1.19	0.017776185	1.08	0.026413922
1451447_at	*C330016O 16RIK*	RIKEN cDNA C330016O16 gene	1.18	0.017776185	1.13	0.012386508
1419130_at	*Deadc1*	deaminase domain containing 1	1.18	0.013925793	1.09	0.006602357
1420952_at	*Son*	Son cell proliferation protein	1.17	0.002274827	1.16	0.046071596
1447640_s_ at	*Pbx3*	pre B-cell leukemia transcription factor 3	1.15	0.035771251	1.27	0.027186297
1449461_at	*Rbp7*	retinol binding protein 7, cellular	1.12	0.022192646	1.39	0.042288878
1426851_a_ at	*Nov*	nephroblastoma overexpressed gene	1.11	0.023572154	1.11	0.033160989
1417462_at	*Cap1*	CAP, adenylate cyclase-associated protein 1 (yeast)	1.10	0.033983868	1.50	0.020072033
1437123_at	*Mmrn2*	multimerin 2	1.10	0.000871383	1.21	0.000313227
1422631_at	*Ahr*	aryl-hydrocarbon receptor	1.09	0.018968038	1.09	0.006196772
1449514_at	*Gprk5*	G protein-coupled receptor kinase 5	1.05	0.049669589	1.32	0.023285335
1417872_at	*Fhl1*	four and a half LIM domains 1	1.05	0.001337287	1.03	0.009154583
1449556_at	*H2-T23*	histocompatibility 2, T region locus 23	1.03	0.02194224	1.10	0.027018405
1456226_x_ at	*Ddr1*	discoidin domain receptor family, member 1	1.02	0.024041634	1.03	0.021976404
1455393_at	*Cp*	ceruloplasmin	1.02	0.019001003	1.11	0.021961097
1434008_at	*Loc384934*	similar to sodium channel beta 4 subunit	-1.07	0.017776185	-1.08	0.023285335
1452590_a_ at	*BC032982*	unknown	-1.11	0.005944427	-1.08	0.015451729
1447802_x_ at	*AV099323*	expressed sequence AV099323	-1.31	0.004421495	-1.03	0.012371525
1427126_at	*M12573*	unknown	-1.91	0.046946097	-1.51	0.043962944
1428991_at	*Hrasls*	HRAS-like suppressor	-2.07	0.003308574	-2.02	0.037734414
1437721_at	*BB543398*	BB543398 RIKEN full-length enriched, 0 day neonate eyeball	-2.08	0.036438465	-1.80	0.018132165
1424105_a_ at	*Pttg1*	pituitary tumor-transforming 1	-2.69	0.013852722	-2.05	0.049414848
1428347_at	*Cyfip2*	cytoplasmic FMR1 interacting protein 2	-2.84	0.007687062	-2.22	0.04909376

Table 4. Top scoring gene ontology (GO) terms listed with corresponding *q*-value and GO identification numbers in hearts from *Lmna*$^{H222P/H222P}$ and *Lmna*$^{H222P/+}$ mice.

GO term	*GO id*	*q*-value	
		H222P/H222P	**H222P/+**
Inflammation			
MHC class II receptor activity	GO:0045012	0.00000015	
antigen processing	GO:0030333	0.00000022	
antigen presentation	GO:0019882	0.00000036	
MHC class I receptor activity	GO:0030106	0.00343037	
complement activation	GO:0006956	0.02981152	
Fibrosis			
vascular endothelial growth factor receptor activity	GO:0005021	0.00661132	
Muscle Components			
contractile fiber	GO:0043292	0.00005914	0.01837139
sarcomere	GO:0030017	0.00022889	0.03241135
muscle myosin	GO:0005859	0.00038115	0.04948603
structural constituent of muscle	GO:0008307	0.0005612	0.0474557
Transcription/Translation			
poly(A) binding	GO:0008143	0.0054132	
specific RNA polymerase II transcription factor activity	GO:0003704	0.0145961	0.01878892
single-stranded DNA binding	GO:0003697	0.01538049	0.03929412
eukaryotic 43S preinitiation complex	GO:0016282	0.02104322	0.04732741
heterogeneous nuclear ribonucleoprotein complex	GO:0030530	0.02280669	
ATP-dependent RNA helicase activity	GO:0004004	0.02928037	0.00315888
transcriptional repressor complex	GO:0017053	0.02961308	0.01050794
tRNA ligase activity	GO:0004812	0.03062475	
double-stranded RNA binding	GO:0003725	0.04470709	0.0136727
regulation of translational initiation	GO:0006446	0.04794275	0.01326877
Signaling Pathways			
insulin-like growth factor binding	GO:0005520	0.00044041	
Ras protein signal transduction	GO:0007265	0.00208363	
Wnt receptor signaling pathway	GO:0016055	0.00237991	0.0185489
heterotrimeric G-protein complex	GO:0005834	0.00414498	0.00283341
JNK cascade	GO:0007254	0.00526864	0.02433549
MAP kinase activity	GO:0004707	0.01475557	
nuclear translocation of MAPK	GO:0000189	0.02418454	
protein phosphatase type 2A activity	GO:0000158	0.03400446	0.02621094
transmembrane receptor protein kinase activity	GO:0019199	0.03446463	0.02434485

Table 5. Genes from MAPK pathways affected as defined by $q<0.05$ in hearts from *Lmna*$^{H222P/H222P}$ mice.

Gene symbol	Gene name	*q*-value
Tgfb2	transforming growth factor, beta 2	2.86E-07
Fgf9	fibroblast growth factor 9	5.67E-06
Mapk8	mitogen activated protein kinase 8	1.49E-05
Evi1	ecotropic viral integration site 1	3.05E-05
Pdgfra	platelet derived growth factor receptor, alpha polypeptide	4.59E-05
Ddit3	DNA-damage inducible transcript 3	4.63E-05
Pdgfa	platelet derived growth factor, alpha	1.61E-04
Ikbkg	inhibitor of kappaB kinase gamma	5.91E-04
Rap1b	RAS related protein 1b	6.48E-04
Tgfbr2	transforming growth factor, beta receptor II	6.56E-04
Rasa1	RAS p21 protein activator 1	7.32E-04
Map3k7	mitogen activated protein kinase kinase kinase 7	8.20E-04
Fgf12	fibroblast growth factor 12	8.94E-04
Flnb	filamin, beta	0.001165294
Tgfbr1	transforming growth factor, beta receptor I	0.001166535
Rasa2	RAS p21 protein activator 2	0.001215545
Ppp3ca	protein phosphatase 3, catalytic subunit, alpha isoform	0.001246963
Stk4	serine/threonine kinase 4	0.001354133
Tgfb3	transforming growth factor, beta 3	0.002364518
Il1b	interleukin 1 beta	0.002765324
Stmn1	stathmin 1	0.002968037
Dusp9	dual specificity phosphatase 9	0.003646724
Mapk7	mitogen activated protein kinase 7	0.003757431
Tnfrsf1a	tumor necrosis factor receptor superfamily, member 1a	0.00415812
Prkx	protein kinase, X-linked	0.004502912
Nfkb2	nuclear factor of kappa light polypeptide gene enhancer in B-cells 2, p49/p100	0.004526246
Pla2g12b	phospholipase A2, group XIIB	0.005008582
Mapk14	mitogen activated protein kinase 14	0.005486382
Arrb2	arrestin, beta 2	0.005499632
Map3k7ip2	mitogen-activated protein kinase kinase kinase 7 interacting protein 2	0.005572035
Fgf14	fibroblast growth factor 14	0.005893794
Map2k4	mitogen activated protein kinase kinase 4	0.006352425
Map3k4	mitogen activated protein kinase kinase kinase 4	0.006428794
Rapgef4	Rap guanine nucleotide exchange factor (GEF) 4	0.00646519
B230120H23Rik	RIKEN cDNA B230120H23 gene	0.007287265
Fgfr1	fibroblast growth factor receptor 1	0.008101899
Nfatc2	nuclear factor of activated T-cells, cytoplasmic, calcineurin-dependent 2	0.008135684
Mapk1	mitogen activated protein kinase 1	0.009114735
Casp3	caspase 3	0.01030442
Atf2	activating transcription factor 2	0.010609392
Pdgfrb	platelet derived growth factor receptor, beta polypeptide	0.011061486
Rasgrp1	RAS guanyl releasing protein 1	0.01152764
Pla2g2f	phospholipase A2, group IIF	0.011765433
Map3k5	mitogen activated protein kinase kinase kinase 5	0.013138994
Map4k4	mitogen-activated protein kinase kinase kinase kinase 4	0.013794331
Ntf3	neurotrophin 3	0.015551899
Prkacb	protein kinase, cAMP dependent, catalytic, beta	0.015732516

Gene symbol	Gene name	*q*-value
Fgf13	fibroblast growth factor 13	0.016029769
Nras	neuroblastoma ras oncogene	0.01603981
Crk	v-crk sarcoma virus CT10 oncogene homolog (avian)	0.016282
Cdc42	cell division cycle 42 homolog (S. cerevisiae)	0.016346284
Mapk9	mitogen activated protein kinase 9	0.016360449
Mef2c	myocyte enhancer factor 2C	0.016628602
Ikbkb	inhibitor of kappaB kinase beta	0.017489001
Pak1	p21 (CDKN1A)-activated kinase 1	0.019850033
Stk3	serine/threonine kinase 3 (Ste20, yeast homolog)	0.020054912
Pla2g4a	phospholipase A2, group IVA (cytosolic, calcium-dependent)	0.020689473
Mapk8ip3	mitogen-activated protein kinase 8 interacting protein 3	0.021525545
Ntrk2	neurotrophic tyrosine kinase, receptor, type 2	0.023029898
Map2k1	mitogen activated protein kinase kinase 1	0.023250303
Elk4	ELK4, member of ETS oncogene family	0.023453863
Il1r2	interleukin 1 receptor, type II	0.024099017
Ppm1a	protein phosphatase 1A, magnesium dependent, alpha isoform	0.02798708
Elk1	ELK1, member of ETS oncogene family	0.028133111
Map3k12	mitogen activated protein kinase kinase kinase 12	0.028611936
Grb2	growth factor receptor bound protein 2	0.030613258
Dusp4	dual specificity phosphatase 4	0.031594265
Atf4	activating transcription factor 4	0.032840296
Ptprr	protein tyrosine phosphatase, receptor type, R	0.034302631
Map3k14	mitogen-activated protein kinase kinase kinase 14	0.034493988
Ppp3cb	protein phosphatase 3, catalytic subunit, beta isoform	0.035522355
Map4k3	mitogen-activated protein kinase kinase kinase kinase 3	0.036013688
Map4k1	mitogen activated protein kinase kinase kinase kinase 1	0.037140547
Mapkapk5	MAP kinase-activated protein kinase 5	0.038864042
Tmem37	transmembrane protein 37	0.039176243
Tnik	TRAF2 and NCK interacting kinase	0.040413687
Prkca	protein kinase C, alpha	0.04096107
Sos1	Son of sevenless homolog 1 (Drosophila)	0.041150981
Hspa5	heat shock 70kD protein 5 (glucose-regulated protein)	0.043896851
Ntrk1	neurotrophic tyrosine kinase, receptor, type 1	0.044662799
Rps6ka4	ribosomal protein S6 kinase, polypeptide 4	0.045486593
Srf	serum response factor	0.048518972
Pdgfb	platelet derived growth factor, B polypeptide	0.049732811

Table 6. Genes from MAPK pathways affected as defined by $q<0.05$ in hearts from *Lmna*$^{H222P/+}$ mice.

Gene symbol	Gene name	*q*-value
Fgf12	fibroblast growth factor 12	3.60E-06
Evi1	ecotropic viral integration site 1	1.08E-04
Raf1	v-raf-leukemia viral oncogene 1	1.11E-04
Tgfbr2	transforming growth factor, beta receptor II	2.29E-04
B230120H23Rik	RIKEN cDNA B230120H23 gene	2.45E-04
Ppm1a	protein phosphatase 1A, magnesium dependent, alpha isoform	2.59E-04
Stmn1	stathmin 1	2.64E-04
Mapk8	mitogen activated protein kinase 8	2.69E-04
Fgf10	fibroblast growth factor 10	4.00E-04
Rasgrp1	RAS guanyl releasing protein 1	4.05E-04
Map3k7ip2	mitogen-activated protein kinase kinase kinase 7 interacting protein 2	4.59E-04
Pdgfra	platelet derived growth factor receptor, alpha polypeptide	4.98E-04
Rap1b	RAS related protein 1b	6.48E-04
Dusp9	dual specificity phosphatase 9	6.53E-04
Srf	serum response factor	7.34E-04
Flnb	filamin, beta	8.02E-04
Map3k5	mitogen activated protein kinase kinase kinase 5	0.00121393
Pak1	p21 (CDKN1A)-activated kinase 1	0.001274338
Tgfb2	transforming growth factor, beta 2	0.001350584
Rasa2	RAS p21 protein activator 2	0.001385751
Rasgrf1	RAS protein-specific guanine nucleotide-releasing factor 1	0.001568889
Fgfr1	fibroblast growth factor receptor 1	0.001913437
Mapk1	mitogen activated protein kinase 1	0.001942955
Tnfrsf1a	tumor necrosis factor receptor superfamily, member 1a	0.002375645
Rasa1	RAS p21 protein activator 1	0.002487897
Pdgfa	platelet derived growth factor, alpha	0.002639407
Stk4	serine/threonine kinase 4	0.002681895
Map4k3	mitogen-activated protein kinase kinase kinase kinase 3	0.002754704
Traf6	Tnf receptor-associated factor 6	0.003022471
Map2k1	mitogen activated protein kinase kinase 1	0.003068013
Ntrk2	neurotrophic tyrosine kinase, receptor, type 2	0.003238241
Arrb2	arrestin, beta 2	0.003281171
Map3k12	mitogen activated protein kinase kinase kinase 12	0.003364804
Ppp3ca	protein phosphatase 3, catalytic subunit, alpha isoform	0.0043393
Ikbkb	inhibitor of kappaB kinase beta	0.004378057
Fgf9	fibroblast growth factor 9	0.004713371
Tgfbr1	transforming growth factor, beta receptor I	0.004829289
Nf1	neurofibromatosis 1	0.004963115
Il1r2	interleukin 1 receptor, type II	0.005098257
Tmem37	transmembrane protein 37	0.005264078
Fgfr4	fibroblast growth factor receptor 4	0.005404511
Elk4	ELK4, member of ETS oncogene family	0.005409921
Pla2g4a	phospholipase A2, group IVA (cytosolic, calcium-dependent)	0.005475986
Prkaca	protein kinase, cAMP dependent, catalytic, alpha	0.005507381
Dusp7	dual specificity phosphatase 7	0.00564084
Map2k7	mitogen activated protein kinase kinase 7	0.006080179
Atf4	activating transcription factor 4	0.006608756
Stk3	serine/threonine kinase 3 (Ste20, yeast homolog)	0.006703101
Casp4	caspase 4, apoptosis-related cysteine peptidase	0.00719374

Gene symbol	Gene name	*q*-value
Map3k7	mitogen activated protein kinase kinase kinase 7	0.007929567
Ptpn5	protein tyrosine phosphatase, non-receptor type 5	0.008807588
Map3k14	mitogen-activated protein kinase kinase kinase 14	0.008979205
Il1b	interleukin 1 beta	0.009114094
Egf	epidermal growth factor	0.009371844
Ikbkg	inhibitor of kappaB kinase gamma	0.009464352
Map2k6	mitogen activated protein kinase kinase 6	0.009745366
Map2k1ip1	mitogen-activated protein kinase kinase 1 interacting protein 1	0.010073412
Acvr1b	activin A receptor, type 1B	0.010415173
Map4k4	mitogen-activated protein kinase kinase kinase kinase 4	0.010658562
Rap1a	RAS-related protein-1a	0.01069035
Mapk9	mitogen activated protein kinase 9	0.010733895
Map3k7ip1	mitogen-activated protein kinase kinase kinase 7 interacting protein 1	0.011029738
Map3k4	mitogen activated protein kinase kinase kinase 4	0.011082817
Kras	v-Ki-ras2 Kirsten rat sarcoma viral oncogene homolog	0.011178974
Casp14	caspase 14	0.011191381
Dusp4	dual specificity phosphatase 4	0.011423174
Casp1	caspase 1	0.01143588
Nfatc2	nuclear factor of activated T-cells, cytoplasmic, calcineurin-dependent 2	0.013223984
Rapgef4	Rap guanine nucleotide exchange factor (GEF) 4	0.01378897
Nr4a1	nuclear receptor subfamily 4, group A, member 1	0.014080154
Map3k3	mitogen activated protein kinase kinase kinase 3	0.014893574
Hspa1l	heat shock protein 1-like	0.015984548
Ntf3	neurotrophin 3	0.016139683
Fgf14	fibroblast growth factor 14	0.017407472
Fasl	Fas ligand (TNF superfamily, member 6)	0.018752911
Mef2c	myocyte enhancer factor 2C	0.019680604
Ppp3cb	protein phosphatase 3, catalytic subunit, beta isoform	0.020361974
Fgf22	fibroblast growth factor 22	0.021250778
Casp6	caspase 6	0.022509927
Mknk1	MAP kinase-interacting serine/threonine kinase 1	0.023706562
Sitpec	signaling intermediate in Toll pathway-evolutionarily conserved	0.02385116
Mapk13	mitogen activated protein kinase 13	0.024399541
Fgfr2	fibroblast growth factor receptor 2	0.024557857
Chuk	conserved helix-loop-helix ubiquitous kinase	0.025051891
Casp9	caspase 9	0.025852039
Mknk2	MAP kinase-interacting serine/threonine kinase 2	0.026408231
Fgf1	fibroblast growth factor 1	0.027300185
Atf2	activating transcription factor 2	0.027981699
Ikbke	inhibitor of kappaB kinase epsilon	0.028390773
Akt3	thymoma viral proto-oncogene 3	0.029365859
Pla2g12b	phospholipase A2, group XIIB	0.029772852
Prkcb1	protein kinase C, beta 1	0.030051395
Nlk	nemo like kinase	0.032550417
Nfkb1	nuclear factor of kappa light chain gene enhancer in B-cells 1, p105	0.03400866
Ntf5	neurotrophin 5	0.035237338
Ppm1b	protein phosphatase 1B, magnesium dependent, beta isoform	0.035547733
Pak2	p21 (CDKN1A)-activated kinase 2	0.03714335
Ppp3r2	protein phosphatase 3, regulatory subunit B, alpha isoform (calcineurin B, type II)	0.038363453

Gene symbol	Gene name	*q*-value
Ntrk1	neurotrophic tyrosine kinase, receptor, type 1	0.039271939
Mapk8ip3	mitogen-activated protein kinase 8 interacting protein 3	0.039579867
Daxx	Fas death domain-associated protein	0.0396163
Prkcc	protein kinase C, gamma	0.039729139
Mapkapk2	MAP kinase-activated protein kinase 2	0.040014548
Crk	v-crk sarcoma virus CT10 oncogene homolog (avian)	0.040886872
Nras	neuroblastoma ras oncogene	0.042562889
Pla2g6	phospholipase A2, group VI	0.042567554
Nfatc4	nuclear factor of activated T-cells, cytoplasmic, calcineurin-dependent 4	0.044083907
Fgf5	fibroblast growth factor 5	0.044422804
Map4k2	mitogen activated protein kinase kinase kinase kinase 2	0.045341238
Hspb1	heat shock protein 1	0.045691236
Ptprr	protein tyrosine phosphatase, receptor type, R	0.049859977

Examination of MAPK Inhibition on Gene Expression in Cells with LMNA Mutations

[00115] Cells transfected with plasmids encoding wild type Lamin A, Lamin A mutants that cause EDMD and other "control" Lamin A mutants that cause lipodystrophy or progeria are treated with either SP600125, PD98059, both together or vehicle (DMSO). To detect JNK and ERK activation, transfected cells are lysed in Laemmli extraction buffer (92) for subsequent immunoblotting and fixed in ice cold methanol for subsequent fluorescence microscopy. To assess activated (phosphorylated) JNK and ERK1/2 by immunoblotting, proteins in cell extracts are separated by SDS-PAGE, transferred to nitrocellulose membranes and detected using antibodies that recognize ERK1/2 (Santa-Cruz), phosphorylated ERK1/2 (Cell Signaling), JNK1 (Santa-Cruz) and phosphorylated JNK1 (Cell Signaling). Recognized proteins are visualized by enhanced chemiluminescence (ECL- Amersham). Antibodies against β-tubulin are used as an internal control to normalize the amounts of protein between blots. Immunoblotting results are quantified as the ratio of signal between the protein of interest and signal of β-tubulin using Scion NIH Image software.

[00116] To assess nuclear translocation of JNK and ERK1/2, fixed cells are incubated with the same antibodies, washed, incubated with Texas Red conjugated secondary antibodies and examined by fluorescence microscopy. GFP fluorescence is simultaneously recorded to know which cells are transfected. Fluorescence microscopy is performed on a Microphot SA (Nikon) microscope attached to a Spot RT Slide camera (Diagnostic Instruments). Transiently transfected cells have been adequate for previous studies to carry out these types of experiments, but, if necessary, stably transfected cell lines expressing A-type lamins can be used, as previously described (90). To measure activation of downstream targets of

activated JNK and ERK, luciferase reporter systems for c-Jun and Elk-1, respectively, are used (Path Detect In Vivo Signal Transduction Pathway Trans-Reporting System; Stratagene). Cells are cultured in the presence of SP600125, PD98059, both or vehicle and transfected with pegfp-N1 constructs encoding wild type and mutant lamins, pFA2-cJun or pFA2-Elk-1 (Stratagene) and pFR-Luc (Stratagene). To correct for transfection efficiency, a plasmid encoding β-galactosidase is co-transfected. After 24 hours, cells are trypsinized, protein lysates obtained and luciferase activity measured using a luminometer.

Example 2. MAP Kinase Inhibition Prevents Cardiomyopathies

Methods

Inhibitors

[00117] PD98059 (Calbiochem) and SP600125 (Calbiochem) were dissolved in Dimethyl Sulfoxide (DMSO, Sigma) at a concentration of 0.5 mg/ml and were delivered to a dose of 3 mg/kg/day for 5 days a week. U0126 (Cat. #662005 EMD Biosciences) and MEK1/2 (Cat. #444939 EMD Biosciences) were also dissolved in DMSO and delivered 5 days a week. The placebo control consisted of DMSO alone. Placebo and inhibitors were administered by intraperitoneal injection using a $27_G{}^5/_8$ syringe. Treatment was started when mice were 8 weeks of age and continued until 16 weeks of age.

Mice

[00118] *Lmna* H222P knock-in mice were generated and genotyped as described (14). Genotyping of mice for the *Lmna* H222P allele was performed by PCR using oligonucleotides 5'-CAGCCATCACCTCTCCTTTG-3' and 5'-AGCACCAGGGAGAGGACAGG-3'. $Lmna^{H222P/H222P}$ mice were separated by sex and were given either vehicle alone (DMSO), the MEK inhibitor PD98059 alone, the JNK inhibitor SP600125 alone, both PD98059 and SP600125 together, the MEK inhibitor U0126 alone, or theMEK inhibitor MEK1/2 alone. All the mice were fed on a chow diet and housed in a barrier facility. The Institutional Animal Care and Use Committee at Columbia University Medical Center approved the use of animals in the study protocol.

Protein Extraction and Western Blots

[00119] Hearts were excised from mice at 16-weeks of age and were homogenized in RIPA extraction buffer (Cell Signalling) containing protease inhibitors (25 mg/ml aprotinin and 10 mg/ml leupeptin). Protein samples were subjected to SDS-PAGE, transferred to nitrocellulose membranes and blotted with primary antibodies against ERK1/2 (Santa-Cruz), phosphorylated ERK1/2 (Cell Signaling), JNK (Santa-Cruz), natriuretic peptide precursor A (Santa-Cruz), phosphorylated JNK (Cell Signaling), and Gapdh (Ambion). Secondary antibodies were HRP–conjugated (Amersham). Recognized proteins were visualized by enhanced chemiluminescence (ECL, Amersham). The signal generated using an ntibody against Gapdh was used as internal controls to normalize the amounts of protein between immunoblots.

RNA Isolation and Quantitative Real-Time RT-PCR Analysis

[00120] Total RNA was extracted using the Rneasy isolation kit (Qiagen) as previously described (96). cDNA was synthesized as previously described (96) using Omniscript Reverse Transcriptase (Qiagen) on total cellular RNA. For each replicate in each experiment, RNA from tissue samples of different animals was used. Primers were designed that correspond to mouse RNA sequences using Primer3 (http://frodo.wi.mit.edu/cgi-bin/primer3/primer3_www.cgi). The real-time RT-PCR reaction contained iQ SYBR green super mix (Bio-Rad), 200 nM of each primer and 0.2 μl of template in a 25 μl reaction volume. Amplification was carried out using appropriate primers and the MyiQ Single-Color Real-Time PCR Detection System (Bio-Rad) with an initial denaturation at 95°C for 2 min followed by 50 cycles at 95°C for 30 s and 62°C for 30 s. Relative levels of mRNA expression were calculated using the CT method (67). Individual expression values were normalized by comparison with *Gapdh* mRNA.

Pathological Analysis of Hearts

[00121] Mice were sacrificed at 16 weeks of age and freshly removed hearts were fixed in 4% formaldehyde for 48 hours, embedded in paraffin, sectioned at 5 μm and stained with hematoxylin and eosin and Masson's trichrome. Representative stained sections were photographed using a Microphot SA (Nikon) light microscope attached to a Spot RT Slide camera (Diagnostic Instruments). Images were processed using Adobe Photoshop 6.0 (Adobe Systems). Length of cardiomyocytes was measured using Scion Image software (Scion Corporation). Data were reported as means ± standard deviations and are compared with respective controls using a two-tailed *t* test.

Transthoracic Echocardiography

[00122] At 16 weeks of age, mice were anesthetized with 1.5% isoflurane in O_2 and placed on a heating pad (37°C). Cardiac function was assessed by echocardiography with a Visualsonics Vevo 770 ultrasound with a 30-MHz transducer applied to the chest wall. Cardiac ventricular dimensions and ejection fraction were measured in 2D-mode and M-mode three times for the number of animals indicated. A "blinded" echocardiographer, unaware of the genotype or treatment, performed the examinations.

Statistical analysis

[00123] To determine significant differences between groups of animals analyzed by echocardiography, we used one-way analysis of variance (ANOVA). For each parameter, there was a global effect between different groups ($p<0.001$). This indicated that at least one group had significantly different results than another. We then used a Tukey adjustment for post hoc multiple comparisons (5% error type I) to determine which groups were significantly different. Homogeneity of variances between groups was validated using Levene test (alpha = 0.05). Normality of residuals was validated using Shapiro-Wilk test. To validate all results, non-parametric tests (Kruskal-Wallis and Mann-Whitney) were performed and concordance checked. Other statistical methods used are described in the figure legends.

Systemic Treatment of Lmna$^{H222P/H222P}$ Mice with PD98050 Inhibits ERK Activity in Heart

[00124] We have demonstrated previously abnormal activation of the extracellular signal-regulated kinase (ERK) branch of the mitogen-activagted protein kinase (MAPK) signaling cascade in hearts of *Lmna* H222P "knock in" mice, a model of autosomal Emery-Dreifuss muscular dystrophy (96). Male *Lmna*$^{H222P/H222P}$ mice develop left ventricular (LV) dilatation and depressed contractile function starting at approximately 8 to 10 weeks of age and invariably develop LV dilatation and decreased cardiac contractility at 16 weeks of age, typically dying between 16 and 36 weeks (14). Based on our observations that ERK is activated in these mice prior to the onset of clinically detectable cardiomyopathy as well as our demonstration that lamin A variants that cause striated muscle disease activate ERK when expressed in cultured cells, we hypothesized that activation of ERK plays a primary pathogenic role in the development of cardiomyopathy (96).

[00125] We further hypothesized that pharmacological inhibition of ERK would prevent or delay development of dilated cardiomyopathy in *Lmna*$^{H222P/H222P}$ mice. To test this hypothesis, we treated *Lmna*$^{H222P/H222P}$ with compounds that inhibits MAPK/ERK kinase (MEK), thereby preventing phosphorylation (activation) of ERK (83). Here we report results of an analysis, using hearts from a mouse model of EDMD, exploring effects of an A-type lamin mutation on gene expression and signaling pathways involved in development of cardiomyopathy.

[00126] We administered PD98059, at a dose of 3 mg/kg/day or 6 mg/kg/day, or placebo (dimethylsulfoxide; DMSO) by intraperitoneal injection 5 days a week to male homozygous

Lmna mutant mice (*Lmna*$^{H222P/H222P}$). PD98059 is a commercially available, potent and selective inhibitor of MEK. PD98059 mediates its inhibitory properties by binding to MEK, therefore preventing phosphorylation of ERK1/2. A comparable dose of PD98059 administered systematically has been shown to inhibit ERK activity in rat hearts (132). The doses of inhibitors used were also in the same range as those previously shown for MAPK inhibitor to be effective on the development of heart failure in the hamster (4).

[00127] Treatment was initiated at 8 weeks of age and continued until the mice were 16 weeks of age. At 16 weeks of age, the mice were analyzed by echocardiography and then sacrificed for histological and biochemical studies. Untreated male *Lmna*$^{+/+}$ and *Lmna*$^{H222P/H222P}$ mice were similarly analyzed for comparisons.

[00128] Systemic administration of PD98059 to mice inhibited phosphorylation of ERK1 and ERK2 in hearts, as shown by immunoblotting of proteins in tissue homogenates with antibodies against phoshorylated ERK1/2 and total ERK1/2 (Figures 11 and 12A). The inhibition was specific of ERK1/2 relative to Jun N-terminal kinase (JNK), as at a dose of 3 mg/kg/day we did not observe inhibition of JNK signaling in heart. To confirm inhibition of ERK1/2 signaling, we monitored the expression of selected downstream genes activated by the kinases using real-time RT-PCR. As expected, inhibition of phosphorylation of ERK1/2 lead to decreased expression of *Elk1*, *Elk4*, *Atf2* and *Atf4* (Figure 12B).

Systemic Treatment of Lmna$^{H222P/H222P}$ *Mice with SP600125 Inhibits JNK Activity in Heart*

[00129] We administered a JNK inhibitor, SP600125, to male *Lmna*$^{H222P/H222P}$ mice as described above. SP600125 is a commercially available inhibitor of JNK. SP600125 blocked the phosphorylation of JNK but did not block the phosphorylation of ERK1/2. We also administered the PD98059 and SP600125 inhibitors together. SP600125 inhibits the phosphorylation of its targets in heart when administered systemically to mice, as shown by western blots of phosphorylated JNK and total JNK (Figure 11).

Treatment with PD98050 and/or SP600125 Prevents Development of Cardiomyopathy

[00130] A feature of dilated cardiomyopathy is the up-regulation of cardiac hormones such as natriuretic peptides (17, 55, 133). Up-regulation of genes involved in sarcomere organization also occurs in dilated cardiomyopathies (18, 55, 134). In hearts from untreated *Lmna*$^{H222P/H222P}$ mice and those treated with placebo, expression of natriuretic peptide precursor A was significantly increased (Figure 13A). In contrast, PD98059-treated

Lmna$^{H222P/H222P}$ mice had a cardiac expression of this peptide similar to *Lmna*+/+ mice (Figure 13A). In hearts from untreated *Lmna*$^{H222P/H222P}$ mice and *Lmna*$^{H222P/H222P}$ mice treated with placebo, expression of *Nppa* and *Nppb* mRNAs encoding natriuretic peptide precursors as well as *Myl4* and *Myl7* mRNAs encoding myosin light chains was significantly increased (Figure 13B). In contrast, PD98059-treated *Lmna*$^{H222P/H222P}$ mice had a cardiac expression of *Nppa*, *Nppb*, *Myl4* and *Myl7* similar to *Lmna*$^{+/+}$ mice (Figure 13B).

[00131] *Lmna*$^{H222P/H222P}$ mice invariably develop dilated cardiomyopathy by 12 weeks of age. We monitored dilation as well as dynamic of the left ventricle in absence or presence of PD98059, SP600125 or both PD98059 and SP600125 in *Lmna*$^{H222P/H222P}$ mice. At 16 weeks, *Lmna*$^{H222P/H222P}$ mice developed left ventricle (LV) dilation. LV dilatation in male *Lmna*$^{H222P/H222P}$ mice at 16 weeks of age was demonstrated by histopathological analysis (Figure 14A). At this age, there was no significant cardiomyocyte disarray or cardiac fibrosis on light microscopic examination.

[00132] As would be measured to confirm cardiomyopathy in humans, we used M-mode transthoracic echocardiography to measure three important parameters of dilation of the LV: left ventricle end systolic diameter (LVESD) and left ventricle end diastolic diameter (LVEDD), the ejection fraction (EF), and the fractional shortening (FS). We also measured thickness of the left ventricular posterior wall (LVPW) and the interventricular septum diameter (IVSD). Treatment with PD98059 prevented development of LV dilatation as measured by histopathology and echocardiography (Fig. 14). Treatment with SP600125 prevented development of LV dilatation as measured by echocardiography (Table 7). *Lmna*$^{H222P/H222P}$ mice showed increased left ventricular end systolic and end diastolic diameters compared to *Lmna*$^{+/+}$ mice (Figure 14B).

[00133] Cardiac and structure and function were further assessed by echocardiography at 16 weeks of age in a total of 43 living mice in the 5 different groups studied (Table 7). Compared to *Lmna*$^{+/+}$ mice, *Lmna*$^{H222P/H222P}$ mice had significantly increased LV end diastolic and end systolic diameters. They also had decreased cardiac contractility indicated by reduced ejection fraction and LV fractional shortening. Ejection fraction in *Lmna*$^{H222P/H222P}$ mice was decreased by approximately 30% compared to *Lmna*$^{+/+}$ mice at 16 weeks age (73.12 ± 6.69 percent vs. 50.78 ± 9.12 percent; $p<0.005$). *Lmna*$^{H222P/H222P}$ mice treated with DMSO had ventricular chamber diameters, ejection fraction and LV fractional shortening similar to

untreated *Lmna*$^{H222P/H222P}$ mice. *Lmna*$^{H222P/H222P}$ mice treated with PD98059 had normal cardiac contractility with ejection fraction and LV fractional shortening virtually identical to *Lmna*$^{+/+}$ mice. With 100% accuracy in real-time, a "blinded" echocardiographer unaware of the genotype or treatment received classified all *Lmna*$^{+/+}$ mice and *Lmna*$^{H222P/H222P}$ mice receiving PD98059 as having normal cardiac function and all *Lmna*$^{H222P/H222P}$ mice that were untreated or treated with placebo as having abnormal cardiac function. Hence, treatment with PD98059 or SP600125 for 8 weeks prevented the development of LV dilatation and cardiac contractile dysfunction in *Lmna*$^{H222P/H222P}$ mice.

[00134] Alterations in nuclear morphology, including abnormal elongation of nuclei, have been described in hearts of mice deficient in A-type lamins that develop dilated cardiomyopathy (108). We observed similar elongation of nuclei in cardiomyocytes of 16 week-old *Lmna*$^{H222P/H222P}$ mice. Treatment with PD98059 prevented this alteration. Nuclei in cardiomyocytes of *Lmna*$^{+/+}$ mice had a well-rounded oval shape whereas nuclei in cardiomyocytes of *Lmna*$^{H222P/H222P}$ mice had an abnormally elongated shape (Figure 15A). Cardiomyocyte nuclei in *Lmna*$^{H222P/H222P}$ mice treated with PD98059 but not placebo had an overall shape that was similar to those in *Lmna*$^{+/+}$ mice (Figure 15A). Means lengths of cardiomyocyte nuclei in untreated and placebo-treated *Lmna*$^{H222P/H222P}$ mice were significantly longer than in *Lmna*$^{+/+}$ mice and *Lmna*$^{H222P/H222P}$ mice treated with PD98059 (Figure 15B).

[00135] Overall, LV diameters, cardiomyocyte nuclear morphology and cardiac ejection fraction were normal in *Lmna*$^{H222P/H222P}$ mice treated with PD98059 at an age when untreated and placebo-treated mice had significant abnormalities in these parameters. Enhanced synthesis of natriuretic peptides and sarcomeric proteins was also prevented. Treatment with an inhibitor of ERK activation therefore delayed the development of significant cardiomyopathy in mice with an *Lmna* mutation that causes Emery-Dreifuss muscular dystrophy in humans.

Table 7. Echocardiographic data at 16 weeks of age for *Lmna*$^{+/+}$ (WT) mice and *Lmna*$^{H222P/H222P}$ mice

Genotype	n	LVEDD (mm)	LVESD (mm)	LVPW (mm)	IVSD (mm)	EF (%)	FS (%)
Lmna$^{+/+}$	12	3.45 ± 0.42	2.00 ± 0.36	0.71 ± 0.10	0.70 ± 0.13	73.12 ± 6.69	41.72 ± 5.76
Lmna$^{H222P/H222P}$ (mock)	6	4.14 ± 0.27##	3.25 ± 0.45##	0.82 ± 0.12	0.70 ± 0.05	50.78 ± 9.12##	25.82 ± 5.70##
Lmna$^{H222P/H222P}$ (DMSO)	5	3.89 ± 0.14#	3.04 ± 0.32##	0.75 ± 0.08	0.69 ± 0.02	52.70 ± 9.03##	26.96 ± 5.68##

Lmna$^{H222P/H222P}$ (PD98059)	7	3.12 ± 0.20**	1.82 ± 0.16**	0.77 ± 0.10	0.69 ± 0.06	73.52 ± 4.68**	41.55 ± 4.29**
Lmna$^{H222P/H222P}$ (SP600125)	13	3.46 ± 0.27**	2.30 ± 0.45**	0.73 ± 0.08	0.72 ± 0.07	69.24 ± 9.59**	38.70 ±7.38**
Lmna$^{H222P/H222P}$ (PD98059 + SP600125)	7	3.65 ± 0.35	2.43 ± 0.37#			71.13 ±6.66	38.33 ± 7.24
Lmna$^{H222P/H222P}$ (U0126)§	3	3.54 ± 0.16	2.47 ± 0.09	0.69 ± 0.11	0.64 ± 0.03	62.83 ± 4.09	33.79 ± 3.10
Lmna$^{H222P/H222P}$ (MEK1/2)§	2	3.77 ± 0.32	2.62 ± 0.28	0.69 ± 0.08	0.60 ± 0.00	64.43 ± 0.77	34.50 ± 0.36

LVEDD: left ventricle end diastolic diameter; LVESD: left ventricle end systolic diameter; LVPW: left ventricular posterior wall; IVSD: interventricular septum diameter; EF: ejection fraction; FS: fractional shortening.

"Mock" indicates untreated *Lmna*$^{H222P/H222P}$ mice. "DMSO" indicates *Lmna*$^{H222P/H222P}$ mice treated only with vehicle.

Values are means ± standard deviations.

*: $p<0.05$ versus *Lmna*$^{H222P/H222P}$ (DMSO); **: $p<0.01$ versus *Lmna*$^{H222P/H222P}$ (DMSO)

#: $p<0.05$ versus *Lmna*$^{+/+}$; ##: $p<0.01$ versus *Lmna*$^{+/+}$

§ Statistical analysis is not provided for U0126 and MEK1/2 due to the small n.

[00136] Our results support the hypothesis that ERK and JNK activation induced by abnormalities in A-type lamins is a pathogenic mechanism in the generation of cardiomyopathy. For example, we demonstrated inhibition of ERK phosphorylation and attenuated activation of downstream genes when PD98059 was administered systemically to *Lmna*$^{H222P/H222P}$ mice. Concurrent with this inactivation of ERK signaling in heart we documented normal LV diameters, normal cardiomyocyte nuclear morphology and normal cardiac ejection fraction in *Lmna*$^{H222P/H222P}$ mice treated with PD98059 at an age when untreated and placebo-treated mice had significant abnormalities in these parameters. These results are consistent with our findings that ERK is abnormally activated in cardiomyocytes of *Lmna*$^{H222P/H222P}$ mice and cells expressing lamin A variants found in human subjects with cardiomypathy (96). Results from Favreau et al. (135) using cultured myoblasts also suggest that the nuclear lamina may serve as scaffold for substrates of the MEK-ERK pathway and that this may be impeded by A-type lamin alterations resulting from *LMNA* mutations that cause Emery-Dreifuss muscular dystrophy.

Example 3. MAP Kinase Inhibition Improves Cardiac Function in Existing Cardiomyopathies

[00137] Using the methods described in Example 2, we treated *Lmna*$^{H222P/H222P}$ mice with PD98059 alone or SP600125 alone, starting at 16 weeks of age, when ejection fraction has already deteriorated and left ventricular end diastolic diameter is increased, until 20 weeks of

age. Treatment with each of these prevented further deterioration in cardiac function (Table 8), suggesting that JNK and ERK inhibition can prevent further deterioration in cardiac function once clinically apparent cardiomyopathy is present.

Table 8. Echocardiographic data at 20 weeks of age for *Lmna*$^{+/+}$ (WT) mice and *Lmna*$^{H222P/H222P}$ mice

Genotype	n	LVEDD (mm)	LVESD (mm)	LVPW (mm)	IVSD (mm)	EF (%)	FS (%)
Lmna$^{+/+}$	12	3.50 ± 0.22	2.07 ± 0.28	0.81 ± 0.10	0.77 ± 0.07	73.21 ± 4.06	41.71 ± 3.50
Lmna$^{H222P/H222P}$ (mock)	7	4.43 ± 0.79##	3.80 ± 1.06##	0.67 ± 0.09	0.62 ± 0.06	43.82 ± 20.41##	22.49 ± 12.08##
Lmna$^{H222P/H222P}$ (DMSO)	22	3.87 ± 0.50#	3.00 ± 0.61##	0.64 ± 0.13	0.63 ± 0.11	53.87 ± 12.12##	27.86 ± 7.22##
Lmna$^{H222P/H222P}$ (PD98059)	19	3.55 ± 0.50	2.41 ± 0.50**#	0.69 ± 0.08	0.66 ± 0.05	65.46 ± 11.49**#	35.91 ± 8.21**
Lmna$^{H222P/H222P}$ (SP600125)	26	3.73 ± 0.42	2.67 ± 0.49*##	0.66 ± 0.09	0.63 ± 0.07	61.88 ± 8.46**##	33.11 ± 5.92**##

LVEDD: left ventricle end diastolic diameter; LVESD: left ventricle end systolic diameter; LVPW: left ventricular posterior wall; IVSD: interventricular septum diameter; EF: ejection fraction; FS: fractional shortening.

Comparison between groups was performed using one-way ANOVA and Tukey adjustment for post hoc multiple comparison (5% type I error). Conditions of homogeneity of variances were validated and non-parametric tests were performed to validate results.

Values are means ± standard deviations.

*: $p<0.05$ versus *Lmna*$^{H222P/H222P}$ (DMSO); **: $p<0.01$ versus *Lmna*$^{H222P/H222P}$ (DMSO)

#: $p<0.05$ versus *Lmna*$^{+/+}$; ##: $p<0.01$ versus *Lmna*$^{+/+}$

Further Clinical Assessment of Knock-in Mice

[00138] We examine effects of JNK and ERK inhibitors on heart function and survival in *Lmna*$^{H222P/H222P}$ mice. Male *Lmna*$^{H222P/H222P}$ and *Lmna*$^{+/+}$ mice are treated with SP600125, PD98059, both or placebo as described above. We begin treatment at 8 weeks of age. Mice are assessed by electrocardiography prior to starting treatment and at 2 weeks, 8 weeks, 16 weeks and 24 weeks after treatment (10 weeks, 16 weeks, 24 weeks and 32 weeks of age, respectively). Ages of 10, 16 and 24 weeks correspond to those at which MAP kinase activities are assessed. Blood is drawn at these times for analysis of complete blood count, routine chemistries and cardiac enzymes. Male *Lmna*$^{H222P/H222P}$ mice typically begin to develop abnormalities detected by echocardiography starting at 8 weeks of age and conduction system abnormalities, primarily an increased PR interval, at 12 weeks of age. If *Lmna*$^{H222P/H222P}$ mice survive beyond 32 weeks of age (medial survival is 28 weeks), analyses continue to be performed at 2 to 4 week intervals in these mice and Lmna+/+ controls.

Kaplan-Meier analysis (95) is performed to compare survival between groups. For electrocardiography, transmitters are placed in the abdominal region under anesthesia with ketamine, xylazine and midazolam. Signals are sent to a computer for display and analysis. Telemetric electrocardiography tracings are also obtained in conscious mice during quiet awake time at daytime, and PR intervals and QRS durations are measured.

[00139] Results demonstrating that MAP kinase inhibition provides a clinical benefit in an animal model of autosomal dominant EDMD pave the way for testing in human subjects and provides a model for drug discovery for the treatment of neuromuscular disorders in which the pathogenesis is unclear.

Example 4. Reduced expression of A-type lamins and emerin activates ERK signaling pathway in cell lines

[00140] Mutations in genes encoding ubiquitously expressed A-type lamins and emerin, proteins of the nuclear envelope, respectively cause autosomal and X-linked Emery-Dreifuss muscular dystrophy (EDMD), which affects skeletal and cardiac muscles. We identified an activation of extracellular signal-regulated kinase (ERK), a branch of the MAP kinase signaling pathway, in hearts from mouse models of these two forms of EDMD, which could explain the pathogenesis of the disease. To examine the relation between the nuclear envelope and the activation of ERK, we studied the effect of decreasing A-type lamins and emerin using model mice and siRNA technology.

[00141] Loss of A-type lamins in mouse heart leads to the activation of ERK. We showed that knock-down of A-type lamins and emerin in HeLa and C2C12 cells using siRNA duplexes induced phosphorylation of ERK and activation of downstream transcription factors. The use of a specific MAPK/ERK kinase (MEK) inhibitor abolished this abnormal activation.

[00142] Our results further demonstrate that abnormalities in the expression of nuclear envelope proteins lead to activation of ERK signaling. This has potential implications for pharmacological therapy of EDMD.

Methods

Mice

[00143] *Lmna*$^{-/-}$ mice were generated and genotyped as described [11]. Hearts were isolated from male *Lmna*$^{-/-}$ and *Lmna*$^{+/+}$ mice at 5 weeks of age. For immunoblotting and real-time RT-PCR experiments, *Lmna*$^{-/-}$ and *Lmna*$^{+/+}$ mice were compared directly to *Lmna*$^{+/+}$ littermates.

Cell Culture

[00144] Human HeLa cells and mouse C2C12 cells were maintained in a 5% CO_2 atmosphere at 37°C. The cells were cultured in Dulbecco's modified Eagle's medium supplemented with 10% calf bovine serum and 0.1% gentamicin.

siRNA

[00145] One day before transfection, HeLa and C2C12 cells were trypsinized, diluted with fresh medium without antibiotics and transferred to 24-well plates. Transient transfection of siRNAs was carried out using Oligofectamine (Invitrogen) as recommended by the manufacturer. Cells were preincubated in 7.5 µl OPTIMEM 1 medium (Life Technologies) and 2 µl Oligofectamine per well for 5 minutes at room temperature. During the time of this incubation, 40 µl OPTIMEM 1 medium were mixed with 2.5 µl siRNA. The two mixtures were combined and incubated for 20 minutes at room temperature for complex formation. The entire mixture was added to the cells in one well resulting in a final concentration of 50 pM for the siRNAs. Cells were assayed 72 hours after transfection for HeLa cells and 48 hours after transfection for C2C12 cells. Reduction of expression of targeted genes was confirmed in at least 3 independent experiments.

RNA Extraction

[00146] At 80% confluence, media was removed from cultures and total RNA was extracted using the Rneasy isolation kit (Qiagen) according to the manufacturer's instructions. Adequacy and integrity of extracted RNA were determined by gel electrophoresis. Concentrations were measured by ultraviolet absorbance spectroscopy.

Indirect Immunofluorescence Microscopy

[00147] HeLa and C2C12 cells were grown on coverslips and washed with phosphate-buffered saline (PBS). Cells were fixed for 10 minutes in methanol at -20°C. HeLa and C2C12 cells were then incubated with the primary antibody in PBS for 1 hour at room

temperature. Primary antibody used was anti-pERK polyclonal (1:100, Cell Signaling). Cells were then washed with PBS and incubated with Texas Red conjugated goat anti-rabbit secondary antibody in PBS (Molecular Probes). Cells were washed with PBS and slides mounted in Mowiol (Santa-Cruz Biotechnologies) with 0.1 μg/ml 4',6-diamidino-2-phenylindole (dapi). Immunofluorescence microscopy was performed using an Axiophot microscope (Carl Zeiss). Micrographs were processed using Adobe Photoshop 6.0 (Adobe Systems).

Real-Time RT-PCR

[00148] Primers were designed corresponding to RNA sequences using Primer3 (http://frodo.wi.mit.edu/cgi-bin/primer3/primer3_www.cgi). RNA was extracted using Rneasy Protect Kit (Qiagen) and subsequently reverse transcribed using SuperScript First-Strand Synthesis System according to the manufacturer's instructions (Invitrogen). Each reaction contained iQ SYBR green super mix (Bio-Rad), 200 nM of primers and 0.2 μl of template in a 25 μl reaction volume. Amplification was carried out using the MyiQ Single-Color Real-Time PCR Detection System (Bio-Rad) with incubation times of 2 minutes at 95°C, followed by 50 cycles of 95°C for 30 seconds and 62°C for 30 seconds. Specificity of the amplification was checked by melting-curve analysis. Relative levels of mRNA expression were calculated according to the $\Delta\Delta C_T$ method, normalized by comparison to *Gapdh* mRNA expression.

Western Blot Analysis

[00149] HeLa and C2C12 cells were harvested from each culture, washed with ice-cold PBS and total protein extracted in buffer (25 mM Tris [pH 7.4], 150 mM NaCl, 5 mM EDTA, 10 mM sodium pyrophosphate, 1 mM Na_3VO_4, 1% SDS, 1 mM dithiothreitol) containing protease inhibitors (25 mg/ml aprotinin and 10 mg/ml leupeptin). Proteins were separated by SDS-PAGE, transferred to nitrocellulose membranes and blotted with primary antibodies against ERK1/2 (Santa-Cruz), pERK1/2 (Cell Signaling), lamin A/C (Santa-Cruz), emerin (Novocatra), β-actin (Sant-Cruz) and Gapdh (Santa-Cruz). Secondary antibodies were HRP–conjugated (Amersham). Recognized proteins were visualized by enhanced chemiluminescence (ECL- Amersham) and visualized using Hyperfilm ECL (Amersham). The signal generated using antibody against β-actin was used as an internal control to normalize the amounts of protein between immunoblots. Band densities were calculated using Scion Image software (Scion Corporation) and normalized to the appropriate total

extract to control for protein loading. Data are reported as means ± standard deviations and are compared with respective controls using a two-tailed *t* test.

Colorimetric Analysis of ERK1/2 Phosphorylation

[00150] HeLa and C2C12 cells were cultured for 24 hours in the presence of PD98059 (45 μM). ERK1/2 phosphorylation was measured using an Enzyme-Linked ImmunoSorbent Assay (ELISA) (SuperArray CASE, ERK1/2 kit) as per the manufacturer's protocol. Briefly, cells were fixed and stained with either phospho-ERK1/2 or ERK1/2 primary antibodies (1 hour at room temperature). After a wash and incubation with secondary antibody (1 hour at room temperature), cells were incubated with color developer (10 minutes at room temperature) and plates were read at an optical density (OD) of 450 nm. Thereafter, relative cell number was assayed in each well (OD of 595 nm) to normalize the antibody reading. To determine the ERK1/2 phosphorylation, we normalized the phospho-ERK1/2 signal ratio (OD_{450nm}/OD_{595nm}) to the total ERK1/2 signal ratio (OD_{450nm}/OD_{595nm}). Data are reported as means ± standard deviations and are compared with respective controls using a two-tailed *t* test.

Activation of ERK1/2 in hearts from mice without A-type lamins

[00151] We have previously shown that a point mutation in Lmna that causes EDMD and loss of emerin both induce activation of ERK, one of the branches of MAP kinase signaling pathway, in hearts of mice prior to cardiac dysfunction [69, 89]. Loss of A-type lamins in mice has been described previously as leading to a muscular dystrophy and cardiomyopathy [101]. To examine if loss of A-type lamins induces an aberrant activation of ERK1/2, we analyzed expression of the phosphorylated ERK1/2 in hearts from mice 5 weeks of age. Phosphorylated ERK1/2 was activated 1.4 ± 0.17 fold in hearts from $Lmna^{-/-}$ mice compared to hearts from control mice when analyzed by immunoblotting (Figure 16A). We also analyzed the expression of genes activated downstream in the ERK1/2 signaling pathway by real-time quantitative RT-PCR. There was significantly increased expression of *c-Jun*, *Mef2c*, *Atf2* and *Atf4* in hearts of $Lmna^{-/-}$ mice compared to $Lmna^{+/+}$ control mice (Figure 16B). These results showed an activation of ERK pathway in hearts of $Lmna^{-/-}$ mice.

Targeted knockdown of Emd and Lmna genes using siRNAs

[00152] To further investigate the role of nuclear envelope proteins in activation of ERK signaling, we used a human cell line (HeLa cells) and a mouse myogenic cell line (C2C12

cells) and knocked down targeted genes using siRNA technology. After a 72 hours treatment for HeLa cells, total RNA and proteins were extracted from cells cultured without siRNA treatment (mock) and from cells cultured with *Gapdh*, *Emd* and *Lmna* siRNAs. When *Gapdh*, *Emd* and *Lmna* siRNAs were transfected into HeLa cells, the corresponding mRNAs (Figure 17A) and proteins (Figure 17B) were reduced of approximately 50%. In C2C12 cells, total RNA and proteins were extracted after 48 hours treatment in mock treated cells and in cells cultured with *Gapdh*, *Emd* and *Lmna* siRNA duplexes. When *Gapdh*, *Emd* and *Lmna* siRNAs were transfected in C2C12 cells, the corresponding mRNAs (Figure 17C) and proteins (Figure 17D) were markedly reduced of 50%. These observations demonstrated that treatment with siRNAs was successful to partially reduce the targeted mRNAs.

Activation of ERK signaling pathway in cells with knocked down A-type lamins or emerin

[00153] To determine if treatment with siRNAs in HeLa and C2C12 cells lead to activation of ERK signaling pathway, we first evaluated phosphorylation of ERK1/2. Immunoblotting with anti-pERK1/2 antibody demonstrated an increase in pERK1/2 in HeLa cells treated with *Emd* and *Lmna* siRNA duplexes whereas no significant increase was observed in mock treated cells or cells treated with *GAPDH* siRNA duplex (Figure 18A). Phosphorylated ERK1/2 activates a series of downstream target genes, including those encoding c-Jun, Elk1 and Elk4. We analyzed the expression of these transcripts using real-time quantitative RT-PCR. While these individual genes were not found to be significantly differentially expressed in mock treated cells and cells treated with *Gapdh* siRNA (Figure 18B), treatment with *Emd* and *Lmna* siRNAs lead to enhanced expression of *c-Jun*, *Elk1* and *Elk4* (Figure 18B). Abnormal activation of pERK1/2 was also observed in C2C12 treated with *Emd* and *Lmna* siRNAs (Figure 18C). We also analyzed the expression of downstream target genes and found an aberrant up-regulation of *c-Jun* and *Elk4* when C2C12 cells were treated with *Emd* and *Lmna* siRNAs (Figure 18D). The expression of *Elk1* was increased only in C2C12 cells treated with *Lmna* siRNA (Figure 18D).

[00154] Translocation of pERK1/2 from cytoplasm to nucleus is necessary for activation of downstream genes. In mock treated HeLa cells and HeLa cells treated with *Gapdh* siRNA, pERK was weakly or not detectable and only approximately 2% of HeLa cells showed a nuclear localization of pERK (Figure 19A). In contrast, treatment with *Emd* and *Lmna* siRNAs induced translocation of pERK into the nucleus in significantly more cells (Figure 19A, arrowheads). Approximately 8% of HeLa cells treated with *Emd* siRNA and 10% of

HeLa cells treated with *Lmna* siRNA showed a nuclear localization of pERK (Figure 4A). In mock treated C2C12 cells and C2C12 cells treated with *Gapdh* siRNA, the activated pERK was detectable in less than 1% of nuclei (Figure 19B). When C2C12 cells were treated with *Emd* or *Lmna* siRNAs, there was a significant increase of cells with a nuclear localization of pERK (Figure 19B, arrowheads). Approximately 6% of C2C12 cells treated with *Emd* or *Lmna* siRNAs showed an intranuclear localization of pERK (Figure 19B). Hence, knocking down expression of *Emd* and *Lmna* induces phosphorylation and translocation of ERK and subsequent activation of downstream targets.

ERK1/2 activity is decreased by a MAPK/ERK kinase (MEK) inhibitor in HeLa cells knocked down for A-type lamins or emerin

[00155] We analyzed the effect of a MEK inhibitor on ERK1/2 activity in HeLa and C2C12 cells treated with siRNA against *Emd* and *Lmna.* Cells were cultured with or without the addition of the MEK inhibitor PD98059 at a concentration of 45 μM for 24 hours. Immunoblotting with anti-pERK1/2 antibody demonstrated that the increase in pERK in HeLa and C2C12 cells treated with *Emd* and *Lmna* siRNAs was reduced when PD98059 is added to the culture medium (Figure 20A and 20B). Inhibition of ERK1/2 by PD98059 in siRNA-treated cells was also confirmed using an ELISA (Figure 20B).

Example 5. Genetic Downregulation of MAPK Signaling

[00156] To show that genetic reductions of ERK improve the cardiac phenotype in $Lmna^{H222P/H222P}$ mice, we cross $Lmna^{H222P/H222P}$ mice to $Erk1^{-/-}$ and $Erk2^{+/-}$ mice (144-147). The progeny are $Lmna^{H222P/H222P}$ mice that are completely deficient in ERK1 and have reduced levels of ERK2. PCR of DNA extracted from tail clippings is performed to determine genotypes of offspring. RT-PCR of RNA extracts and immunoblotting of protein extracts from cardiac muscle, skeletal muscle, and other tissues, confirms deficiency or reduced levels of ERK1 and ERK2. Approximately 16 each of male $Lmna^{H222P/H222P}/Erk1^{+/+}/Erk2^{+/+}$, $Lmna^{H222P/H222P}/Erk1^{-/-}/Erk2^{+/+}$, and $Lmna^{H222P/H222P}/Erk1^{+/+}/Erk2^{+/-}$ mice are assessed by echocardiography and electrocardiography at 16 and 24 weeks of age.

[00157] We have shown that left ventricular tissue from *Lmna* H222P mice have a "molecular signature" of cardiomyopathy at the mRNA and protein expression level (96, 148; Example 1). These alterations in mRNA and protein expression occur prior to the onset of histological or clinical abnormalities in $Lmna^{H222P/H222P}$ mice. We perform molecular analysis

at the level of mRNA profiling and protein expression to examine the effects of ERKdeficiencies on a "molecular signature" indicative of cardiomyopathy in hearts of *Lmna*$^{H222P/H222P}$ mice. Approximately 8 mice per group are sacrified at 16 or 24 weeks of age. RNA and proteins are isolated as described previously (96, 148, 149). Real-time RT-PCR is used to quantify mRNAs encoded by downstream genes in MAPK cascade. Proteins encoded by several of these RNAs are examined by immunoblotting. Expression of muscle-specific genes, such as those encoding myosins and sarcolipin, and fibrosis and inflammatory markers are also measured. We also measure the amounts of phosphorylated (active) and non-phosphorylated ERK using specific antibodies. Genetic reduction of ERK isoforms reduce or abolish the "molecular signature" indicative of cardiomyopathy and prevent dilated cardiomyopathy with heart block and skeletal muscle myopathy. These experiments are repeated with mice that are deficient in JNK1 and/or JNK2.

REFERENCES

The following references are referred to in this disclosure.

1. Emery, A.E.H. 2000. Emery-Dreifuss muscular dystrophy – a 40 year retrospective. *Neuromusc. Disord.* **10**:228-232.
2. Bione, S., Maestrini, E., Rivella, S., Manchini, M., Regis, S., Romei, G., and Toniolo, D. 1994. Identification of a novel X-linked gene responsible for Emery-Dreifuss muscular dystrophy. *Nature Genet.* **8**:323-327.
3. Manilal, S., Nguyen, T.M., Sewry, C.A., and Morris, G.E. 1996. The Emery-Dreifuss muscular dystrophy protein, emerin, is a nuclear membrane protein. *Hum. Mol. Genet.* **5**:801-808.
4. Nagano, A., Koga, R., Ogawa, M., Kurano, Y., Kawada, J., Okada, R., Hayashi, Y. K., Tsukahara, T., and Arahata, K. 1996. Emerin deficiency at the nuclear membrane in patients with Emery-Dreifuss muscular dystrophy. *Nature Genet.* **12**:254-259.
5. Bonne, G., Di Barletta, M.R., Varnous, S., Becane, H., Hammouda, E.H., Merlini, L., Muntoni, F., Greenberg, C.R., Gary, F., Urtizberea, J.A., et al. 1999. Mutations in the gene encoding lamin A/C cause autosomal dominant Emery-Dreifuss muscular dystrophy. *Nature Genet.* **21** :285-288.
6. Di Barletta, M.R.Ricci, E., Galluzzi, G., Tonali, P., Mora, M., Morandi, L., Romorini, A., Voit, T., Orstavik, K.H., Merlini, L., et al. 2000. Different mutations in the LMNA gene cause autosomal dominant and autosomal recessive Emery-Dreifuss muscular dystrophy. *Am. J. Hum. Genet.* **66**:1407-1412.
7. Muchir, A., and Worman, H.J. 2004. The nuclear envelope and human disease. *Physiology* **19**: 309-314.
8. Lin, F., and Worman, H.J. 1993. Structural organization of the human gene encoding nuclear lamin A and nuclear lamin C. *J. Biol. Chem.* **268**:16321-16326.
9. Aebi, U., Cohn, J., Buhle, L., and Gerace, L. 1986. The nuclear lamina is a meshwork of intermediate-type filaments. *Nature* **323**:560-564.
10. Fisher, D.Z., Chaudhary, N., and Blobel, G. 1986. cDNA sequencing of nuclear lamins A and C reveals primary and secondary structural homology to intermediate filament proteins. *Proc. Natl. Acad. Sci. USA.* **83**:6450-6454.
11. Goldman, A.E., Maul, G., Steinert, P.M., Yang, H.Y., and Goldman, R.D. 1986. Keratin-like proteins that co-isolate with intermediate filaments of BHK- 21 cells are nuclear lamins. *Proc. Natl. Acad. Sci. USA.* **83**:3839-3843.

12. McKeon, F.D., Kirschner, M.W., and Caput, D. 1986. Homologies in both primary and secondary structure between nuclear envelope and intermediate filament proteins. *Nature* **319**:463-468.

13. Lammerding, J., Schulze, P.C., Takahashi, T., Kozlov, S., Sullivan, T., Kamm, R.D., Stewart, C.L., and Lee, R.T. 2004. Lamin A/C deficiency causes defective nuclear mechanics and mechanotransduction. *J. Clin. Invest.* **113** :370-378.

14. Arimura, T., Helbling-Leclerc, A., Massart, C., Varnous, S., Niel, F., Lacene, E., Fromes, Y., Toussaint, M., Mura, A.M., Keller, D.I., et al. 2005. Mouse model carrying H222P-lmna mutation develops muscular dystrophy and dilated cardiomyopathy similar to human striated muscle laminopathies. *Hum. Mol. Genet.* **14**:155-169.

15. Hwang, J.J., Allen, P.D., Tseng, G.C., Lam, C.W., Fananapazir, L., Dzau, V.J., and Liew, C.C. 2002. Microarray gene expression profiles in dilated and hypertrophic cardiomyopathic end-stage heart failure. *Physiol. Genomics* **10**:31-44.

16. Mukherjee, S., Belbin, T.J., Spray, D.C., Iacobas, D.A., Weiss, L.M., Kitsis, R.N., Wittner, M., Jelicks, L.A., Scherer, P.E., Ding, A., et al. 2003. Microarray analysis of changes in gene expression in a murine model of chronic chagasic cardiomyopathy. *Parasitol. Res.* **91**:187-196.

17. Barrans, J.D., Allen, P.D., Stamatiou, D., Dzau, V.J., and Liew, C.C. 2002. Global gene expression profiling of end-stage dilated cardiomyopathy using a human cardiovascular-based cDNA microarray. *Am. J. Pathol.* **160**:2035-2043.

18. Grzeskowiak, R., Witt, H., Drungowski, M., Thermann, R., Hennig, S., Perrot, A., Osterziel, K.J., Klingbiel, D., Scheid, S., Spang, R., et al. 2003. Expression profiling of human idiopathic dilated cardiomyopathy. *Cardiovasc. Res.* **59**:400-411.

19. Petrich, B.G., Gong, X., Lerner, D.L., Wang, X., Brown, J.H., Saffitz, J.E., and Wang, Y. 2002. c-Jun N-terminal kinase activation mediates downregulation of connexin43 in cardiomyocytes. *Circ. Res.* **91**:640-647.

20. Petrich, B.G., Molkentin, J.D., and Wang, Y. 2003. Temporal activation of c-Jun N-terminal kinase in adult transgenic heart via cre-loxP-mediated DNA recombination. *Faseb J.* **17**:749-751.

21. Chen, Z., Gibson, T.B., Robinson, F., Silvestro, L., Pearson, G., Xu, B., Wright, A., Vanderbilt, C., and Cobb, M.H. 2001. MAP kinases. *Chem. Rev.* **101**:2449-2476.

22. Garrington, T.P., and Johnson, G.L. 1999. Organization and regulation of mitogen-activated protein kinase signaling pathways. *Curr. Opin. Cell Biol.* **11**:211-218.

23. Baines, C.P., and Molkentin, J.D. 2005. STRESS signaling pathways that modulate cardiac myocyte apoptosis. *J. Mol. Cell. Cardiol.* **38**:47-62.

24. Brunet, A., Roux, D., Lenormand, P., Dowd, S., Keyse, S., and Pouyssegur, J. 1999. Nuclear translocation of p42/p44 mitogen-activated protein kinase is required for growth factor-induced gene expression and cell cycle entry. *Embo J.* **18**:664-674.

25. Hochholdinger, F., Baier, G., Nogalo, A., Bauer, B., Grunicke, H.H., and Uberall, F. 1999. Novel membrane-targeted ERK1 and ERK2 chimeras which act as dominant negative, isotype-specific mitogen-activated protein kinase inhibitors of Ras-Raf-mediated transcriptional activation of c-fos in NIH 3T3 cells. *Mol. Cell. Biol.* **19**:8052-8065.

26. Qin, L.X., Beyer, R.P., Hudson, F.N., Linford, N.J., Morris, D.E., and Kerr, K.F. 2006. Evaluation of methods for oligonucleoyides array data via quantitative real time PCR. *BMC Bioinformatics* **7**:23.

27. Millenaar, F.F., Okyere, J., May, S.T., van Zanten, M., Voesenek, L.A., and Peeters, A.J. 2006. How to decide? Different methods of calculating gene expression from short oligonucleotide array data will give different results. *BMC Bioinformatics* **7**:137.

28. Widmann, C., Gibson, S., Jarpe, M.B., and Johnson, G.L. 1999. Mitogen-activated protein kinase: conservation of a three-kinase module from yeast to human. *Physiol. Rev.* **79**:143-180.

29. Chi, H., Barry, S.P., Roth, R.J., Wu, J.J., Jones, E.A., Bennett, A.M., and Flavell, R.A. 2006. Dynamic regulation of pro- and anti-inflammatory cytokines by MAPK phosphatase 1 (MKP-1) in innate immune responses. *Proc. Natl. Acad. Sci. USA* **103**:2274-2279.

30. Gillespie-Brown, J., Fuller, S.J., Bogoyevitch, M.A., Cowley, S., and Sugden, P.H. 1995. The mitogen-activated protein kinase kinase MEK1 stimulates a pattern of gene expression typical of the hypertrophic phenotype in rat ventricular cardiomyocytes. *J. Biol. Chem.* **270**:28092-28096.

31. Thorburn, J., Carlson, M., Mansour, S.J., Chien, K.R., N G Ahn, N.G., and Thorburn, A. 1995. Inhibition of a signaling pathway in cardiac muscle cells by active mitogen-activated protein kinase kinase. *Mol. Biol. Cell.* **6**:1479–1490.

32. Braz, J.C., Bueno, O.F., Liang, Q., Wilkins, B.J., Dai, Y.S., Parsons, S., Braunwart, J., Glascock, B.J., Klevitsky, R., Kimball, T.F., et al. 2003. Targeted inhibition of p38 MAPK promotes hypertrophic cardiomyopathy through upregulation of calcineurin-

NFAT signaling. *J. Clin. Invest.* **111**:1475-1486.

33. Nicol, R.L., Frey, N., Pearson, G., Cobb, M., Richardson, J., and Olson, E.N. 2001. Activated MEK5 induces serial assembly of sarcomeres and eccentric cardiac hypertrophy. *Embo J.* **20**:2757-2767.
34. Cook, S.A., Sugden, P.H., and Clerk, A. 1999. Activation of c-Jun N-terminal kinases and p38-mitogen-activated protein kinases in human heart failure secondary to ischaemic heart disease. *J. Mol. Cell. Cardiol.* **31**:1429-1434.
35. Haq, S., Choukroun, G., Lim, H., Tymitz, K.M., del Monte, F., Gwathmey, J., Grazette, L., Michael, A., Hajjar, R., Force, T., et al. 2001. Differential activation of signal transduction pathways in human hearts with hypertrophy versus advanced heart failure. *Circulation* **103**:670-677.
36. Rodriguez-Viciana, P., Tetsu, O., Tidyman, W.E., Estep, A.L., Conger, B.A., Santa Cruz, M., McCormick, F., and Rauen, K.A. 2006. Germline mutations in genes within the MAPK pathway cause cardio-facio-cutaneous syndrome. *Science* **311**:1287-1290.
37. Bueno, O.F., De Windt, L.J., Tymitz, K.M., Witt, S.A., Kimball, T.R., Klevitsky, R., Hewett, T.E., Jones, S.P., Lefer, D.J., Peng, C.F., et al. 2000. The MEK1-ERK1/2 signaling pathway promotes compensated cardiac hypertrophy in transgenic mice. *Embo J.* **19**:6341-6350.
38. Woodman, S.E., Park, D.S., Cohen, A.W., Cheung, M.W., Chandra, M., Shirani, J., Tang, B., Jelicks, L.A., Kitsis, R.N., Christ, G.J., et al. 2002. Caveolin-3 knock-out mice develop a progressive cardiomyopathy and show hyperactivation of the p42/44 MAPK cascade. *J. Biol. Chem.* **277**:38988-38997.
39. Cohen, A.W., Park, D.S., Woodman, S.E., Williams, T.M., Chandra, M., Shirani, J., Pereira de Souza, A., Kitsis, R.N., Russell, R.G., Weiss, L.M., et al. 2003. Caveolin-1 null mice develop cardiac hypertrophy with hyperactivation of p42/44 MAP kinase in cardiac fibroblasts. *Am. J. Physiol. Cell. Physiol.* **284**:457-474.
40. Luo, J., McMullen, J.R., Sobkiw, C.L., Zhang, L., Dorfman, A.L., Sherwood, M.C., Logsdon, M.N., Horner, J.W., DePinho, R.A., Izumo, S., et al. 2005. Class IA phosphoinositide 3-kinase regulates heart size and physiological cardiac hypertrophy. *Mol. Cell. Biol.* **25**:9491-9502.
41. Malarkey, K., Belham, C.M., Paul, A., Graham, A., McLees, A., Scott, P.H., and Plevin, R. 1995. The regulation of tyrosine kinase signalling pathways by growth factor and G-protein-coupled receptors. *Biochem J.* **309**:361-375.

42. Rosette, C., and Karin, M. 1996. Ultraviolet light and osmotic stress: activation of the JNK cascade through multiple growth factor and cytokine receptors. *Science* **274**:1194-1197.

43. Coleman, M.L., Densham, R.M., Croft, D.R., and Olson, M.F. 2006. Stability of p21 (Waf1/Cip1) CDK inhibitor protein is responsive to RhoA-mediated regulation of the actin cytoskeleton. *Oncogene* **25***:* 2708-2716**.**

44. Smith, E.R., Smedberg, J.L., Rula, M.E., and Xu, X.X. 2004. Regulation of Ras-MAPK pathway mitogenic activity by restricting nuclear entry of activated MAPK in endoderm differentiation of embryonic carcinoma and stem cells. *J. Cell Biol.* **164**:689-699.

45. Ivorra, C., Kubicek, M., González, J.M., Sanz-González, S.M., Álvarez-Barrientos, A., O'Connor, J.E., Burke, B., and Andrés, V. 2006. A mechanism of AP-1 suppression through interaction of c-Fos with lamin A/C. *Genes Dev.* **20**: 307-320.

46. Schwartz, K., Boheler, K.R., de la Bastie, D., Lompre, A.M., and Mercadier, J.J. 1992. Switches in cardiac muscle gene expression as a result of pressure and volume overload. *Am. J. Physiol.* **262**:364-369.

47. Chien, K.R., Zhu, H., Knowlton, K.U., Miller-Hance, W., van-Bilsen, M., O'Brien, T.X., and Evans, S.M. 1993. Transcriptional regulation during cardiac growth and development. *Annu. Rev. Physiol.* **55** :77-95.

48. Hwang, J.J., Allen, P.D., Tseng, G.C., Lam, C.W., Fananapazir, L., Dzau, V.J., and Liew, C.C. 2002. Microarray gene expression profiles in dilated and hypertrophic cardiomyopathic end-stage heart failure. *Physiol. Genomics* **10**:31-44.

49. Yung, C.K., Halperin, V.L., Tomaselli, G.F., and Winslow, R.L. 2004. Gene expression profiles in end-stage human idiopathic dilated cardiomyopathy: altered expression of apoptotic and cytoskeletal genes. *Genomics* **83**:281-297.

50. Swynghedauw, B. 1999. Molecular mechanisms of myocardial remodeling. *Physiol. Rev.* **79**:215-262.

51. Swynghedauw, B., and Baillard, C. 2000. Biology of hypertensive cardiopathy. *Curr. Opin. Cardiol.* **15**:247-253.

52. Yoshimine, K., Horiuchi, M., Suzuki, S., Kobayashi, K., Abdul, J.M., Masuda, M., Tomomura, M., Ogawa, Y., Itoh, H., Nakao, K., et al. 1997. Altered expression of atrial natriuretic peptide and contractile protein genes in hypertrophied ventricle of JVS mice with systemic carnitine deficiency. *J. Mol. Cell. Cardiol.* **29**:571-578.

53. Liao, P., Georgakopoulos, D., Kovacs, A., Zheng, M., Lerner, D., Pu, H., Saffitz, J., Chien, K., Xiao, R.P., Kass, D.A., and Wang, Y. 2001. The in vivo role of p38 MAP kinases in cardiac remodeling and restrictive cardiomyopathy. *Proc. Natl. Acad. Sci. USA.* **98**:12283-12288.

54. Zheng, M., Dilly, K., Dos Santos Cruz, J., Li, M., Gu, Y., Ursitti, J.A., Chen, J., Ross, J.Jr., Chien, K.R., Lederer, J.W., and Wang, Y. 2004. Sarcoplasmic reticulum calcium defect in Ras-induced hypertrophic cardiomyopathy heart. *Am. J. Physiol. Heart Circ. Physiol.* **286**:424-433.

55. Wang, J., Xu, N., Feng, X., Hou, N., Zhang, J., Cheng, X., Chen, Y., Zhang, Y., and Yang, X. 2005. Targeted disruption of Smad4 in cardiomyocytes results in cardiac hypertrophy and heart failure. *Circ. Res.* **97**:821-828.

56. Takahashi, T., Allen, P.D., and Izumo, S. 1992. Expression of A-, B-, and C-type natriuretic peptide genes in failing and developing human ventricles. Correlation with expression of the Ca(2+)-ATPase gene. *Circ. Res.* **71**:9-17.

57. Schwartz, K., de la Bastie, D., Bouveret, P., Oliviero, P., Alonso, S.,and Buckingham, M. 1986. Alpha-skeletal muscle actin mRNA's accumulate in hypertrophied adult rat hearts. *Circ. Res.* **59**:551-555.

58. Izumo, S., Nadal-Ginard, B., Mahdavi, V. 1988. Protooncogene induction and reprogramming of cardiac gene expression produced by pressure overload. *Proc. Natl. Acad. Sci. U S A.* **85**:339-343.

59. Ferrandi, C., Ballerio, R., Gaillard, P., Giachetti, C., Carboni, S., Vitte, P.A., Gotteland, J.P., and Cirillo, R. 2004. Inhibition of c-Jun N-terminal kinase decreases cardiomyocyte apoptosis and infarct size after myocardial ischemia and reperfusion in anaesthetized rats. *Br. J. Pharmacol.* **142** :953-960.

60. Borsello, T., Clarke, P.G., Hirt, L., Vercelli, A., Repici, M., Schorderet, D.F., Bogousslavsky, J., and Bonny, C. 2003. A peptide inhibitor of c-Jun N-terminal kinase protects against excitotoxicity and cerebral ischemia. *Nature Med.* **9**:1180-1186.

61. Wang, J., Van De Water, T.R., Bonny, C., de Ribaupierre, F., Puel, J.L., and Zine, A. 2003. A peptide inhibitor of c-Jun N-terminal kinase protects against both aminoglycoside and acoustic trauma-induced auditory hair cell death and hearing loss. *J. Neurosci.* **23**:8596-8607.

62. Minogue, A.M., Schmid, A.W., Fogarty, M.P., Moore, A.C., Campbell, V.A., Herron, C.E., and Lynch, M.A. 2003. Activation of the c-Jun N-terminal kinase signaling

cascade mediates the effect of amyloid-beta on long term potentiation and cell death in hippocampus: a role for interleukin-1beta? *J. Biol. Chem.* **278**:27971-27980.

63. Kuida, K., and Boucher, D.M. 2004. Functions of MAP kinases: Insights from gene-targeting studies. *J. Biochem.* **135**: 653-656.
64. Mounkes, L.C., Kozlov, S.V., Rottman, J.N., and Stewart, C.L. 2005. Expression of an LMNA-N195K variant of A-type lamins results in cardiac conduction defects and death in mice. *Hum. Mol. Genet.* **14**:2167-2180.
65. Pavlidis, P., Lewis, D.P., and Noble, W.S. 2002. Exploring gene expression data with class scores. *Pac. Symp. Biocomput.* 474-485.
66. Dennis, G. Jr., Sherman, B. T., Hosack, D. A., Yang, J., Gao, W., Lane, H. C., and Lempicki, R. A. 2003. DAVID: Database for Annotation, Visualization, and Discovery. *Genome Biology.* **4**:P3.
67. Ponchel, F., Toomes, C., Bransfield, K., Leong, F. T., Douglas, S. H., Field, S. L., Bell, S. M., Combaret, V., Puisieux, A., Mighell, A. J., et al. 2003. Real-time PCR based on SYBR-Green I fluorescence: An alternative to the TaqMan assay for a replicative quantification of gene rearrangements, gene amplifications and micro gene deletions. *BMC Biotechnol.* **13**:18.
68. Fatkin, D., MacRae, C, Sasaki, T., Wolff, M.R., Porcu, M., Frenneaux, M., Atherton, J., Vidaillet, H.J., Spudich, S., De Girolami, U., et al. 1999. Missense mutations in the rod domain of the lamin A/C gene as causes of dilated cardiomyopathy and conduction-system disease. *N. Engl. J. Med.* **341**:1715-1724.
69. Muchir, A., Bonne, G., van der Kooi, A.J., van Meegen, M., Baas, F., Bolhuis, P.A., de Visser, M., and Schwartz, K. 2000. Identification of mutations in the gene encoding lamins A/C in autosomal dominant limb girdle muscular dystrophy with atrioventricular conduction disturbances (LGMD1B). *Hum. Mol. Genet.* **9**:1453-1459.
70. De Sandre-Giovannoli, A., Chaouch, M., Kozlov, S., Vallat, J. M., Tazir, M., Kassouri, N., Szepetowski, P., Hammadouche, T., Vandenberghe, A., Stewart, C. L., etal. 2002. Homozygous defects in LMNA, encoding lamin A/C nuclear envelope proteins, cause autosomal recessive axonal neuropathy in human (Charcot- Marie-Tooth Disorder Type 2) and mouse. *Am. J. Hum. Genet.* **70**:726-736.
71. Cao, H., and Hegele, R. A. 2000. Nuclear lamin A/C R482Q mutation in Canadian kindreds with Dunnigan-type familial partial lipodystrophy. *Hum. Mol. Genet.* **9**:109-112.

72. Shackleton, S., Lloyd, D.J., Jackson, S.N., Evans, R., Niermeijer, M.F., Singh, B.M., Schmidt, H., Brabant, G., Kumar, S., Durrington, P.N., et al. 2000. LMNA, encoding lamin A/C, is mutated in partial lipodystrophy. *Nature Genet.* **24**:153-156.

73. Speckman, R.A., Garg, A., Du, F., Bennett, L., Veile, R., Arioglu, E., Taylor, S.I., Lovett, M., and Bowcock, A.M. 2000. Mutationai and hapiotype analyses of families with familial partial lipodystrophy (Dunnigan variety) reveal recurrent missense mutations in the globular C-terminal domain of lamin A/C. *Am. J. Hum. Genet.* **66**:1192-1198.

74. Dunnigan, M.G., Cochrane, M.A., Kelly, A., and Scott, J.W. 1974. Familial lipoatrophic diabetes with dominant transmission. A new syndrome. *Q. J. Med.* **43**:33-48.

75. Novelli, G., Muchir, A., Sangiuolo, F., Helbiing-Leclerc, A., Rosaria d'Apice, M., Massart, C, Capon, F., Sbraccia, P., Federici, M., Lauro, R., et al. 2002. Mandibuloacral dysplasia is caused by a mutation in LMNA encoding lamins A/C. *Am. J. Hum. Genet.* **71**:426-431.

76. Eriksson, M., Brown, W.T., Gordon, L.B., Glynn, M.W., Singer, J., Scott, L, Erdos, M.R., Robbins, C. M., Moses, T.Y., Berglund, P., et al. 2003. Recurrent de novo point mutations in lamin A cause Hutchinson-Gilford progeria syndrome. *Nature* **423** :293-298.

77. De Sandre-Giovannoli, A., Bernard, R., Cau, P., Navarro, C, Amiel, J., Boccaccio, I., Lyonnet, S., Stewart, C.L., Munnich, A., Le Merrer, M., et al. 2003. Lamin A truncation in Hutchinson-Gilford progeria. *Science* **300**:2055.

78. Chen, L., Lee, L., Kudlow, B., Dos Santos, H., Sletvold, O., Shafeghati, Y., Botha, E., Garg, A., Hanson, N., Martin, G., et al. 2003. LMNA mutations in atypical Werner's syndrome. *Lancet* **362**:440-445.

79. Navarro, C.L., De Sandre-Giovannoli, A., Bernard, R., Boccaccio, I., Boyer, A., Genevieve, D., Hadj-Rabia, S., Gaudy-Marqueste, C, Smitt, H.S., Vabres, P., et al. 2004. Lamin A and ZMPSTE24 (FACE-1) defects cause nuclear disorganization and identify restrictive dermopathy as a lethal neonatal laminopathy. *Hum. Mol. Genet.* **13**:2493-2503.

80. Bennett, B.L., Sasaki, D.T., Murray, B.W., O'Leary, E.C., Sakata, ST., Xu, W., Leisten, J.C., Motiwala, A., Pierce, S., Satoh, Y., et. al. 2001. SP600125, an anthrapyrazolone inhibitor of Jun N-terminal kinase. *Proc. Natl. Acad. Sci. USA*. **98**:13681-13686.

81. Han, Z., Boyle, D.L., Chang, L., Bennett, B., Karin, M., Yang, L., Manning, A.M., and Firestein, G.S. 2001. c-Jun N-terminal kinase is required for metalloproteinase expression and joint destruction in inflammatory arthritis. *J. Clin. Invest.* **108**:73-81.

82. Shin, M., Yan, C, and Boyd D. 2002. An inhibitor of c-jun aminoterminal kinase (SP600125) represses c-Jun activation, DNA-binding and PMA-inducible 92-kDa type IV collagenase expression. *Biochim, Biophys. Acta.* **1589**:311-316.

83. Dudley, D.T., Pang, L, Decker, S.J., Bridges, A.J., and Saltiel, A.R. 1995. A synthetic inhibitor of the mitogen-activated protein kinase cascade. *Proc. Natl. Acad. Sci. USA.* **92**:7686-7689.

84. Pang, L., Sawada, T., Decker, S.J., and Saltiel, A.R. 1995. Inhibition of MAP kinase kinase blocks the differentiation of PC-12 cells induced by nerve growth factor. *J. Biol. Chem.* **270**:13585-13588.

85. Waters, S.B., Holt, K.H., Ross, S.E., Syu, L.J., Guan, K.L., Saltiel, A.R., Koretzky, G.A., and Pessin, J.E. 1995. Desensitization of Ras activation by a feedback disassociation of the SOS-Grb2 complex. *J. Biol. Chem.* **270**:20883-20886.

86. Langlois, W.J., Sasaoka, T., Saltiel, A.R., and Olefsky, J.M. 1995. Negative feedback regulation and desensitization of insulin- and epidermal growth factor-stimulated p21ras activation. *J. Biol. Chem.* **270**:25320-25323.

87. Kultz, D., Madhany, S., and Burg, M.B. 1998. Hyperosmolality causes growth arrest of murine kidney cells. Induction of GADD45 and GADD153 by osmosensing via stress-activated protein kinase 2. *J. Biol. Chem.* **273**:13645-13651.

88. Means, T.K., Pavlovich, R.P., Roca, D., Vermeulen, M.W., and Fenton, MJ. 2000. Activation of TNF-alpha transcription utilizes distinct MAP kinase pathways in different macrophage populations. *J. Leukoc. Biol.* **67**:885-893.

89. Ostlund, C, Bonne, G., Schwartz, K., and Worman, H.J. 2001. Properties of lamin A mutants found in Emery-Dreifuss muscular dystrophy, cardiomyopathy and Dunnigan-type partial lipodystrophy. *J. Cell Sci.* **114**:4435-4445.

90. Boguslavsky, R.L., Stewart, C.L., Worman, H.J. 2006. Nuclear lamin A inhibits adipocyte differentiation: implications for Dunnigan-type familial partial lipodystrophy. *Hum. Mol. Genet.* **15**:653-663.

91. Paradisi, M., McClintock, D., Boguslavsky, R.L., Pedicelli, C, Worman, H.J., and Djabaii, K. 2006. Dermal fibroblasts in Hutchinson-Gilford progeria syndrome with the lamin A G608G mutation have dysmorphic nuclei and are hypersensitive to heat stress.

BMC Cell Biol. **6**:27.

92. Laemmli, U.K. 1970. Cleavage of structural proteins during the assembly of the head of bacteriophage T4. *Nature* **227**:680-685.
93. Daigle, C, Martens, F.M., Girardot, D., Dao, H.H., Touyz, R.M., and Moreau, P. 2004. Signaling of angiotensin ll-induced vascular protein synthesis in conduit and resistance arteries in vivo. *BMC Cardiovasc Disord.* **10**;4:6.
94. Wang, Y., Herron, A.J., and Worman, H.J. 2006. Pathology and nuclear abnormalities in hearts of transgenic mice expressing M371K lamin A encoded by an LMNA mutation causing Emery-Dreifuss muscular dystrophy. *Hum. Mol. Genet.* **15**(16):2479-89.
95. Kaplan, E.L., and Meier, P. 1958. Nonpararnetric estimation from incomplete observations. *J. Amer. Statist. Assn.* **53**:457-481.
96. Muchir, A. et al., Activation of MAPK pathways links *LMNA* mutations to cardiomyopathy in Emery-Dreifuss muscular dystrophy. *J. Clin. Invest.* **117**, 1282 (2007).
97. Kyoi, S., Otani, H., Matsuhisa, S., Akita, Y., Tatsumi, K., Enoki, C., et al. (2006). Opposing effects of p38 MAP kinase and JNK inhibitors on the development of heart failure in the cardiomyopathic hamster. *Cardiovasc Res* **69**, 888-898.
98. Lorusso, P. M. et al., *J. Clin. Oncol.* **23**, 5281 (2005).
99. Adjei, A. A.et al., *J. Clin. Oncol.* **26**, 2139 (2008).
100. Miller RG., Layzer RB, Mellenthin MA, Golabi M, Francoz RA, Mall JC: Emery-Dreifuss muscular dystrophy with autosomal dominant transmission. *Neurology* 1985, **35:**1230-1233.
101. Sullivan T, Escalante-Alcalde D, Bhatt H, Anver M, Bhat N, Nagashima K, Stewart CL, Burke B: Loss of A-type lamin expression compromises nuclear envelope integrity leading to muscular dystrophy. *J Cell Biol* 1999, **147**:913-920.
102. de Nadal E, Alepuz PM, Posas F: Dealing with osmostress through MAP kinase activation. *EMBO Rep* 2002, **3**:735-40
103. Cowan KJ, Storey KB: Mitogen-activated protein kinases: new signaling pathways functioning in cellular responses to environmental stress. *J Exp Biol* 2003, **206**:1107-15.

104. Lammerding J, Hsiao J, Schulze PC, Kozlov S, Stewart CL, Lee RT: Abnormal nuclear shape and impaired mechanotransduction in emerin-deficient cells. *J Cell Biol* 2005, **170**:781-791.

105. Muchir A, van Engelen BGM, Lammens M, Mislow JM, McNally E, Schwartz K, Bonne G: Nuclear envelope alterations in fibroblasts from LGMD1B patients carrying nonsense Y259X heterozygous or homozygous mutation in lamin A/C gene. *Exp Cell Res* 2003, **291**:352-362.

106. Ozawa R, Hayashi YK, Ogawa M, Kurokawa R, Matsumoto H, Noguchi S, Nonaka I, Nishino I: Emerin-lacking mice show minimal motor and cardiac dysfunctions with nuclear-associated vacuoles. *Am J Pathol* 2006, **168**:907-917.

107. Melcon G, Kozlov S, Cutler DA, Sullivan T, Hernandez L, Zhao P, Mitchell S, Nader G, Bakay M, Rottman JN, Hoffman EP, Stewart CL: Loss of emerin at the nuclear envelope disrupts the Rb1/E2F and MyoD pathways during muscle regeneration. *Hum Mol Genet* 2006, **15**:637-651.

108. Nikolova V, Leimena C, McMahon AC, Tan JC, Chandar S, Jogia D, Kesteven SH, Michalicek J, Otway R, Verheyen F, Rainer S, Stewart CL, Martin D, Feneley MP, Fatkin D. Defects in nuclear structure and function promote dilated cardiomyopathy in lamin A/C–deficient mice. *J Clin Invest* 2004, **113**:357-369.

109. Ishitani T, Ninomiya-Tsuji J, Nagai S, Nishita M, Meneghini M, Barker N, Waterman M, Bowerman B, Clevers H, Shibuya H, Matsumoto K: The TAK1-NLK-MAPK-related pathway antagonizes signalling between beta-catenin and transcription factor TCF. *Nature* 1999, **399**:798–802.

110. Kim D, Rath O, Kolch W, Cho KH: A hidden oncogenic positive feedback loop caused by crosstalk between Wnt and ERK Pathways. *Oncogene* 2007, **26**:4571–4579.

111. Massague J: How cells red Tgf- β signals. *Nat Rev Mol Cell Biol* 2000, **1**:169-78.

112. Hocevar BA, Brown TL, Howe PH: Tgf- β induced fibronectin synthesis through a c-Jun N-terminal kinase-dependent, SMAD4-independent pathway. *The EMBO J* 1999, **18**:1345-1356.

113. Wolf CM, Wang L, Alcalai R, Pizard A, Burgon PG, Ahmad F, Sherwood M, Branco DM, Wakimoto H, Fishman GI, See V, Stewart CL, Conner DA, Berul CI, Seidman CE, Seidman JG: Lamin A/C haploinsufficiency causes dilated cardiomyopathy and apoptosis-triggered cardiac conduction system disease. *J Mol Cell Cardiol* 2008, **44**:293-303.

114. Yoon S, Seger R: The extracellular signal-regulated kinase: Multiple substrates regulate diverse cellular functions. *Growth Factors* 2006, **24**:21-44.

115. Torres M, Forman HJ: Redox signaling and the MAP kinase pathways. *Biofactors* 2003, **17**:287-96

116. Michel MC, Li Y, Heusch G: Mitogen-activated protein kinases in the heart. *Naunyn-Schmiedeberg Arch Pharmacol* 2001, **363**:245-266.

117. Crisp M, Liu Q, Roux K, Rattner JB, Shanadan C, Burke B, Stahl PD, Hodzic D: Coupling of the nucleus and cytoplasm: role of the LINC complex. *J Cell Biol* 2006, **172**:41-53.

118. English JM, Cobb MH: Pharmacological inhibitors of MAPK pathways. *Trends Pharmacol Sci* 2002, **23**:40-45.

119. US Patent No. 6,924,415 "Transgenic mice comprising a constitutively-activated MEK5 and exhibiting cardiac hypertrophy and dilated cardiomyopathy"

120. Barancik, M., Htun, P., Srrohm, C., Kilian, S., & Schaper, W. (2000). Inhibition of the cardiac g38-MAPK pathway by SB203580 delays ischemic cell death. *J Cardiovasc Pharmacol* **35**, 474-483.

121. Sanada, S., Kitakaze, M., Papst, P. J., Hatanaka, K., Asanuma, H., Aki, T., et al. (2001). Role of Phasic Dynamism of p38 Mitogen-Activated Protein Kinase Activation in Ischemic Preconditioning of the Canine Heart. *Circ Res* **88**, 175-180.

122. See, F., Thomas,W.,Way, K., Tzanidis, A., Kompa, A., Lewis, D., et al. (2004). p38 mitogen-activated protein kinase inhibition improves cardiac function and attenuates left ventricular remodeling following myocardial infarction in the rat. *J Am Coll Cardiol* **44**, 1679-1689.

123. Yada, M., Shimamoto, A., Hampton, C. R., Chong, A. J., Takayama, H., Rothnie, C. L., et al. (2004). FR167653 diminishes infarct size in a murine model of myocardial ischemia-reperfusion injury. *J Thorac Cardiovasc Surg* **128**, 588-594.

124. Liu, Y. H., Wang, D., Rhaleb, N. E., Yang, X. P., Xu, J., Sankey, S. S., et al. (2005). Inhibition of p38 mitogen-activated protein kinase protects the heart against cardiac remodeling in mice with heart failure resulting from myocardial infarction. *J Card Fail* **11**, 74-81.

125. Engel, F. B., Hsieh, P. C., Lee, R. T., & Keating, M. T. (2006). FCFl/p38 MAP kinase inhibitor therapy induces cardiomyocyte mitosis, reduces scarring, and rescues function after myocardial infarction. *Proc Natl Acad Sci USA* **103**, 15546-15551.

126. Li, M., Georgakopoulos, D., Lu, G., Hester, L., Kass, D. A, Hasday, J., et al. (2005). p38 MAP kinase mediates inflammatory cytokine induction in cardiomyocytes and extracellular matrix remodeling in heart. *Circulation* **111**, 2494-2 502.

127. Nakamura, T., Colbert, M., Krenz, M., Molkentin, J. D., Hahn, H. S., Dorn, G. W. 2nd, Robbins, J. (2007) Mediating ERK 1/2 signaling rescues congenital heart defects in a mouse model of Noonan syndrome. *J Clin Invest* **117**, 2123-2132.

128. Worman, H.J. and Bonne, G (2007) "Laminopathies": a wide spectrum of human diseases. *Exp. Cell Res.*, **313,** 2121-2133.

129. Taylor, M.R., Fain, P.R., Sinagra, G., Robinson, M.L., Robertson, A.D., Carniel, E., Di Lenarda, A., Bohlmeyer, T.J., Ferguson, D.A., Brodsky, G.L. *et al.* (2003) Natural history of dilated cardiomyopathy due to lamin A/C gene mutations. *J. Am. Coll. Cardiol.*, **41,** 771-780.

130. Bécane, H.M., Bonne, G., Varnous, S., Muchir, A., Ortega, V., Hammouda, E.H., Urtizberea, J.A., Lavergne, T., Fardeau, M., Eymard, B. *et al.* (2000) High incidence of sudden death with conduction system and myocardial disease due to lamins A and C gene mutation. *Pacing Clin. Electrophysiol.*, **23,** 1661-1666.

131. Meune, C., Van Berlo, J.H., Anselme, F., Bonne, G., Pinto, Y.M. and Duboc D. (2006) Primary prevention of sudden death in patients with lamin A/C gene mutations. *N. Engl. J. Med.*, **354,** 209-210.

132. Sanada, S., Node, K., Minamino, T., Takashima, S., Ogai, A., Asanuma, H., Ogita, H., Liao, Y., Asakura, M., Kim, J. *et al.* (2003) Long-acting Ca^{2+} blockers prevent myocardial remodeling induced by chronic NO inhibition in rats. *Hypertension*, **41,** 963-967.

133. Mizuno, Y., Yoshimura, M., Harada, E., Nakayama, M., Sakamoto, T., Shimasaki, Y., Ogawa, H., Kugiyama, K., Saito, Y., Nakao, K. *et al.* (2000) Plasma levels of A- and B-type natriuretic peptides in patients with hypertrophic cardiomyopathy or idiopathic dilated cardiomyopathy. *Am. J. Cardiol.*, **86,** 1036-1040.

134. Abraham, W.T., Gilbert, E.M., Lowes, B.D., Minobe, W.A., Larrabee, P., Roden, R.L., Dutcher, D., Sederberg, J., Lindenfeld, J.A., Wolfel, E.E. *et al.* (2002) Coordinate changes in myosin heavy chain isoform gene expression are selectively associated with alterations in dilated cardiomyopathy phenotype. *Mol. Med.*, 8, 750-760.

135. Favreau, C., Delbarre, E., Courvalin, J.C. and Buendia B. (2008) Differentiation of C2C12 myoblasts expressing lamin A mutated at a site responsible for Emery-Dreifuss

muscular dystrophy is improved by inhibition of the MEK-ERK pathway and stimulation of the PI3-kinase pathway. *Exp. Cell Res.*, **314,** 1392-1405.

136. Alessi, D.R., Cuenda, A., Cohen, P., Dudley, D.T. and Saltiel, A.R. (1995) PD 098059 is a specific inhibitor of the activation of mitogen-activated protein kinase kinase in vitro and in vivo. *J. Biol. Chem.*, **270,** 27489-27494.
137. Börsch-Haubold, A.G., Pasquet, S. and Watson, S.P. (1998) Direct inhibition of cyclooxygenase-1 and -2 by the kinase inhibitors SB 203580 and PD 98059. SB 203580 also inhibits thromboxane synthase. *J. Biol. Chem.*, **273,** 28766-28772.
138. Mamdani, M., Juurlink, D.N., Lee, D.S., Rochon, P.A., Kopp, A., Naglie, G., Austin, P.C., Laupacis, A. and Stukel, T.A. (2004) Cyclo-oxygenase-2 inhibitors versus non-selective non-steroidal anti-inflammatory drugs and congestive heart failure outcomes in elderly patients: a population-based cohort study. *Lancet*, **363,** 1751-1756.
139. Hudson, M., Richard, H. and Pilote, L. (2005) Differences in outcomes of patients with congestive heart failure prescribed celecoxib, rofecoxib, or non-steroidal anti-inflammatory drugs: population based study. *BMJ*, **330,** 1370.
140. Manilal, S., Nguyen, T.M., Sewry, C.A. and Morris, G.E. (1996) The Emery-Dreifuss muscular dystrophy protein, emerin, is a nuclear membrane protein. *Hum. Mol. Genet.*, **5,** 801-808.
141. Yang, S.H., Meta, M., Qiao, X., Frost, D., Bauch, J., Coffinier, C., Majumdar, S., Bergo, M.O., Young, S.G. and Fong, L.G. (2006) A farnesyltransferase inhibitor improves disease phenotypes in mice with a Hutchinson-Gilford progeria syndrome mutation. *J. Clin. Invest.*, **116,** 2115-2121.
142. Yang, S.H., Qiao, X., Fong, L.G. and Young, S.G. (2008) Treatment with a farnesyltransferase inhibitor improves survival in mice with a Hutchinson-Gilford progeria syndrome mutation. *Biochim. Biophys. Acta*, **1781,** 36-39.
143. Lo Russo, P.M., Adjei, A.A., Varterasian, M., Gadgeel, S., Reid, J., Mitchell, D.Y., Hanson, L., DeLuca, P., Bruzek, L., Piens, J. *et al.* (2005) Phase I and pharmacodynamic study of the oral MEK inhibitor CI-1040 in patients with advanced malignancies. *J. Clin. Oncol.*, **23,** 5281-5293.
144. Pages, G. et al. (1999) Defective thymocyte maturation in p44 MAP kinase (*Erk1*) knockout mice. *Science* **286**:1374-1377.
145. Yao, Y. et al. (2003) Extracellular signal-regulated kinase 2 is necessary for mesoderm differentiation. *Proc. Natl. Acad. Sci. U.S.A.* **100**:12759-12764.

146. Hatano, N. et al. (2003) Essential role for ERK2 mitogen-activated protein kinase in placental development. *Genes Cells* **8**:847-856.
147. Saba-El-Leil, M.K. et al. (2003) An essential function of the mitogen-activated protein kinase Erk2 in mouse trophoblast development. *EMBO Rep.* **4**:964-968.
148. Muchir, A. et al. (2009) Inhibition of extracellular signal-regulated kinase signaling to prevent cardiomyopathy caused by mutation in the gene encoding A-type lamins. *Hum. Mol. Genet.* **18**:241-247.
149. Muchir, A. et al. (2007) Activation of MAPK in hearts of *Emd* null mice: similarities between mouse models of X-linked and autosomal dominant Emery-Dreifuss muscular dystrophy. *Hum. Mol. Genet.* **16**: 1884-1895.
150. Heinke, J., Molkentin, J.D. (2006) Regulation of cardiac hypertrophy by intracellular signaling pathways. *Nat. Rev. Mol. Cell. Biol.* **7**:589-600.
151. Maosong & Elion (2005) MAP kinase pathways. *J. Cell. Sci.* **118**: 3569-3572.
152. Chang & Karin (2001) Mammalian MAP kinase signaling cascade. *Nature* **410**: 37-40.
153. Chen *et al.* (2000) The c-Jun N-terminal kinase pathway and apoptotic signaling. *Int. J. Oncol.* **16:** 651–62.
154. Pearson *et al.* (2001) Mitogen-activated protein (MAP) kinase pathways: regulation and physiological functions. *Endocr. Rev.* **22**: 53–83.
155. Davis *et al.* (2000) Signal transduction by the JNK group of MAP kinases. *Cell* **103**: 239-252.
156. Roux & Blenis (2004) ERK and p38 MAPK-activated protein kinases: a family of protein kinases with diverse biological functions. *Microbiol. Mol. Biol. Rev.* **68**: 320-344.
157. Hetman, M., *et al.* (2002) *J. Biol. Chem.* **277**, 49577.
158. Ohno, M., *et al.* (2001) *Nat. Neurosci.* **4**, 1238.
159. Wang, H., *et al.* (2001) *Biochem. Biophys. Res. Commun.* **286**, 869.
160. Scherle, P.A., *et al.* (2000) *J. Biol. Chem.* **275**, 37086.
161. Valjent, E., *et al.* (2000) *J. Neurosci.* **20**, 8701.
162. Watabe, A.M., *et al.* (2000) *J. Neurosci.* **20**, 5924.
163. Atkins, C.M., *et al.* (1998) *Nat. Neurosci.* **1**, 602.
164. DeSilva, D.R., *et al.* 1998. *J. Immunol.* **160**, 4175.
165. Duncia, J.V., *et al.* 1998. *Biorg. Med. Chem. Lett.* **8**, 2839.
166. Favata, M.F., *et al.* 1998. *J. Biol. Chem.* **273**, 18623.

167. Ahn et al. (1999) *Promega Notes*. 71: 4.

168. Kohno & Pouyssegur (2003) Pharmacological inhibitirs of the ERK signaling pathway: application as anticancer drugs. *Prog. Cell. Cyc. Res.* **5**: 219-224.

169. Ohori, M. et al. (2005) Identification of a selective ERK inhibitor and structural determination of the inhibitor-ERK2 complex. *Biochem. Biophys. Res. Comm.* **336**: 357-363.

170. Chen, F. et al. (2006) Characterization of ATP-independent ERK inhibitors identified through in silico analysis of the active ERK2 structure. *Bioorg. Med. Chem.* **16**:6281-6288.

171. Hancock, C.N. et al. (2005) Identification of novel extracellular signal-regulated kinase docking domain inhibitors. *J. Med. Chem.* **48**: 4586-4595.

172. National Cancer Institute NCI Drug Dictionary, available at www.cancer.gov.

173. Stebbins, J.L. et al. (2008) Identification of a new JNK inhibitor targeting the JNK-JIP interaction site. *Proc. Natl. Acad. Sci., U.S.A.* **105**: 16809-16813.

174. Wiegler, K. et al. (2008) The JNK inhibitor XG-102 protects from ischemic damage with delayed intravenous administration also in the presence of recombinant tissue plasminogen activator. *Cerebrovasc. Dis.* **26**: 360-366.

175. Carboni, S. et al. (2004) AS601245: a JNK inhibitor with neuroprotective properties. *J. Pharmacol. Exp. Ther.* **310**: 25-32.

CLAIMS

We claim:

1. A method of treating or preventing a cardiomyopathy associated with activation of at least one kinase in the mitogen-activated protein kinase (MAPK) signaling pathway in heart tissue, the method comprising providing to a subject an inhibitor of at least one kinase in the extracellular signal-regulated kinase (ERK) signaling pathway, or an inhibitor of at least one kinase in the c-Jun N-terminal kinase (JNK) signaling pathway, or both.

2. The method of claim 1, wherein the cardiomyopathy is associated with one or more mutations in *LMNA* or *EMD*.

3. The method of claim 1, wherein the at least one kinase in the ERK signaling pathway is a MAPK/ERK kinase (MEK).

4. The method of claim 1, wherein the at least one kinase in the ERK signaling pathway is MEK1 or MEK2.

5. The method of claim 1, wherein the at least one kinase in the JNK signaling pathway is a JNK.

6. The method of claim 1, wherein the inhibitor of at least one kinase in the ERK signaling pathway is selected from the group consisting of a chromone and a flavone.

7. The method of claim 1, wherein the inhibitor of at least one kinase in the ERK signaling pathway is selected from the group consisting of 2-(2-amino-3-methoxyphenyl)-4H-1-benzopyran-4-one (PD98059), 1,4-diamino-2,3-dicyano-1,4-bis(2-aminophenylthio)butadiene (U0126), and Z-& E-a-(amino-((4-aminophenyl)thio)methylene)-2-(trifluoromethyl)benzeneacetonitrile (MEK1/2).

8. The method of claim 7, wherein the inhibitor of at least one kinase in the ERK signaling pathway is PD98059.

9. The method of claim 1, wherein the inhibitor of at least one kinase in the ERK signaling pathway is selected from the group consisting of PD0325901, AZD6244/ARRY-142886, and ARRY-438162.

10. The method of claim 1, wherein the inhibitor of at least one kinase in the JNK signaling pathway is an anthrapyrazolone.

11. The method of claim 10, wherein the inhibitor of at least one kinase in the JNK signaling pathway is anthra[1,9-cd]pyrazol-6(2H)-one (SP600125).

12. The method of claim 10, wherein the inhibitor of at least one kinase in the JNK signaling pathway is CC-401.

13. The method of claim 1, wherein the cardiomyopathy is dilated cardiomyopathy or a hypertrophic cardiomyopathy.

14. The method of claim 1, wherein the treating comprises improving cardiac function or preventing deterioration in cardiac function.

15. The method of claim 14, wherein the improving or preventing deterioration comprises increasing at least one of ejection fraction or fractional shortening.

16. The method of claim 14, wherein the improving or preventing deterioration comprises decreasing at least one of left ventricular end systolic diameter or left ventricular end diastolic diameter.

17. The method of claim 1, wherein the treating or the preventing comprises reducing expression of at least one molecular marker of cardiomyopathy.

18. The method of claim 17, wherein the molecular marker is selected from the group consisting of atrial natriuretic factor, brain natriuretic factor, Bcl-2, Elk-1, c-Jun, JunD, Vegf, Myl7, Sln, and Elk 4.

19. The method of claim 17, wherein the molecular marker is a sarcomere structure protein.

20. The method of claim 19, wherein the sarcomere structure protein is myosin.

Figure 1

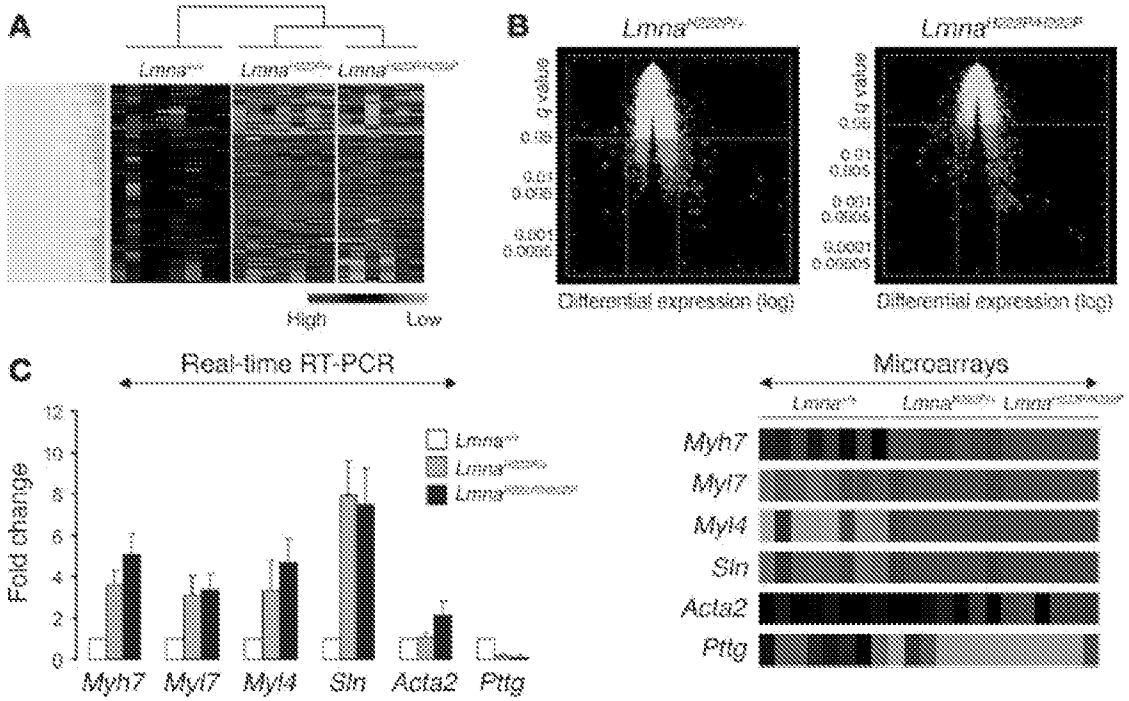
A
High
Low
B
Differential expression (log)
Differential expression (log)
C
Real-time RT-PCR
Fold change
Myh7
Myl7
Myl4
Sln
Acta2
Ptg
Microarrays
Myh7
Myl7
Myl4
Sln
Acta2
Ptg

Figure 2

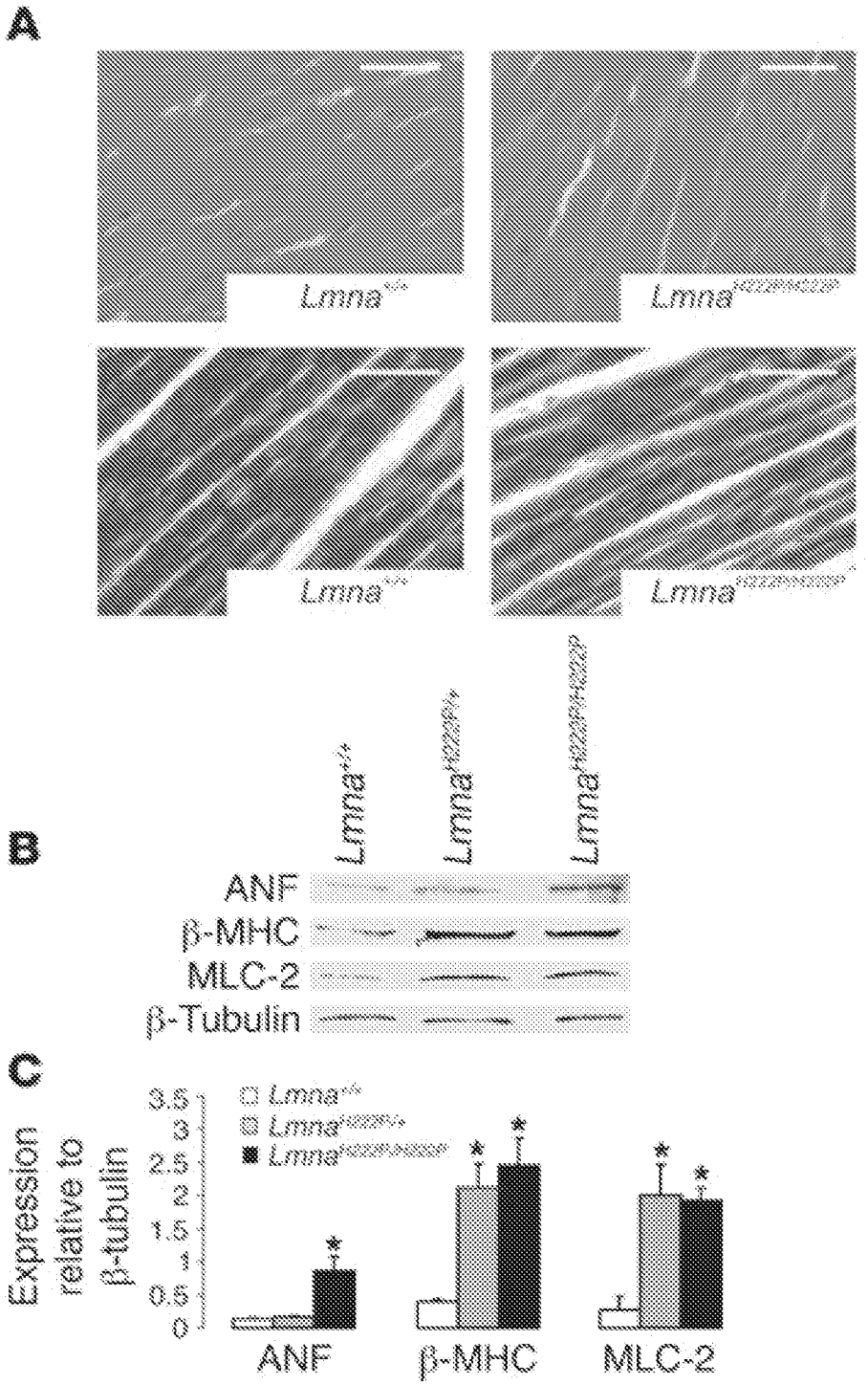
A
B
C
ANF
β-MHC
MLC-2
β-Tubulin
Expression relative to β-tubulin
3.5
3
2.5
2
1.5
1
0.5
0
ANF
β-MHC
MLC-2

Figure 3

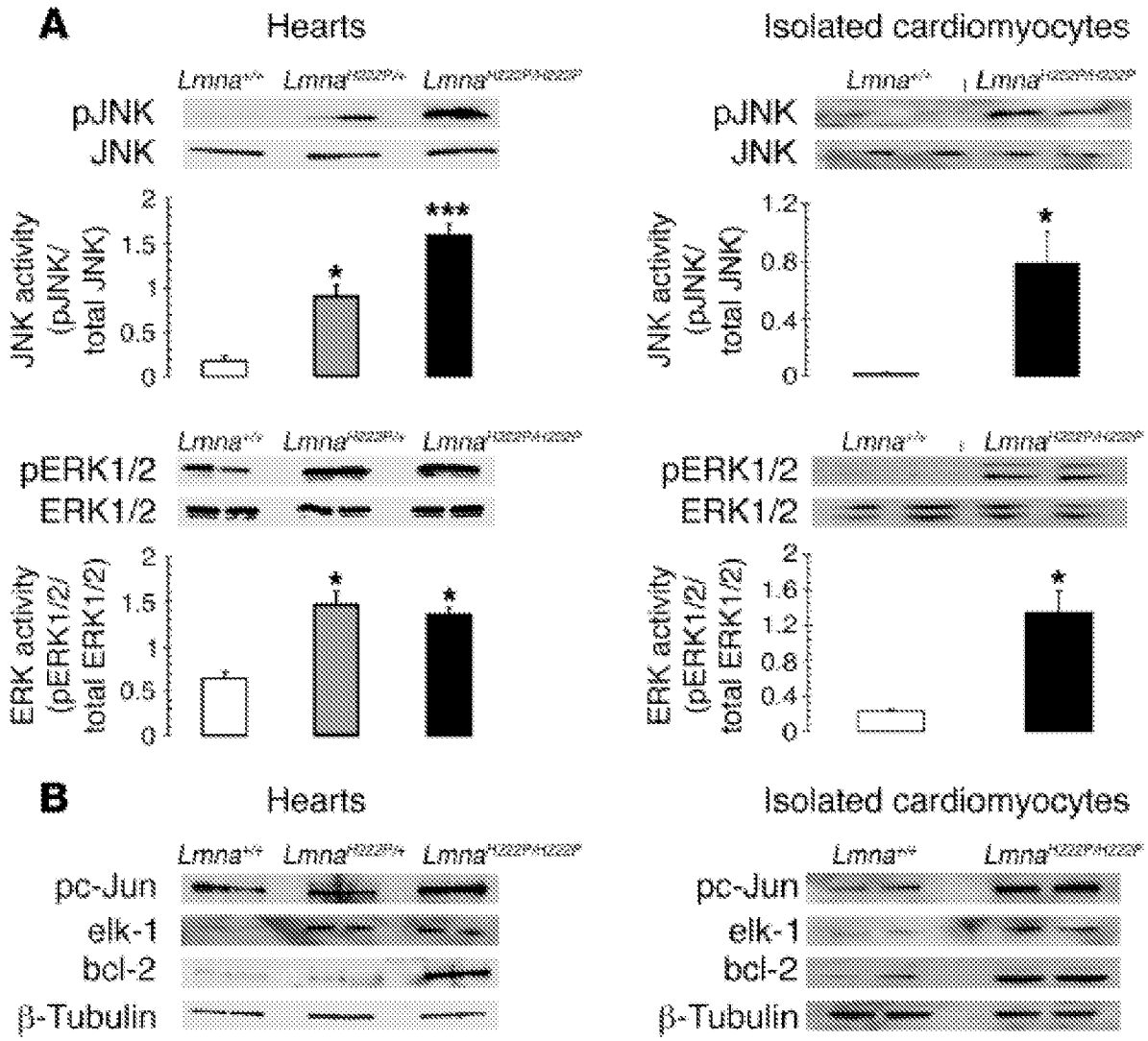
A
Hearts
Isolated cardiomyocytes
pJNK
JNK
JNK activity (pJNK/ total JNK)
pERK1/2
ERK1/2
ERK activity (pERK1/2/ total ERK1/2)
B
Hearts
Isolated cardiomyocytes
pc-Jun
elk-1
bcl-2
β-Tubulin

Figure 4

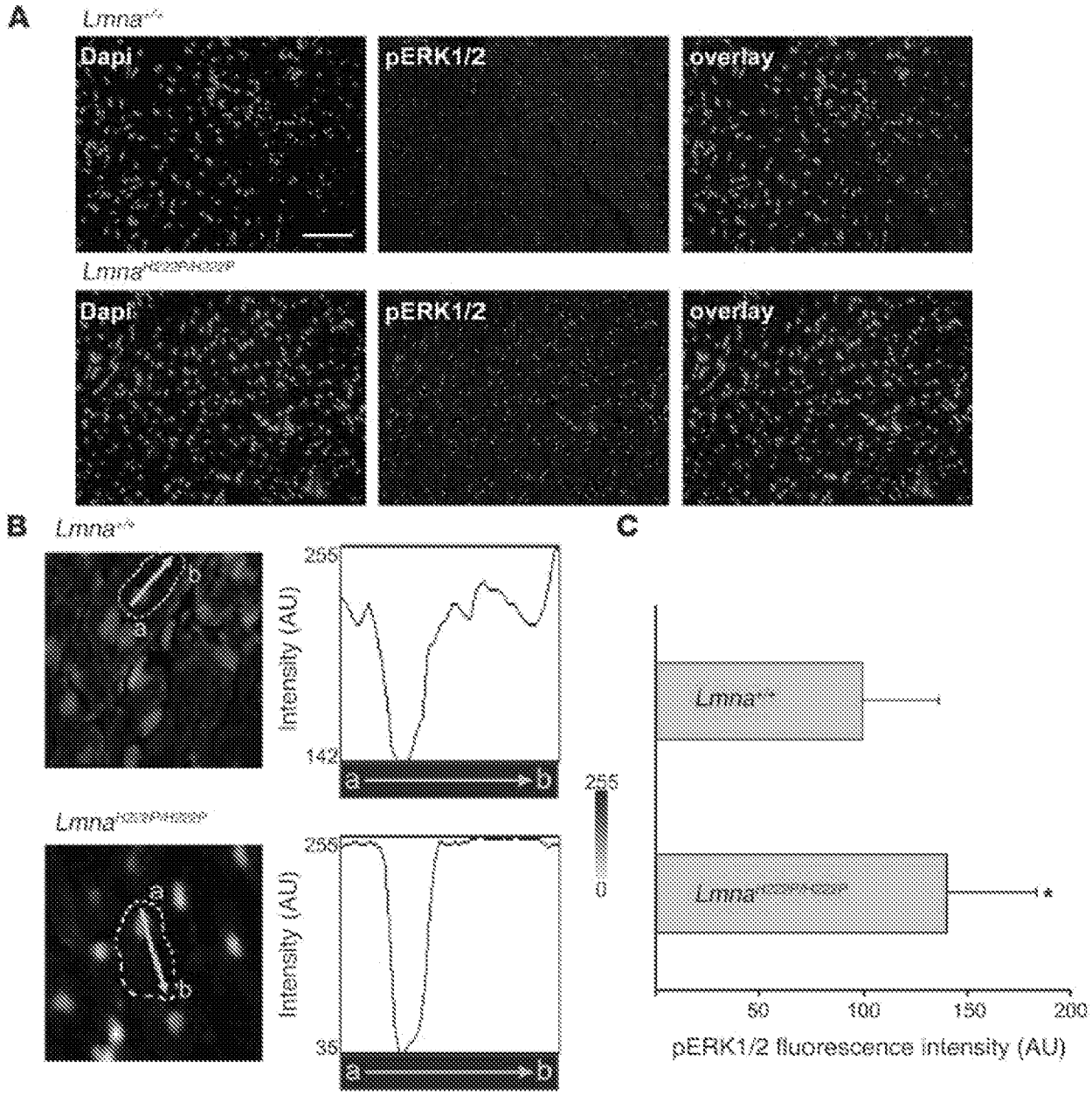
A
Lmna+/+
Dapi
pERK1/2
overlay
Lmna
Dapi
pERK1/2
overlay
B
Lmna+/+
255
Intensity (AU)
142
a
b
Lmna
255
Intensity (AU)
35
a
b
255
0
C
Lmna+/+
Lmna
*
50
100
150
200
pERK1/2 fluorescence intensity (AU)

Figure 5

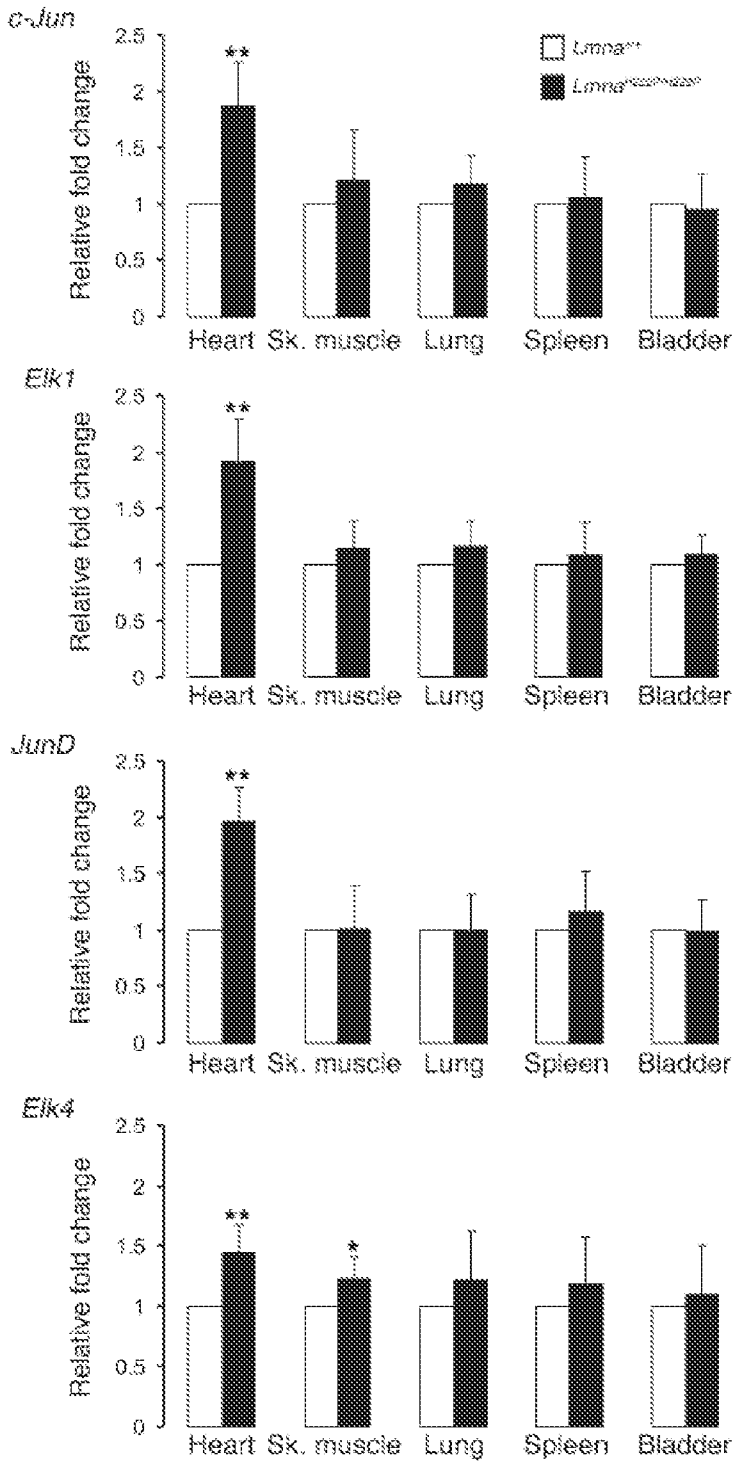
c-Jun
Elk1
JunD
Elk4
Relative fold change
2.5
2
1.5
1
0.5
0
**
*
Heart
Sk. muscle
Lung
Spleen
Bladder

Figure 6

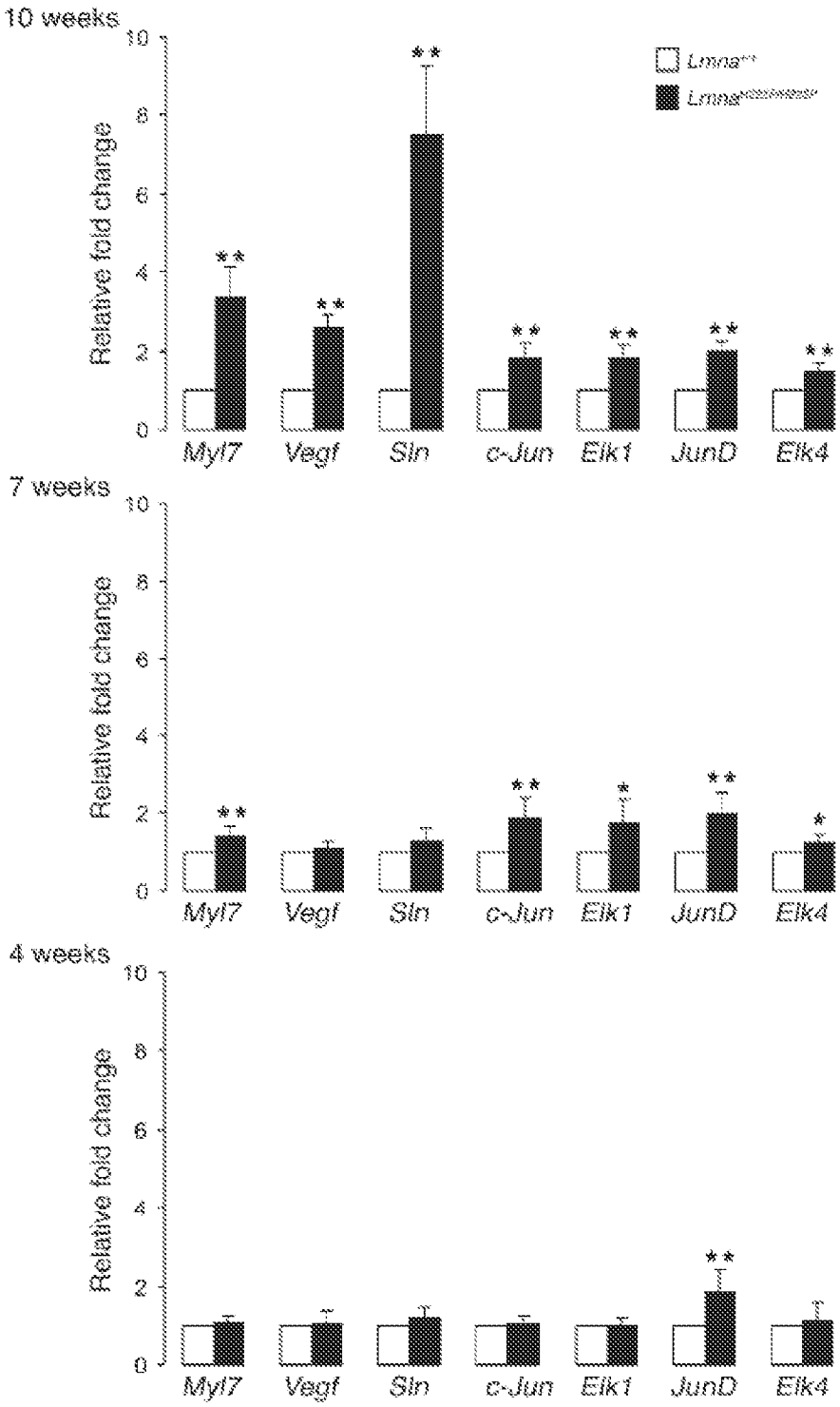
10 weeks
7 weeks
4 weeks
Relative fold change
0
2
4
6
8
10
Myl7
Vegf
Sln
c-Jun
Elk1
JunD
Elk4
**
*

Figure 7

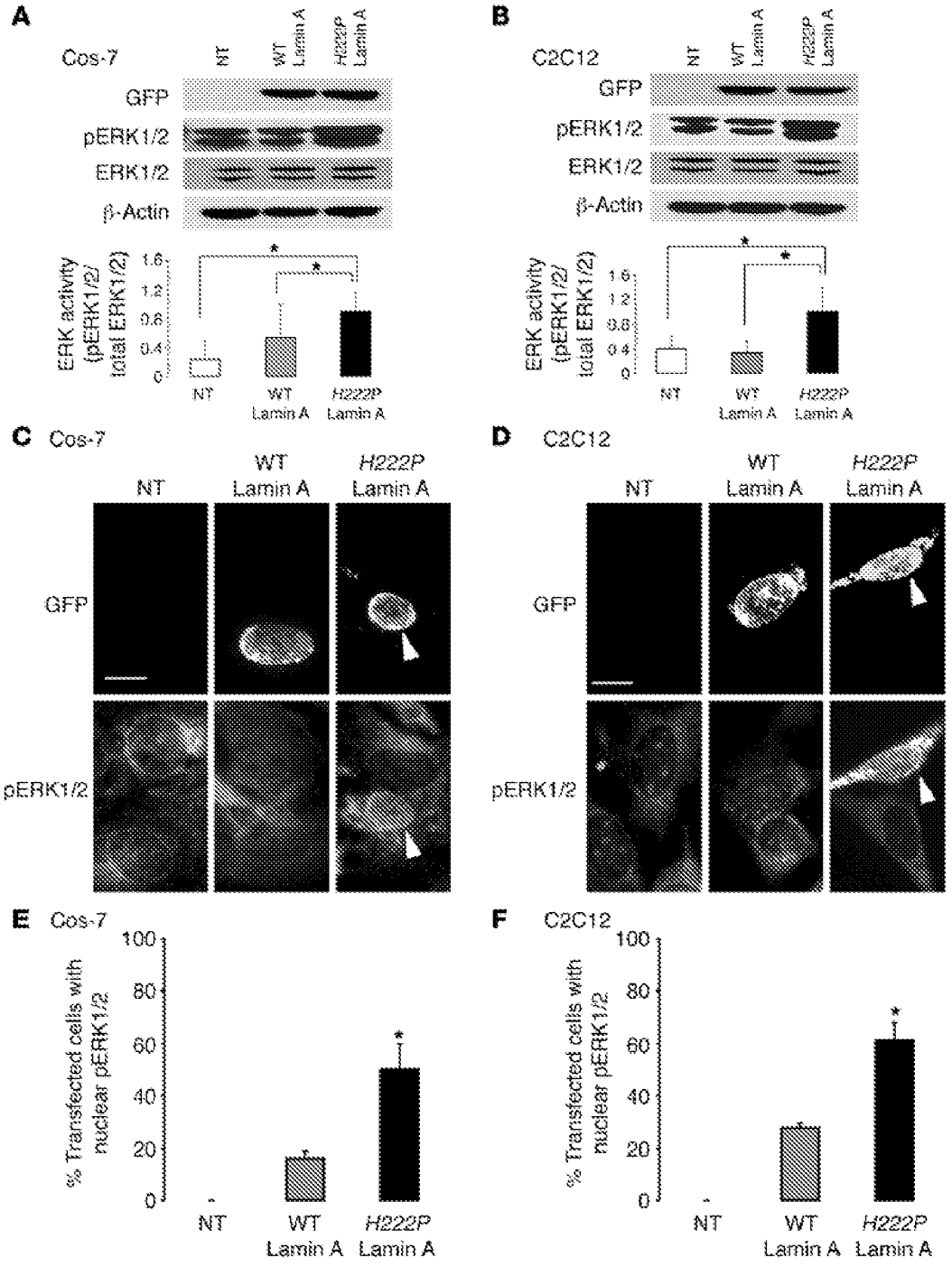
A
Cos-7
NT
WT Lamin A
H222P Lamin A
GFP
pERK1/2
ERK1/2
β-Actin
ERK activity (pERK1/2/ total ERK1/2)
1.6
1.2
0.8
0.4
0
NT
WT Lamin A
H222P Lamin A
B
C2C12
C Cos-7
D C2C12
pERK1/2
E Cos-7
F C2C12
% Transfected cells with nuclear pERK1/2
100
80
60
40
20
0

Figure 8

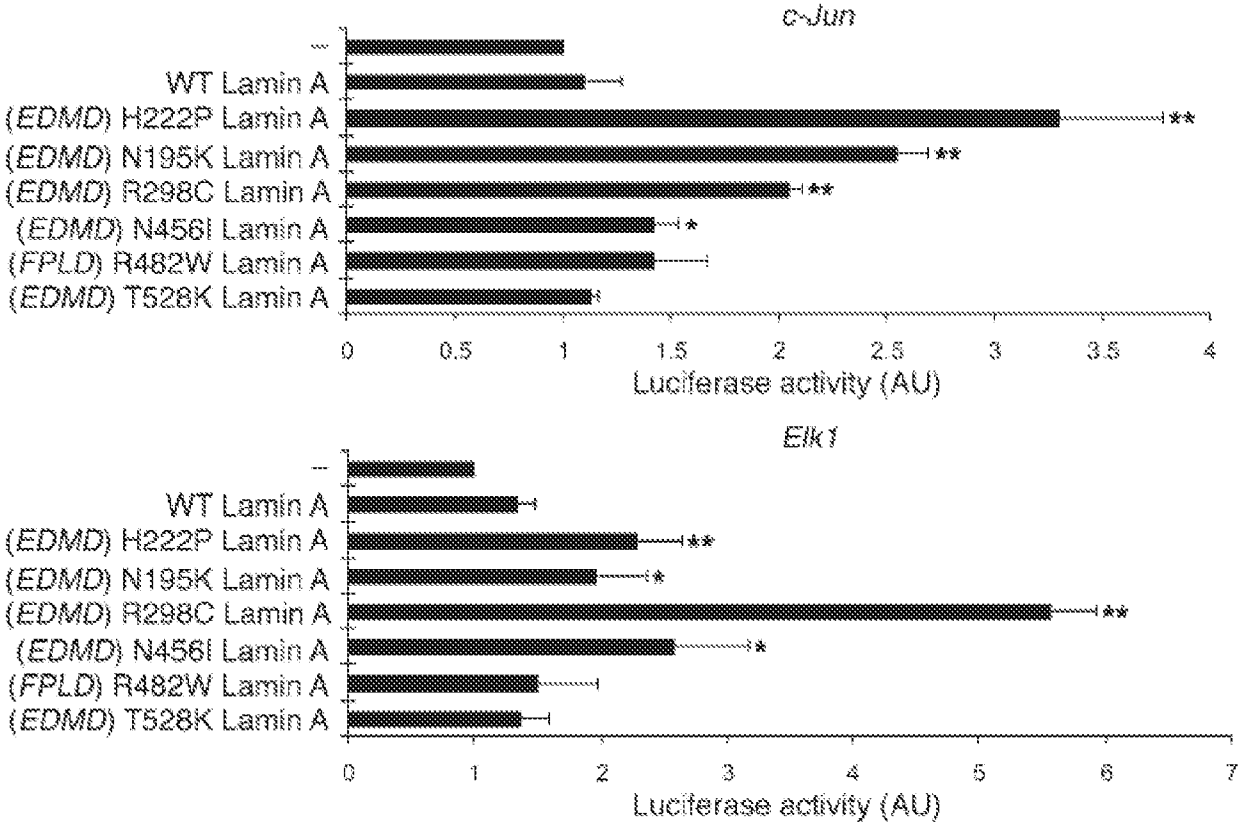
c-Jun
–
WT Lamin A
(EDMD) H222P Lamin A
(EDMD) N195K Lamin A
(EDMD) R298C Lamin A
(EDMD) N456I Lamin A
(FPLD) R482W Lamin A
(EDMD) T528K Lamin A
**
**
**
*
0
0.5
1
1.5
2
2.5
3
3.5
4
Luciferase activity (AU)
Elk1
–
WT Lamin A
(EDMD) H222P Lamin A
(EDMD) N195K Lamin A
(EDMD) R298C Lamin A
(EDMD) N456I Lamin A
(FPLD) R482W Lamin A
(EDMD) T528K Lamin A
**
*
**
*
0
1
2
3
4
5
6
7
Luciferase activity (AU)

Figure 9

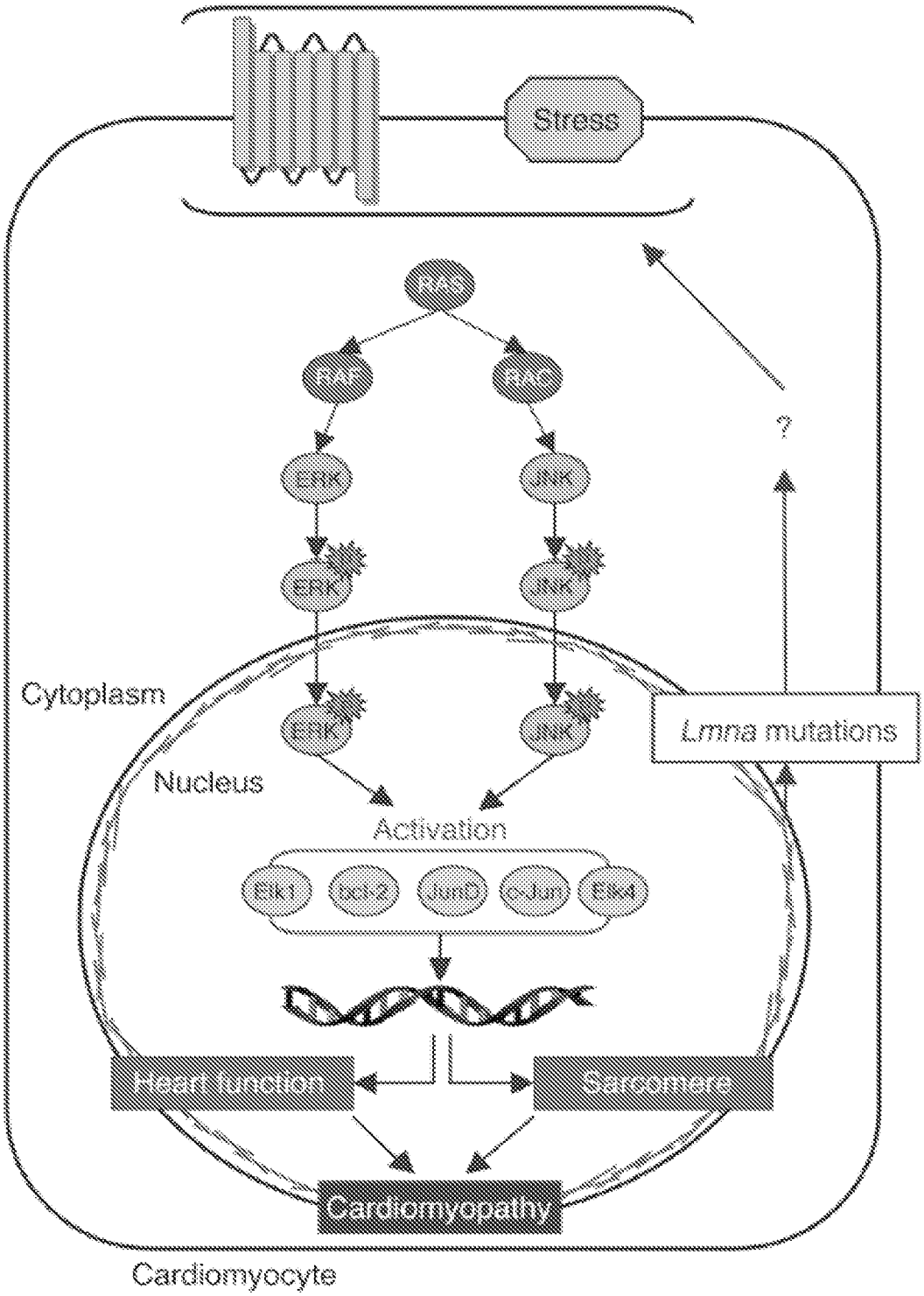
Stress
Ras
Raf
Raf
?
ERK
JNK
ERK
JNK
Cytoplasm
ERK
JNK
Lmna mutations
Nucleus
Activation
Elk1
Jun-2
JunD
c-Jun
Elk4
Heart function
Sarcomere
Cardiomyopathy
Cardiomyocyte

Figure 10

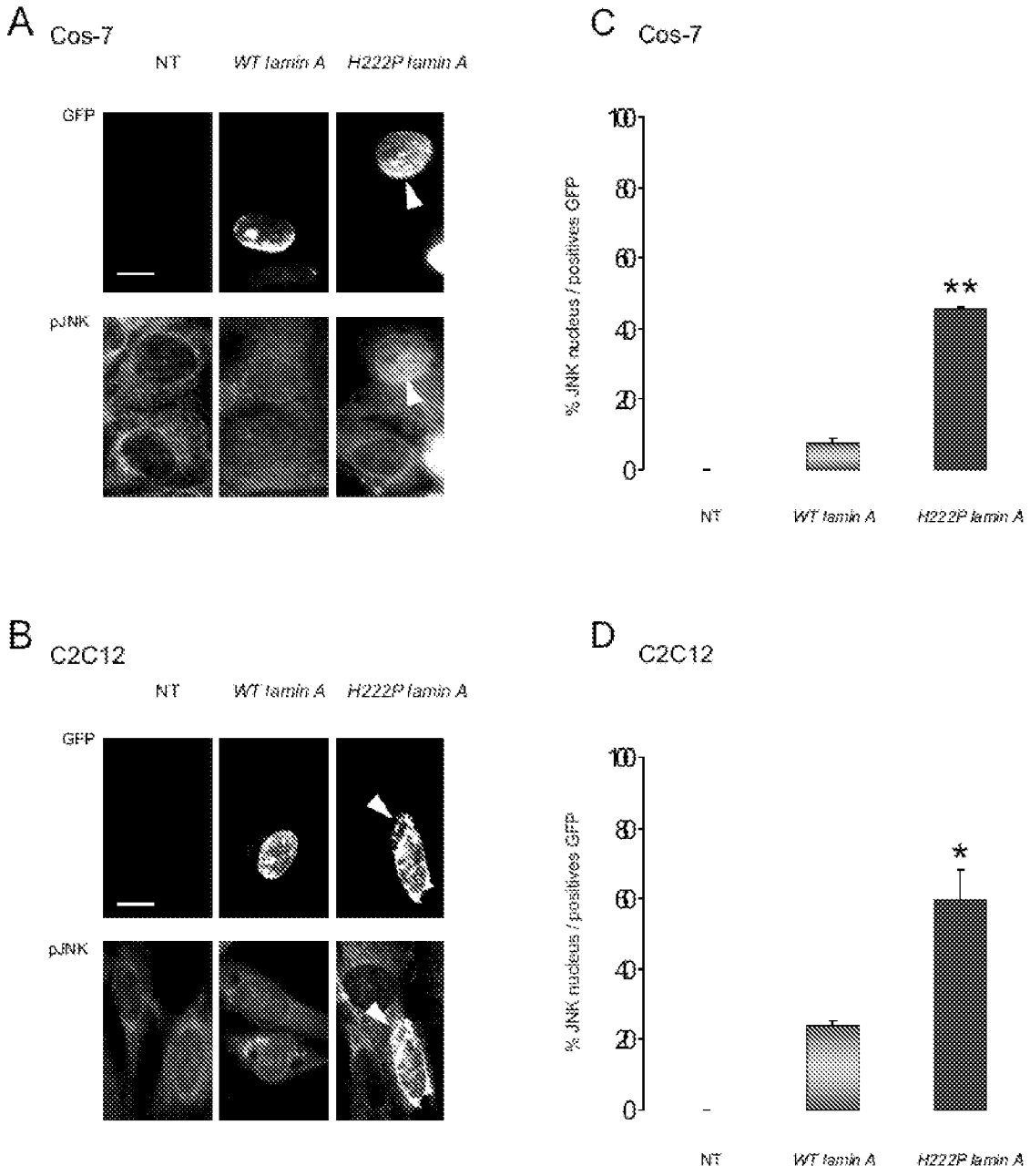
A
Cos-7
NT
WT lamin A
H222P lamin A
GFP
pJNK
B
C2C12
NT
WT lamin A
H222P lamin A
GFP
pJNK
C
Cos-7
% JNK nucleus / positives GFP
0
20
40
60
80
100
-
**
NT
WT lamin A
H222P lamin A
D
C2C12
% JNK nucleus / positives GFP
0
20
40
60
80
100
-
*
NT
WT lamin A
H222P lamin A

Figure 11

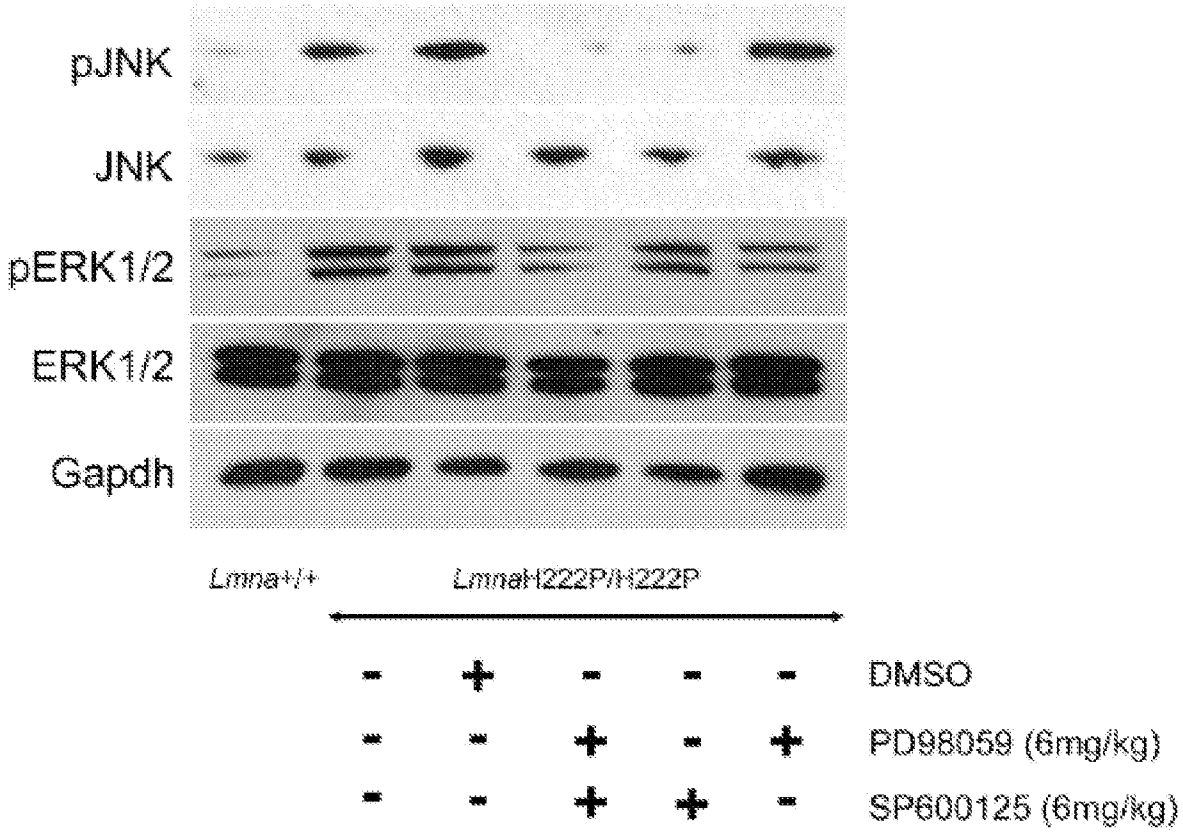
pJNK
JNK
pERK1/2
ERK1/2
Gapdh
Lmna+/+
LmnaH222P/H222P
- + - - - DMSO
- - + - + PD98059 (6mg/kg)
- - + + - SP600125 (6mg/kg)

Figure 12

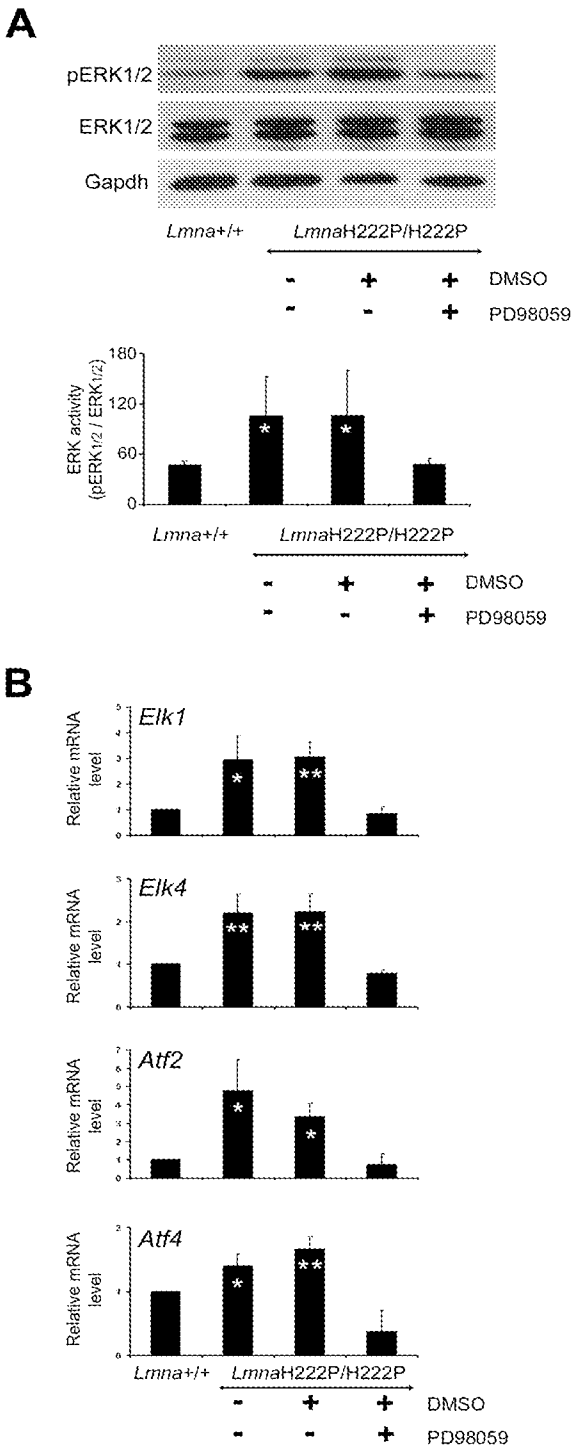
A
pERK1/2
ERK1/2
Gapdh
Lmna+/+
LmnaH222P/H222P
DMSO
PD98059
ERK activity (pERK1/2 / ERK1/2)
180
120
60
0
B
Elk1
Elk4
Atf2
Atf4
Relative mRNA level

Figure 13

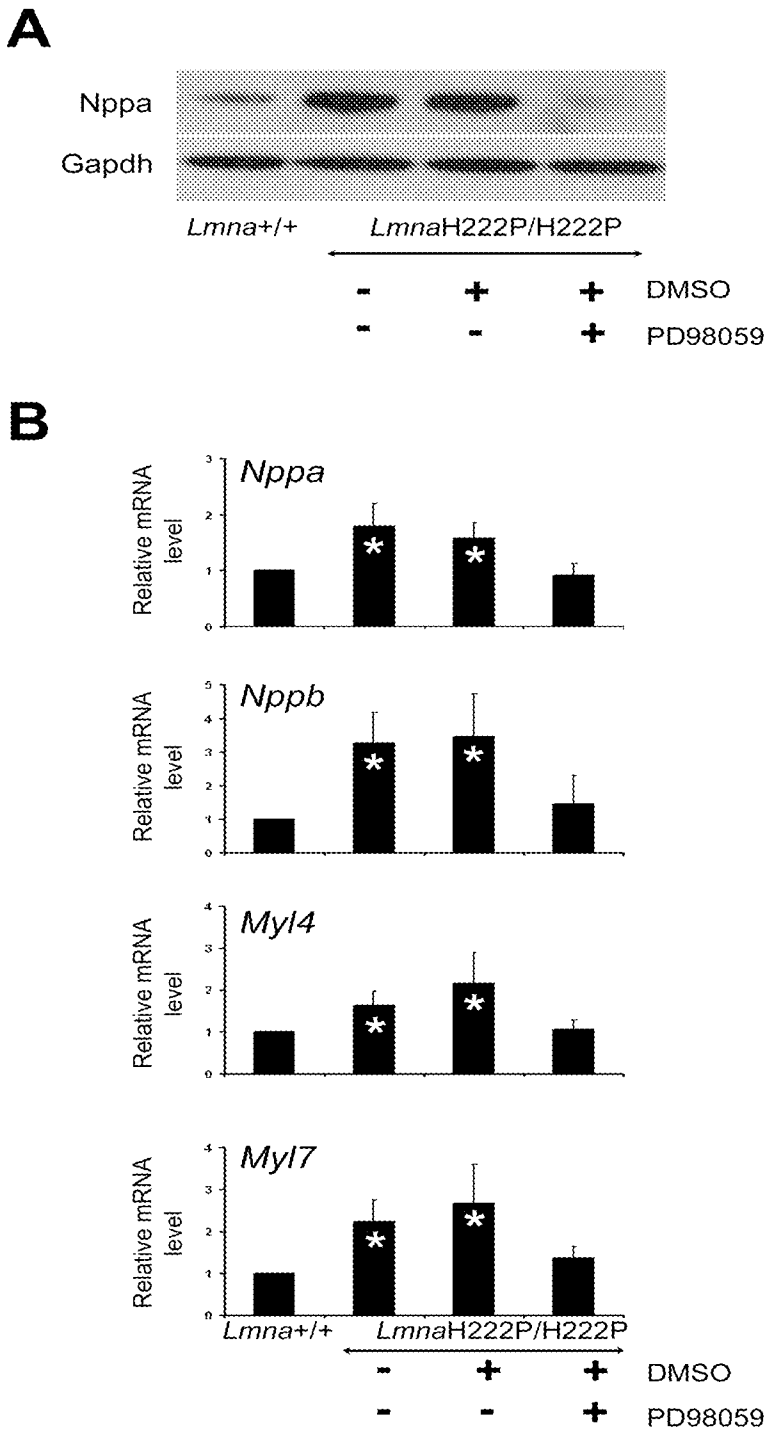
A
Nppa
Gapdh
Lmna+/+
LmnaH222P/H222P
DMSO
PD98059
B
Nppa
Nppb
Myl4
Myl7
Relative mRNA level
Lmna+/+
LmnaH222P/H222P
DMSO
PD98059

Figure 14

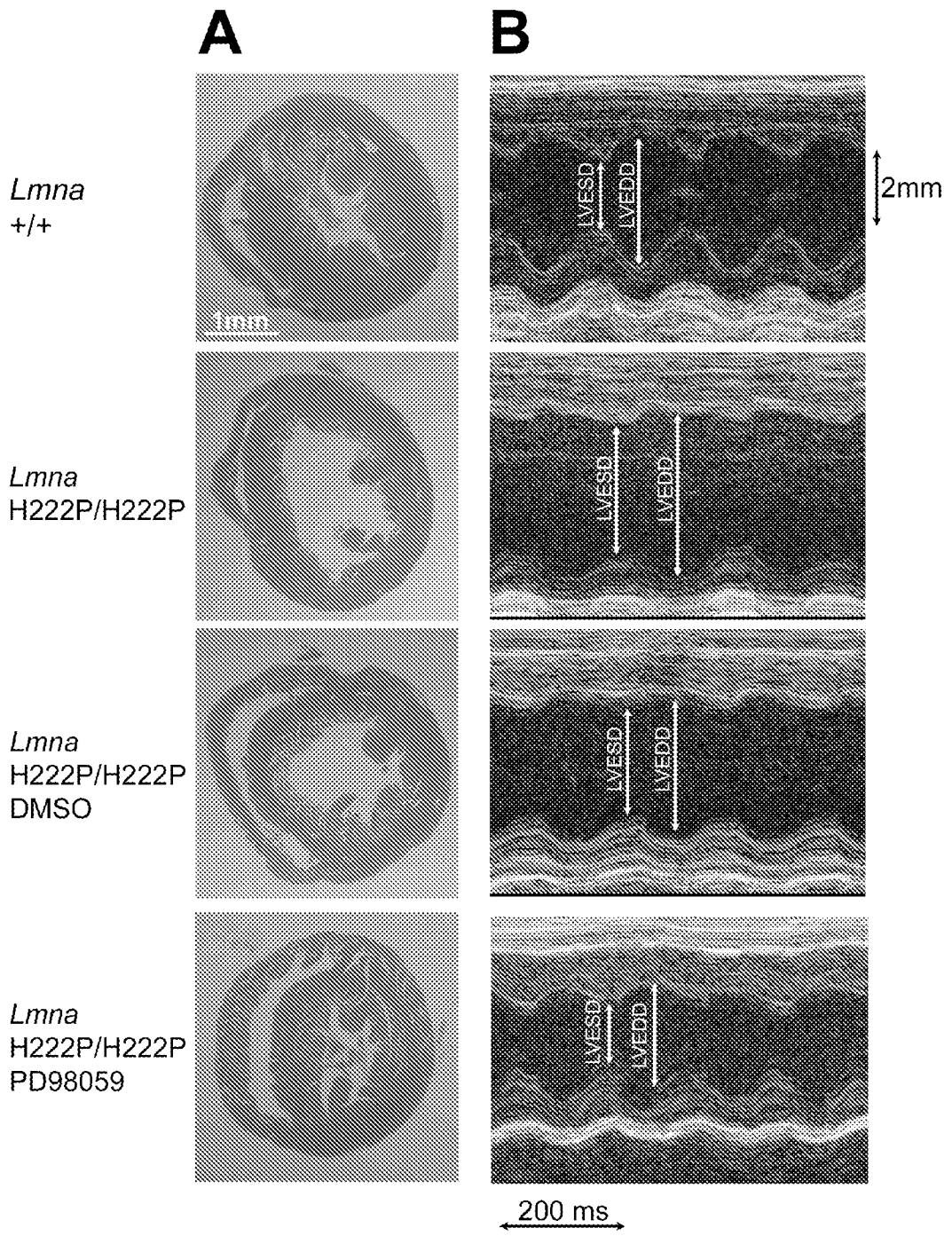
A
B
Lmna
+/+
Lmna
H222P/H222P
Lmna
H222P/H222P
DMSO
Lmna
H222P/H222P
PD98059
1mm
LVESD
LVEDD
2mm
200 ms

Figure 15

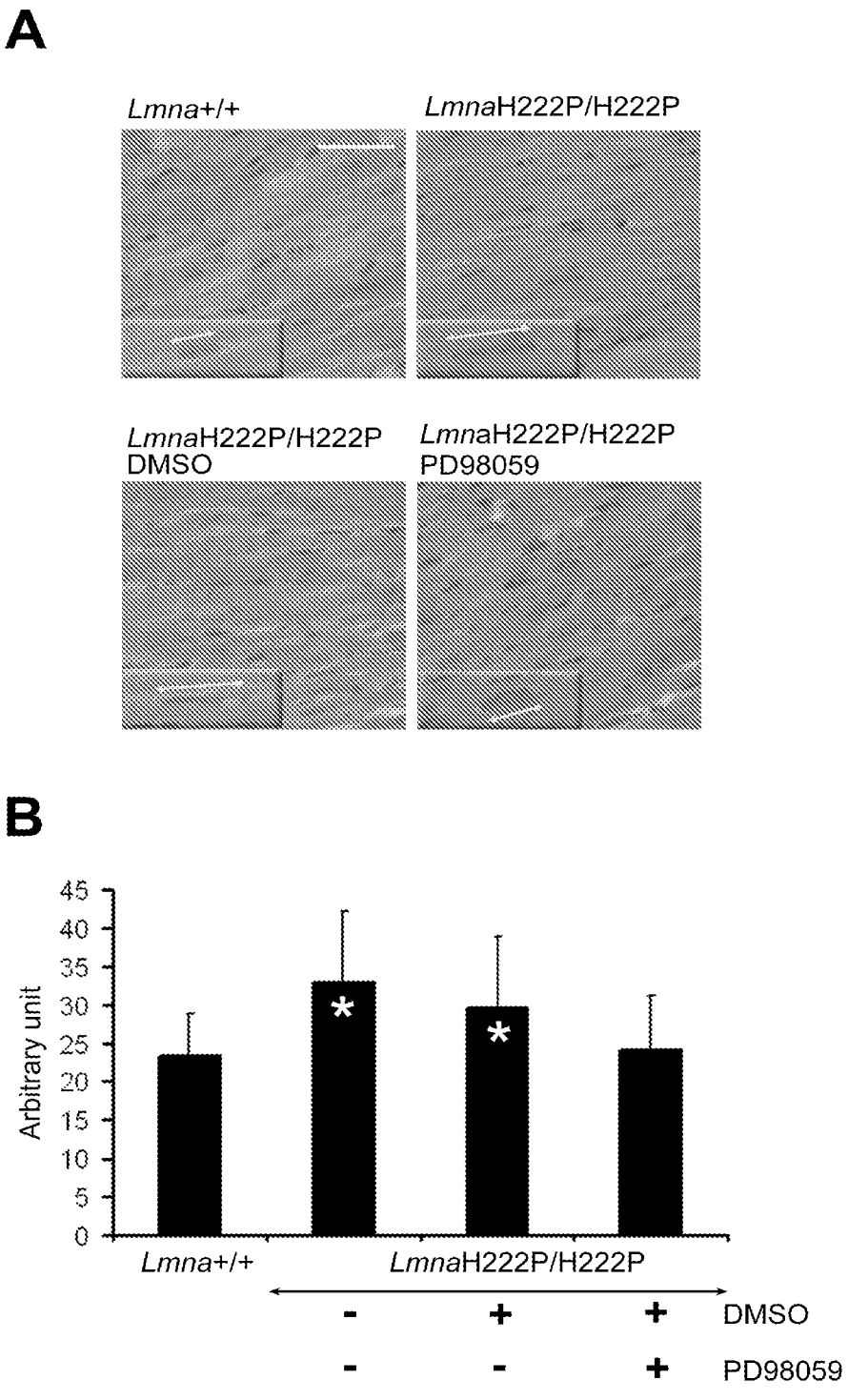
A
Lmna+/+
LmnaH222P/H222P
LmnaH222P/H222P
DMSO
LmnaH222P/H222P
PD98059
B
Arbitrary unit
45
40
35
30
25
20
15
10
5
0
*
*
Lmna+/+
LmnaH222P/H222P
-
+
+
DMSO
-
-
+
PD98059

Figure 16

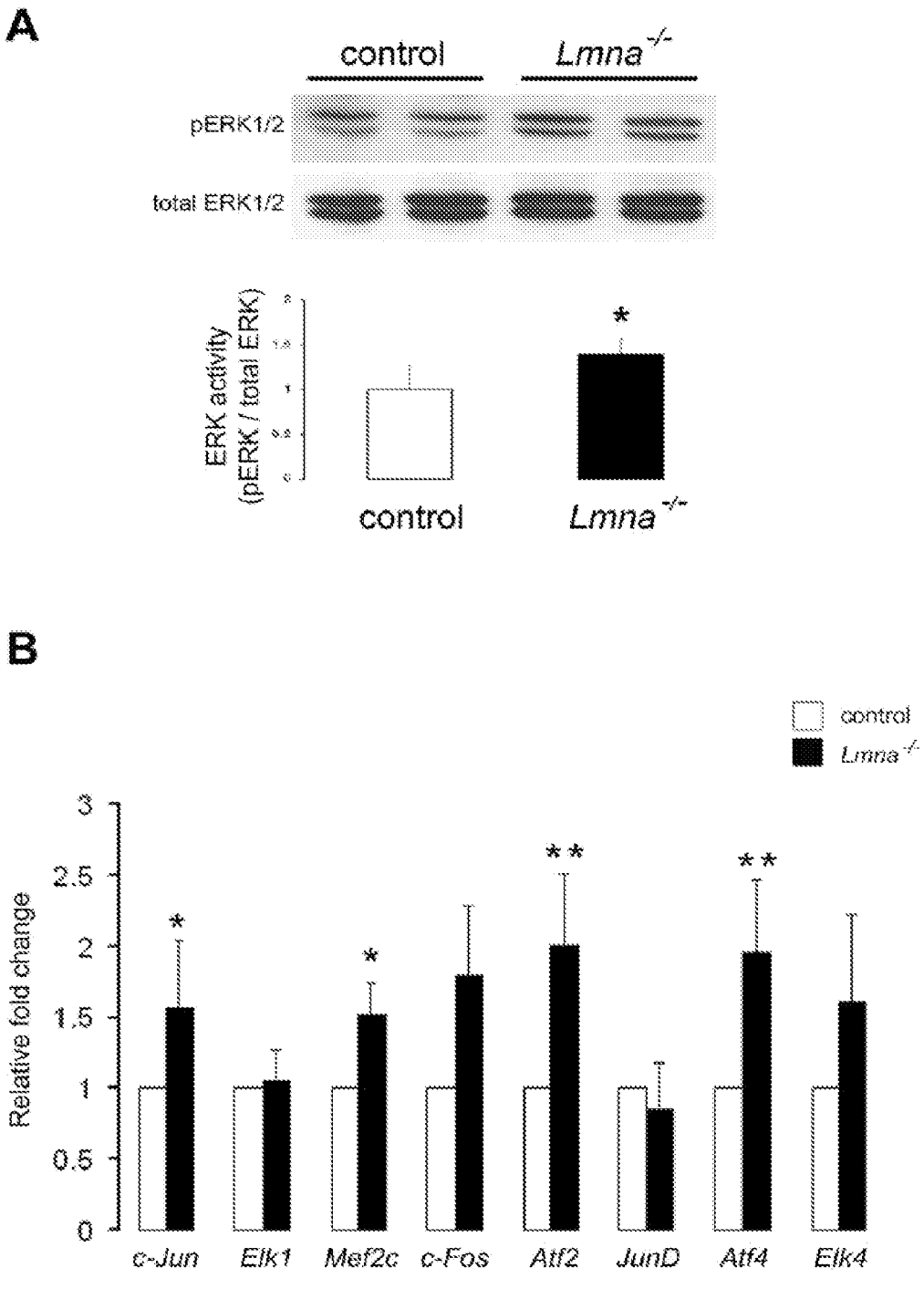
A
control
Lmna-/-
pERK1/2
total ERK1/2
ERK activity
(pERK / total ERK)
*
control
Lmna-/-
B
control
Lmna-/-
Relative fold change
0
0.5
1
1.5
2
2.5
3
*
*
**
**
c-Jun
Elk1
Mef2c
c-Fos
Atf2
JunD
Atf4
Elk4

Figure 17

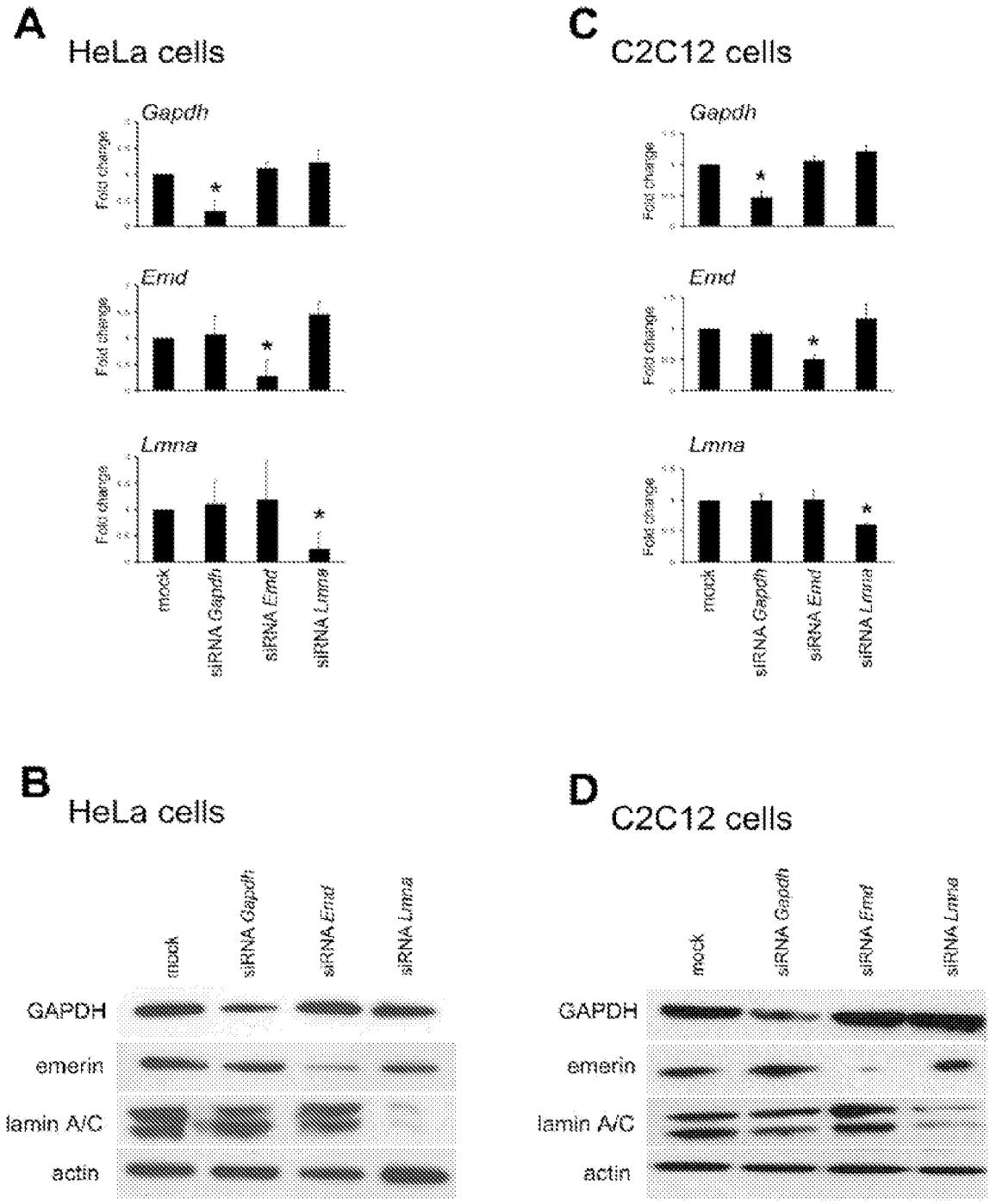
A
HeLa cells
Gapdh
Emd
Lmna
Fold change
mock
siRNA Gapdh
siRNA Emd
siRNA Lmna
C
C2C12 cells
Gapdh
Emd
Lmna
Fold change
mock
siRNA Gapdh
siRNA Emd
siRNA Lmna
B
HeLa cells
mock
siRNA Gapdh
siRNA Emd
siRNA Lmna
GAPDH
emerin
lamin A/C
actin
D
C2C12 cells
mock
siRNA Gapdh
siRNA Emd
siRNA Lmna
GAPDH
emerin
lamin A/C
actin

Figure 18

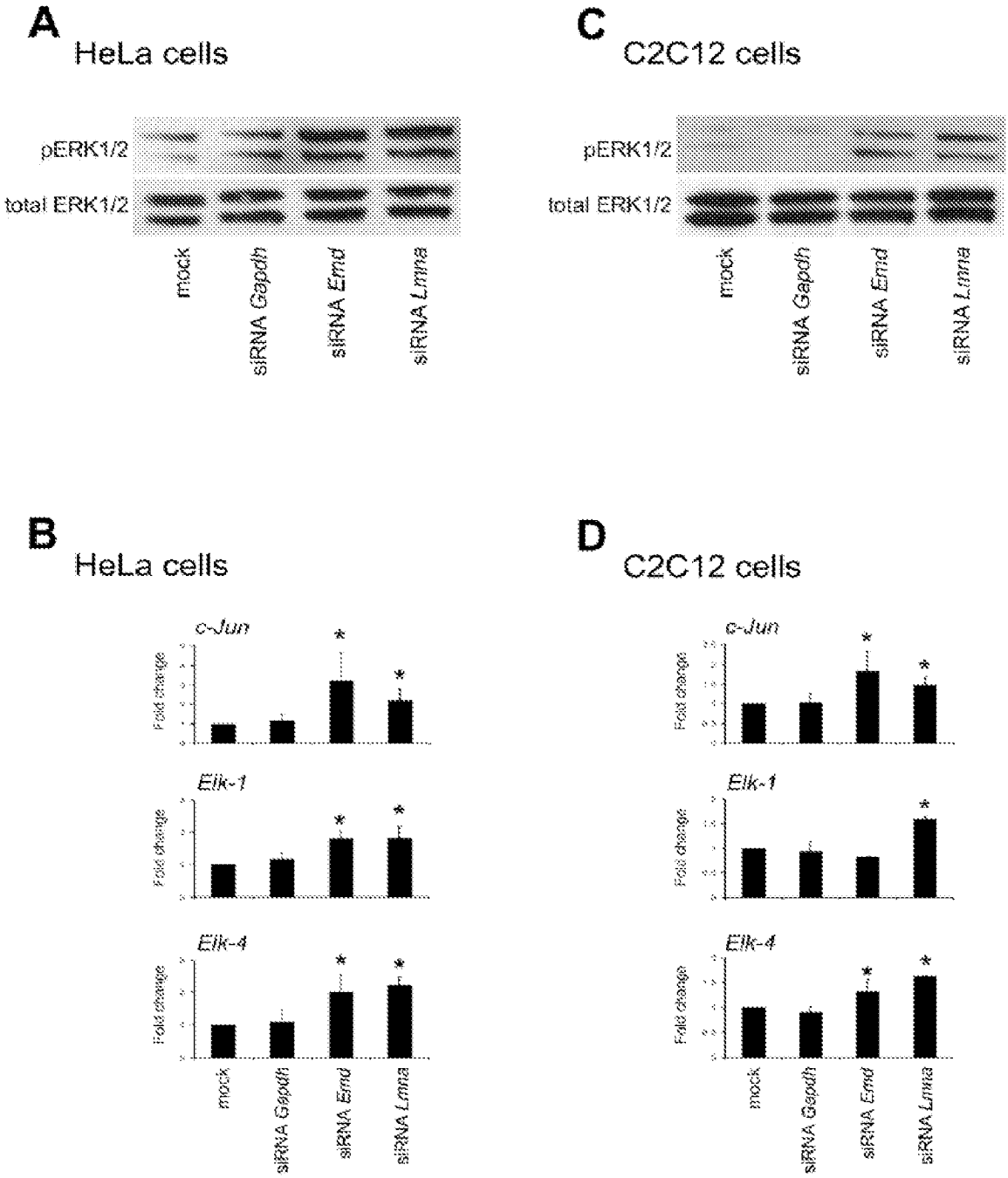
A
HeLa cells
pERK1/2
total ERK1/2
mock
siRNA Gapdh
siRNA Emd
siRNA Lmna
C
C2C12 cells
pERK1/2
total ERK1/2
mock
siRNA Gapdh
siRNA Emd
siRNA Lmna
B
HeLa cells
c-Jun
Elk-1
Elk-4
Fold change
mock
siRNA Gapdh
siRNA Emd
siRNA Lmna
D
C2C12 cells
c-Jun
Elk-1
Elk-4
Fold change
mock
siRNA Gapdh
siRNA Emd
siRNA Lmna

Figure 19

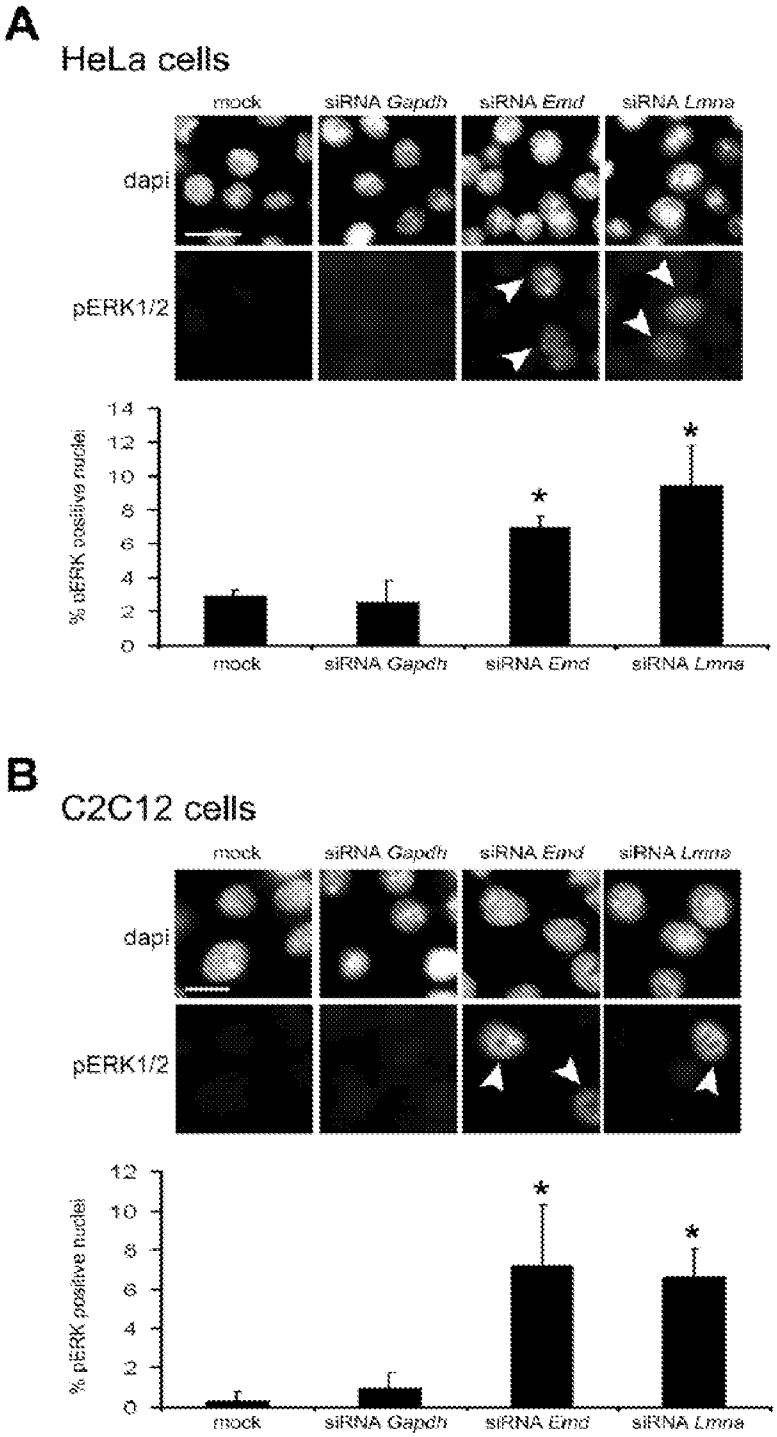
A
HeLa cells
mock
siRNA Gapdh
siRNA Emd
siRNA Lmna
dapi
pERK1/2
% pERK positive nuclei
0
2
4
6
8
10
12
14
*
*
mock
siRNA Gapdh
siRNA Emd
siRNA Lmna
B
C2C12 cells
mock
siRNA Gapdh
siRNA Emd
siRNA Lmna
dapi
pERK1/2
% pERK positive nuclei
0
2
4
6
8
10
12
*
*
mock
siRNA Gapdh
siRNA Emd
siRNA Lmna

Figure 20

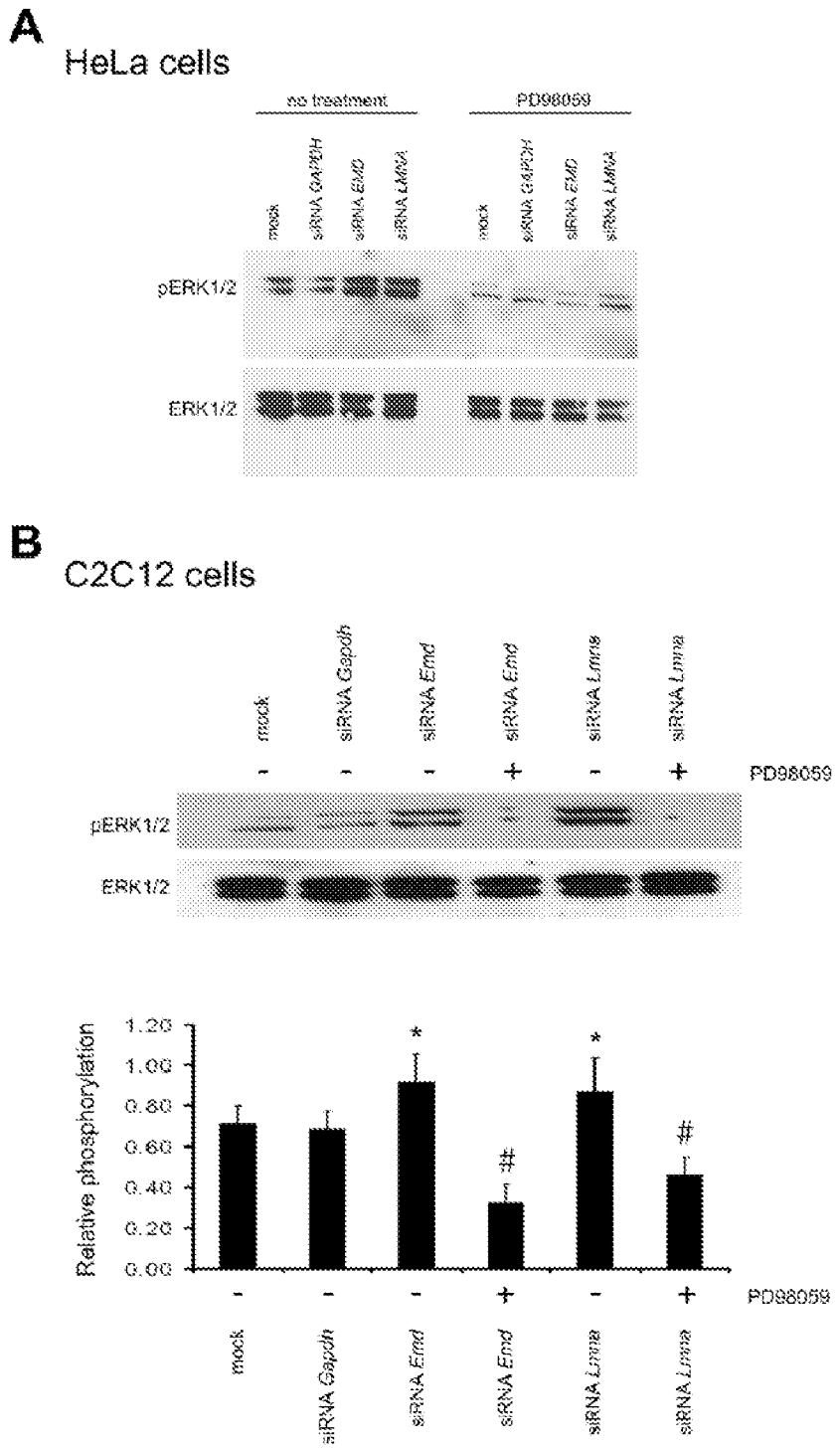
A
HeLa cells
no treatment
PD98059
mock
siRNA GAPDH
siRNA EMD
siRNA LMNA
pERK1/2
ERK1/2
B
C2C12 cells
mock
siRNA Gapdh
siRNA Emd
siRNA Lmna
PD98059
pERK1/2
ERK1/2
Relative phosphorylation
1.20
1.00
0.80
0.60
0.40
0.20
0.00
*
#